

# The Investigation and Analysis of RAFT-mediated Block Copolymers in Aqueous Dispersed Media

Dissertation presented in partial fulfillment of requirements for the degree:



MSc (Polymer Science)

by

Nadine O. Pretorius

Supervisor Prof R.D. Sanderson

Co supervisor Dr J. B. McLeary

December 2007

Stellenbosch

## *Declaration*

**I, the undersigned, hereby declare that the work contained in this dissertation is my own original work and that I have not previously in its entirety or in part submitted it at any university for a degree.**

---

Nadine O. Pretorius

**December 2007**

Stellenbosch

Dedicated To

*my late father Jacob, my mom Marechia and brother Vincent*

## *Abstract*

Polymers prepared via radical techniques are very common in our every day environment. The technique is however limited by a lack of control over the polymerization and an inability to produce block copolymers. Block copolymers have a significant number of potential applications in advanced materials and as a result are a field in which significant research is being conducted. Reversible Addition-Fragmentation chain transfer (RAFT) is a living free radical process that overcomes the disadvantages inherent in the traditional process.

In this study the mediation behaviour of two inherently different RAFT agents was investigated by the “living” free radical polymerization of model monomers via the RAFT process in homogeneous and aqueous dispersed media with the focus on differentiating between the two types of agents. To ensure that the agents were comparable a new RAFT agent had to be prepared which has not previously been documented. The efficiency of the RAFT agents was compared in terms of rate effects, the predictability of the molecular weights of the polymers, the polydispersities of the polymers and their ability to allow block copolymer formation via sequential addition of monomers. Block copolymerizations were conducted by the addition of new monomer to the already existing RAFT end-capped chains. Monomer addition was done via three different approaches; namely shot addition, feed addition and pre-swelling (in the case of emulsions). Chromatographic analysis was conducted on the resulting block copolymers via liquid chromatography at critical conditions (LC-CC), and its online coupling with size-exclusion chromatography (SEC) to obtain two-dimensional information on the differences in heterogeneity of their molecular distributions. Other analyses included dynamic light scattering analysis (DLS) and transmission electron microscopy (TEM).

The detailed analysis enabled the understanding of the different products that are produced via the two different classes of RAFT agent. Potential causes for the differences are discussed and possible areas for future research are highlighted. The work presented here is the most detailed investigation of this class of polymerization to date and will provide new insight for researchers working in this vibrant and important research field.

## *Opsomming*

Polimere gesintetiseer deur die gebruik van radikaal tegnieke is algemeen in ons daaglikse omgewing.

Die tegniek is egter beperk deur die gebrek aan beheer oor die polimerisasie en die onvermoë om blokkopolimere te sintetiseer. Blokkopolimere beskik oor 'n aansienlike hoeveelheid potensiele toepassings in gevorderde materiale en is gevolglik 'n belangrike navorsingsgebied. Omkeerbare addisie fragmentasie ketting oordrag (OAF0) is 'n lewende vrye radikaal proses wat die inherente nadele van die tradisionele proses oorkom.

In die betrokke studie is die mediasie gedrag van twee verskillende OAF0 agente bestudeer deur die lewende vrye radikaal polimerisasie van model monomere deur die OAF0 proses in homogene en waterig dispersie media met die fokus op differensiering tussen die twee tipes agente. Om te verseker dat die twee agente vergelykbaar is, is 'n nuwe OAF0 agent voorberei wat tot op hede nog nie gedokumenteer is nie. Die effektiwiteit van die OAF0 agente is vergelyk in terme van tempo effekte, die voorspelbaarheid van die molekulêre massa van die polimere, die polidispersiteit van die polimere en die moontlikheid om blokkopolimerisasie deur kronologiese byvoeging van monomere te fasiliteer. Blokkopolimerisasie is uitgevoer deur die byvoeging van nuwe monomeer tot die alreeds bestaande OAF0 eind-groep kettings. Monomeer byvoegings is uitgevoer deur drie verskillende metodes; naamlik vulskoot addisie, voer addisie en vooraf swelling (in die geval van emulsies). Chromatografiese analise is uitgevoer op die resulterende blokkopolimere deur vloeistof chromatografie by kritieke kondisie (LC-CC) en die aanlyn koppeling met grootte-uitsluiting vloeistof chromatografie, om twee-dimensionele informasie omtrent die verskille in heterogeniteit van hul molekulere verdeling te bepaal. Verdere analise sluit dinamiese verstrooiing mikroskopie en transmissie elektron mikroskopie in.

Die gedetailleerde analise onthul die samestelling van die verskillende produkte wat geproduseer is deur die verskillende klasse van OAF0 agente. Potensiele oorsake vir die verskille is bespreek en moontlike areas vir toekomstige navorsing is benadruk. Die werk hier voorgestel is die mees gedetailleerde navorsing van hierdie tipe klas van polimerisasie tot op hede en beloof nuwe insig vir navorsers betrokke in hierdie dinamiese en belangrike navorsingsveld.

# ***Index***

<i>Abstract</i> .....	<i>I</i>
<i>Opsomming</i> .....	<i>II</i>
<i>Index</i> .....	<i>III</i>
<i>List of Figures</i> .....	<i>IX</i>
<i>List of Schemes</i> .....	<i>XVII</i>
<i>List of Tables</i> .....	<i>XIX</i>
<i>List of Acronyms</i> .....	<i>XXI</i>
<i>List of Symbols</i> .....	<i>XXIII</i>
<i>Chapter 1: Introduction and Aims</i> .....	<i>1</i>
1.1 General Introduction.....	2
1.2 Aims .....	3
1.3 Thesis Layout.....	4
Chapter 1- Introduction and aims .....	4
Chapter 2- Historical and theoretical background.....	4
Chapter 3- RAFT agents “made easy”.....	4
Chapter 4- The living character of CVADTB and CVATTB in homogeneous polymerization.....	4
Chapter 5- RAFT mediated miniemulsion polymerizations .....	4

*Indexes and lists*


---

Chapter 6- Chromatographic investigation of block copolymers via hyphenated techniques.....	4
Chapter 7- Conclusions and Recommendations.....	5
1.4 References.....	6
<b><i>Chapter 2: Historical and Theoretical Background .....</i></b>	<b><i>7</i></b>
2.1. Radical Polymerization.....	8
2.1.1 The nature of radical chain polymerization .....	8
2.1.2 The mechanism and radical kinetics.....	8
2.2. Living Radical Polymerization .....	16
2.2.1 Overview.....	16
2.2.2 Reversible-addition fragmentation transfer (RAFT).....	18
2.2.2.1 History of RAFT.....	18
2.2.2.2 The RAFT mechanism .....	18
2.2.2.3 The choice of RAFT agents.....	20
2.2.2.4 Block copolymers via RAFT .....	22
2.3. Homogeneous Systems.....	24
2.4. Heterogeneous Systems .....	24
2.5. The Basic Framework of Radical Emulsion Polymerization Mechanism and Kinetics .....	25
2.5.1 The different intervals in emulsion polymerization .....	26
Interval I.....	27
Interval II.....	28
Interval III .....	28
2.5.2 Phase transfer events in emulsion polymerization .....	28
CASE 1: $\bar{n} \ll 0.5$ .....	30
CASE 2: $\bar{n} = 0.5$ .....	30
CASE 3: $\bar{n} \gg 0.5$ .....	30
2.6. Miniemulsion Polymerization.....	31
2.6.1 Preparation of miniemulsion by ultrasound homogenization .....	31
2.6.2 Mechanism and kinetics of miniemulsion polymerization .....	32
2.6.2.1 Mechanism of particle nucleation.....	32
2.6.2.2 Stability of miniemulsions.....	33

*Indexes and lists*


---

2. 7. Characterization of Polymers with Complex Architectures by Liquid Chromatography .....	34
2.7.1 Overview .....	34
2.7.2 Critical point of adsorption .....	35
2.7.3 Two-dimensional chromatography .....	36
2.7.3.1 “Comprehensive” 2D-LC setup .....	37
2.8. References .....	39
<i>Chapter 3: RAFT Agents “Made Easy” .....</i>	<i>42</i>
3.1 Introduction .....	43
3.2 Experimental .....	44
3.2.1 Cyanovaleric acid dithiobenzoate .....	44
Materials .....	44
Procedure .....	44
3.2.2 Cyanovaleric acid benzyl trithiocarbonate .....	46
Materials .....	46
Procedure .....	46
3.3 Conclusions .....	48
3.4 References .....	49
<i>Chapter 4: The Living Character of CVADTB and CVATTB in Homogeneous Polymerization .....</i>	<i>50</i>
4.1 Introduction .....	51
4.2 Experimental .....	52
4.2.1 Materials/Reagents .....	52
4.2.2 RAFT agents used .....	52
4.2.3 Polymerizations .....	52
4.2.3.1 RAFT mediated solution polymerization of styrene and methyl methacrylate. ....	52
4.2.3.2 Block copolymer polymerizations .....	53
4.2.4 Kinetic analysis .....	54
4.2.5 SEC analysis .....	54

*Indexes and lists*


---

4.3 Results and Discussion .....	54
4.3.1 Styrene and methyl methacrylate polymers .....	54
4.3.1.1 Rates of reaction .....	55
4.3.1.2 Molecular weight distributions .....	57
4.3.1.3 UV-RI overlays.....	61
4.3.2 Chain extension of starting blocks .....	64
4.3.2.1 PS-b-PMMA .....	66
4.3.2.2 PMMA-b-PS .....	71
4.4 Conclusions.....	76
4.5 References.....	78
<i>Chapter 5: RAFT Mediated Miniemulsion Polymerizations .....</i>	<i>79</i>
5.1 Introduction.....	80
5.2 Experimental .....	81
5.2.1 Materials/Reagents .....	81
5.2.2 General.....	81
5.2.3 Miniemulsion preparation procedure.....	82
5.2.4 Polymerizations .....	82
5.2.4.1 RAFT mediated miniemulsion homopolymerization of styrene and methyl methacrylate.....	82
5.2.4.2 Chain extension of starting block polymers .....	83
5.2.5 Kinetic analysis .....	84
5.2.6 SEC analysis.....	84
5.2.7 Particle size analysis.....	84
5.2.8 Transmission electron microscopy .....	84
5.3 Results and Discussion .....	85
5.3.1 Styrene and methyl methacrylate polymers .....	85
5.3.1.1 Rate of reactions .....	87
5.3.1.2 Molecular weight distribution in RAFT mediated miniemulsion polymerization.....	89
5.3.1.3 UV-RI analysis .....	94
5.3.2 Chain extension of the starting block polymers .....	97
5.3.2.1 PS-b-PMMA copolymers .....	99

*Indexes and lists*

---



---

5.3.2.2 PMMA-b-PS copolymers .....	103
5.3.3. Latex investigations: A closer look at the prepared latexes with dynamic light scattering (DLS) and transmission electron microscopy (TEM) .....	108
5.3.3.1 PS-b-PMMA sequence .....	109
5.3.3.2 PMMA-b-PS sequence .....	112
5.4 Conclusion .....	116
5.5 References .....	119

*Chapter 6: Chromatographic Investigation of Block*

*Copolymers via Hyphenated Techniques.....121*

6.1 Introduction .....	122
6.2 Experimental .....	123
6.2.1 Synthesis of block copolymers .....	123
6.2.2 Analysis of block copolymers .....	123
6.2.2.1 Liquid chromatography under critical conditions: The first separation step .....	123
6.2.2.2 Size-exclusion chromatography (SEC): The second separation step .....	124
6.2.2.3 On-line two-dimensional chromatography .....	124
6.2.2.4 Analytical software programs .....	125
6.3 Results and Discussion .....	126
6.3.1 Critical conditions of polystyrene and poly(methyl methacrylate) .....	126
6.3.2 Chromatographic analysis of RAFT mediated block copolymers prepared in homogeneous media .....	129
6.3.2.1 LC- CC .....	129
6.3.2.2 Two-dimensional chromatography .....	131
6.3.3 Online 2-D chromatography analysis of RAFT mediated block copolymers prepared in heterogeneous media .....	135
6.3.3.1 PS-b-PMMA copolymers .....	135
6.3.3.2 PMMA-b-PS copolymers .....	138
6.4 Conclusions .....	141
6.5 References .....	142

*Chapter 7: Conclusions and Recommendations .....143*

*Indexes and lists*

---

7.1 Conclusions to the study ..... 144  
7.2 Recommendations for future investigation..... 147

*Acknowledgements*.....148

## List of Figures

Figure 2.1 Guidelines for the selection of RAFT agents for various polymerizations. For Z, addition rates decrease and fragmentation increases from left to right. For R, fragmentation rates decrease from left to right. ....	21
Figure 2.2 The three regions involved in a conventional batch emulsion polymerization and their kinetics. (Adapted from Qui <i>et al</i> <sup>50</sup> ) .....	27
Figure 2.3 The possible fates of exited free radicals. ....	29
Figure 2.4 The preparation steps involved in creating a miniemulsion latex. (Adapted from Antoniette and Landfester. <sup>61</sup> ) .....	32
Figure 2.5 A schematic representation of the different chromatographic modes found in liquid chromatography brought about by change in the eluent composition or analysis temperature. (Kind courtesy of Deutsches Kunststoff- Institut (DKI)) .....	36
Figure 2.6 Schematic representation of a typical online 2D-chromatography system. (With kind courtesy of DKI). The first dimension represents separation with regard to chemical composition, while the second dimension involves separation with regard to hydrodynamic volume.....	38
Figure 4.1 Chemical structures of RAFT agents 4-cyano-4-((thiobenzoyl)sulfonyl)pentanoic acid (cyanovaleric acid dithiobenzoate) (CVADTB) (1) and S-4-cyanopentanoic acid-S'-benzyltrithiocarbonate (CVATTB) (2).....	52
Figure 4.2 A comparison of the first-order kinetics of the polystyrene polymerizations using the two different RAFT agents synthesized in this study. See Table 4.2.....	55
Figure 4.3 A comparison of the first-order kinetics of the poly(methyl methacrylate) polymerizations using the two different RAFT agents synthesized in this study (See Table 4.2 for details). ....	57
Figure 4.4 The molecular weight and polydispersity index of the polystyrene polymerizations as a function of conversion. The dashed (Sty06, CVADTB) and	

*Indexes and lists*

---

solid (Sty08, CVATTB) lines are the theoretically derived molecular weights for the respective data sets.....	58
Figure 4.5 Size-exclusion chromatograms of two of the polystyrene polymerizations as a function of increasing conversion. See Table 4.2. Sty06 (CVADTB) exhibits a high molecular weight shoulder at higher conversions; a phenomenon that is absent in Sty08 (CVATTB). .....	59
Figure 4.6 The molecular weight and polydispersity index of the poly(methyl methacrylate) polymerizations as a function of conversion. The dashed (MMA05) and solid (MMA07) lines are the theoretically derived molecular weights. ....	60
Figure 4.7 Size-exclusion chromatograms of two of the poly(methyl methacrylate) polymerizations as a function of increasing conversion (See Table 4.2). .....	61
Figure 4.8 UV-RI overlays of the final styrene polymers end-capped with the respective RAFT agents (See Table 4.2). The UV determinations for both reactions were done at a wavelength of 320nm.....	63
Figure 4.9 UV-RI overlays of the final poly(methyl methacrylate) polymers end-capped with the respective RAFT agents (See Table 4.2). The UV determinations for both reactions were done at a wavelength of 320nm.....	63
Figure 4.10 A: Size-exclusion chromatograms of the block formation of Sty06 mediated by dithiobenzoate CVADTB extended with PMMA via shot addition of monomer. See Table 4.3 for experimental details. B: The UV-RI response overlays of the final sample of the block copolymerization reaction of the same polymer in A. The dotted line represents UV absorbance at 254nm, while the dashed line represents UV absorbance at 320nm. ....	67
Figure 4.11 A: Size-exclusion chromatograms of the block formation of Sty07 mediated by the trithiocarbonate CVATTB chain extended with PMMA via shot addition of monomer. See Table 4.3 for experimental details. B: The UV-RI response overlays of the final sample in the block copolymerization reaction of the same polymer in A. The dotted line represents UV absorbance at 254nm; while the dashed line represents UV absorbance at 320nm. ....	68

*Indexes and lists*

- 
- Figure 4.12 Size-exclusion chromatograms of the block formation of Sty06 mediated by the CVADTB extended with PMMA via a monomer feed system (b). See Table 4.3 for experimental details. The UV-response overlays of the block copolymer are presented: the dotted line represents UV absorbance at 254nm, while the dashed line represents UV absorbance at 320nm. The RI response of the starting block material (a) is also included. .... 70
- Figure 4.13 Size-exclusion chromatograms of the block formation of Sty07 mediated by CVATTB extended with PMMA via a monomer feed system. See Table 4.3 for experimental details. The UV-response overlays of the block copolymer are presented: the dotted line represents UV absorbance at 254nm, while the dashed line represents UV absorbance at 320nm. The RI response of the starting block material (a) is also included. .... 71
- Figure 4.14 A: Size-exclusion chromatograms of the block formation of MMA05 mediated by CVADTB extended with PS via monomer shot addition. See Table 4.3 for experimental details. B: The UV-RI response overlays of the final sample in the block copolymerization reaction of the same polymer in A. The dotted line represents UV absorbance at 254nm, while the dashed line represents UV absorbance at 320nm. .... 72
- Figure 4.15 A: Size-exclusion chromatograms of the block formation of MMA07 mediated by CVATTB extended with PS via a monomer feed system. See Table 4.3 for experimental details. B: The UV-RI response overlays of the final sample in the block copolymerization reaction of the same polymer in A. The dotted line represents UV absorbance at 254nm; while the dashed line represents UV absorbance at 320nm. .... 73
- Figure 4.16 Size-exclusion chromatograms of the block formation of MMA05 mediated by CVADTB extended with PS via a monomer feed system (b). See Table 4.3 for experimental details. The UV-response overlays of the block copolymer are presented: the dotted line represents UV absorbance at 254nm; while the dashed line represents UV absorbance at 320nm. The RI response of the starting block material (a) is also included. .... 74

*Indexes and lists*


---

Figure 4.17 Size-exclusion chromatograms of the block formation of MMA07 mediated by CVATTB extended with PS via a monomer feed system (b). See Table 4.3 for experimental details. The UV-response overlays of the block copolymer are presented; the dotted line represents UV absorbance at 254nm; while the dashed line represents UV absorbance at 320nm. The RI response of the starting block material (a) is also included. ....	75
Figure 5.1 Chemical structures of RAFT agents 4-cyano-4-((thiobenzoyl) sulfonyl) pentanoic acid (cyanovaleric acid dithiobenzoate) (CVADTB) (1) and S-4-cyanopentanoic acid-S'-benzyltrithiocarbonate (CVATTB) (2).....	82
Figure 5.2 Semilogarithmic plots of monomer conversion versus reaction time. A: The styrene miniemulsion polymerization reactions of mSty08 and mSty14 at 75°C. B: The methyl methacrylate miniemulsion polymerizations reactions of mMMA01 and mMMA07 at 80°C. All reaction conditions were kept constant, apart from the RAFT agent type for the purpose of comparison .....	88
Figure 5.3 Evolution of Mn and PDI with conversion. A: The miniemulsion polymerization of styrene at 75°C in the presence of CVADTB (mSty08) and CVATTB (mSty14). B: The miniemulsion polymerization of methyl methacrylate at 80°C in the presence of CVADTB (mMMA01) and CVATTB (mMMA07). ....	90
Figure 5.4 Size-exclusion chromatograms of the molecular weight distribution of polystyrene synthesized in the presence of CVADTB (mPS08). The high molecular weight secondary distribution creating the increase in polydispersity values in Figure 5.3 A is encircled. ....	91
Figure 5.5 Size-exclusion chromatograms of the molecular weight distribution of polystyrene synthesized in the presence of CVATTB (mPS14). ....	92
Figure 5.6 Size-exclusion chromatograms of the molecular weight distribution of poly(methyl methacrylate) synthesized in the presence of CVATTB (mPMMA07). ....	93
Figure 5.7 Size-exclusion chromatograms of the molecular weight distribution of poly(methyl methacrylate) synthesized in the presence of CVADTB (mPMMA01). ....	94

*Indexes and lists*

- 
- Figure 5.8 UV-RI overlays of the styrene miniemulsion polymers. Illustration of the deviation of UV signals from the RI with increasing conversion. (- - -) UV signal at 320nm. (—) RI signal. (a) Results from mPS08 (CVADTB). (b) Results from mPS14 (CVATTB). ..... 95
- Figure 5.9 UV-RI overlays of the methyl methacrylate miniemulsion polymers. Illustration of the deviation of UV signals from the RI with increasing conversion. (- - -) UV signal at 320nm. (—) RI signal. (a) Results from mPMMA01 (CVADTB). (b) Results from mPMMA14 (CVATTB). ..... 96
- Figure 5.10 Normalized SEC chromatograms of the block formation from mPS08 mediated by CVADTB via the three different addition methods of MMA monomer. See Table 5.3 for experimental details. .... 100
- Figure 5.11 The UV-RI response overlay chromatograms of the block formation from mPS08 mediated by CVADTB via the three different addition methods of MMA monomer. The starting block as well as the final sample in the block copolymerization reaction is shown. The dotted line represents UV absorbance at 254nm, while the dashed line represents the UV absorbance at 320nm. The arrows indicate the presence of terminated high molecular weight chains. .... 101
- Figure 5.12 Normalized SEC chromatograms of the block formation from mPS14 mediated by CVATTB via the three different addition methods of MMA monomer. See Table 5.3 for experimental details. .... 102
- Figure 5.13 The UV-RI response overlay chromatograms of the block formation from mPS14 by CVATTB via the three different addition methods of MMA monomer. The starting block as well as the final sample in the block copolymerization reaction is shown. The dotted line represents UV absorbance at 254nm, while the dashed line represents UV absorbance at 320nm. .... 103
- Figure 5.14 Normalized SEC chromatograms of the block formation from mPMMA01 mediated by CVADTB via the three different addition methods of styrene monomer. See Table 5.3 for experimental details. .... 104
- Figure 5.15 The UV-RI response overlay chromatograms of the block formation from mPMMA01 mediated by CVADTB via the three different addition methods of styrene monomer. The starting block as well as the final sample in the block

*Indexes and lists*

---

copolymerization reaction is shown. The dotted line represents UV absorbance at 254nm, while the dashed line represents UV absorbance at 320nm. .... 105

Figure 5.16 Normalized SEC chromatograms of the block formation from mPMMA07 chains mediated by CVATTB) via the three different addition methods of styrene monomer. See Table 5.3 for experimental details..... 106

Figure 5.17 UV-RI response overlay chromatograms of the block formation from mPMMA07 chains mediated by CVATTB) via the three different addition methods of styrene monomer. The starting block as well as the final sample in the block copolymerization reaction is shown. The dotted line represents UV absorbance at 254nm, while the dashed line represents UV absorbance at 320nm. .... 107

Figure 5.18 TEM images of the PS-b-PMMA block copolymer latexes obtained from the chain extension of mPS08, mediated by CVADTB, indicated by A. The three addition methods are identified as B=shot addition, C=pre-swelling and D=feed addition. (Refer to Table 5.3 for latex compositions.)..... 111

Figure 5.19 TEM images for the PS-b-PMMA block copolymer latexes obtained from the chain extension of mPS14, mediated by CVATTB, indicated by A. The three addition methods are identified as B=shot addition, C=pre-swelling and D=feed addition. (Refer to Table 5.3 for latex compositions)..... 112

Figure 5.20 TEM images for the PMMA-b-PS block copolymer latexes obtained from the chain extension of mPMMA01, indicated by A. The three addition methods are identified as B=shot addition, C=pre-swelling and D=feed addition. (Refer to Table 5.3 for latex compositions)..... 114

Figure 5.21 TEM images for the PMMA-b-PS block copolymer latexes obtained from the chain extension of mPMMA07, indicated by A. The three addition methods are identified as B=shot addition, C=pre-swelling and D=feed addition. (Refer to Table 5.3 for latex compositions)..... 115

Figure 6.1 Critical conditions diagram of molar mass vs retention time for PS standards under solvent/non-solvent conditions. Stationary phase: C18 guard; Waters Symmetry C18 300 Å, 5µm average particle size, 4.6x250mm (ID); Supelco Nucleosil Si C18 100 Å, 5µm average particle size, 250x4.6mm (ID); mobile

*Indexes and lists*

phase: THF and ACN; separation temperature: 30°C. Critical conditions were found at 50.3THF/49.7 ACN. Standards ranged between 1480 to 63350 g/mol. .... 127

Figure 6.2 Critical conditions chromatograms for a range of PMMA standards at the critical point of PMMA. Stationary phase: Supelco Si 300 Å, 5µm average particle size, 250x4.6mm (ID); Supelco Nucleosil Si C18 100 Å, 5µm average particle size, 250x4.6mm (ID); mobile phase: MEK-cyclohexane 70.7:29.3(v/v%); separation temperature: 30°C..... 128

Figure 6.3 LC-CC elugrams of the PS-b-PMMA copolymers at the critical conditions for styrene. Stationary phase: C18 guard, Waters Symmetry C18 300 Å, Supelco Nucleosil Si C18 100 Å. Mobile phase: 50.3/49.7% (v/v %) THF/ACN. Analysis temp: 30°C. (A) Shot addition, (B) Feed addition ..... 130

Figure 6.4 LC-CC elugrams of the PMMA-b-PS copolymers at the critical conditions for PMMA. Stationary phase: Supelco Si 300 Å, Nucleosil Si 100 Å. Mobile phase: 70.7/29.3 (v/v %) MEK/Cyclohexane. Analysis temp: 30°C. (A) Shot addition, (B) Feed addition..... 131

Figure 6.5 Two-dimensional LC-CC versus SEC contour plots of the CVADTB-mediated PS-b-PMMA block copolymer prepared via shot addition. (a) Critical conditions for Sty, (b) critical conditions for PMMA. (The arrows indicate the respective critical points.)..... 132

Figure 6.6 Two-dimensional LC-CC versus SEC contour plots of the CVADTB-mediated PS-b-PMMA block copolymer prepared via feed addition. (a) Critical conditions for Sty, (b) critical conditions for PMMA. .... 133

Figure 6.7 Two-dimensional LC-CC versus SEC contour plots of the CVADTB-mediated PMMA-b-PS block copolymer prepared via shot addition. (a) Critical conditions for PMMA, (b) critical conditions for Sty. (The arrows indicate the respective critical points.)..... 134

Figure 6.8 Two-dimensional LC-CC versus SEC contour plots of the CVADTB-mediated PMMA-b-PS block copolymer prepared via feed addition. (a) Critical condition for PMMA, (b) critical conditions for Sty. .... 134

*Indexes and lists*

---

Figure 6.9 Two-dimensional LC-CC versus SEC contour plots of the CVADTB-mediated PS-b-PMMA miniemulsion block copolymer prepared via shot addition. (a) Critical conditions for PS, (b) critical conditions for PMMA. (The arrows indicate the respective critical points.) ..... 135

Figure 6.10 Two-dimensional LC-CC versus SEC contour plots of the CVADTB-mediated PS-b-PMMA miniemulsion block copolymer prepared via pre-swelling. (a) Critical conditions for PS, (b) critical conditions for PMMA..... 136

Figure 6.11 Two-dimensional LC-CC versus SEC contour plots of the CVADTB-mediated PS-b-PMMA miniemulsion block copolymer prepared via feed addition. (a) Critical conditions for PS, (b) critical conditions for PMMA..... 137

Figure 6.12 Two-dimensional LC-CC versus SEC contour plots of the CVATTB-mediated PS-b-PMMA miniemulsion block copolymer prepared via feed addition. (a) Critical conditions for PS, (b) critical conditions for PMMA..... 137

Figure 6.13 Two-dimensional LC-CC versus SEC contour plots of the CVADTB-mediated PMMA-b-PS miniemulsion block copolymer prepared via shot addition. (a) Critical conditions for PMMA, (b) critical conditions for PS. (The arrows indicate the respective critical points.) ..... 138

Figure 6.14 Two-dimensional LC-CC versus SEC contour plots of the CVADTB-mediated PMMA-b-PS miniemulsion block copolymer prepared via pre-swelling (a) Critical conditions for PMMA, (b) critical conditions for PS..... 139

Figure 6.15 Two-dimensional LC-CC versus SEC contour plots of the CVADTB-mediated PMMA-b-PS miniemulsion block copolymer prepared via feed addition. (a) Critical conditions for PMMA, (b) critical conditions for PS..... 139

Figure 6.16 Two-dimensional LC-CC versus SEC contour plots of the CVATTB-mediated PMMA-b-PS miniemulsion block copolymer prepared via feed addition. (a) Critical conditions for PMMA, (b) Critical conditions for PS..... 140

## List of Schemes

Scheme 2.1 Homolytic cleavage of the initiator and the chain initiating steps.....	9
Scheme 2.2 Chain propagation by the addition of monomer units.....	9
Scheme 2.3 Possibilities of monomer insertion linkages.....	9
Scheme 2.4 Termination of chains via combination.....	10
Scheme 2.5 Termination of chains via disproportionation .....	10
Scheme 2.6 Chain transfer to a non-radical species .....	11
Scheme 2.7 Inhibition .....	12
Scheme 2.8 Initiation .....	12
Scheme 2.9 Propagation.....	13
Scheme 2.10 Termination.....	13
Scheme 2.11 Chain transfer.....	14
Scheme 2.12 Reversible deactivation .....	17
Scheme 2.13 Reversible chain transfer .....	17
Scheme 2.14 Initiator decomposition and formation of oligomeric, propagating radicals.....	18
Scheme 2.15 Initial reaction of oligomeric radical with RAFT agent.....	19
Scheme 2.16 Reinitiation .....	19
Scheme 2.17 Establishment of equilibrium between active and dormant species in the RAFT process.....	19
Scheme 2.18 Termination to give dead polymer .....	20
Scheme 2.19 Sequential block copolymer synthesis via the RAFT process.....	23
Scheme 3.1 General RAFT agent structure.....	43

*Indexes and lists*

---

Scheme 3.2 The preparation of cyanovaleric acid dithiobenzoate .....	44
Scheme 3.3 The preparation of bis(benzylsulfanyl thiocarbonyl) disulfide .....	46
Scheme 3.4 The preparation of cyanovaleric acid benzyl trithiocarbonate .....	47

## List of Tables

Table 4.1: Experimental details of the RAFT mediated solution polymerizations of styrene (Sty) and methyl methacrylate (MMA) with RAFT agents CVADTB and CVATTB.....	53
Table 4.2: Final polymers produced by the RAFT mediated homogeneous polymerization of styrene and methyl methacrylate with RAFT agents CVADTB and CVATTB. The data is representative of the reactions run tabulated in Table 4.1 .....	55
Table 4.3: Experimental details of the block copolymerization of the RAFT end-capped PS and PMMA polymers.....	64
Table 5.1 Quantities of reagents and temperatures used for the RAFT-mediated polymerizations of styrene and methyl methacrylate in miniemulsion. The Sty polymerizations was carried out at 75°C, while the MMA polymerizations were done at 80°C. ....	83
Table 5.2: Final polymers produced by the RAFT-mediated miniemulsion polymerizations of styrene and methyl methacrylate. The data is representative of the reactions run as shown in Table 5.1. $f = 0$ .....	85
Table 5.3: Experimental details of the block copolymerization of the RAFT end-capped styrene and methyl methacrylate polymers from the seeded latexes. The PS-b-PMMA polymerizations were carried out at 80°C, while the PMMA-b-PS polymerizations were carried out at 75°C.....	99
Table 5.4 Particle size analysis of the seed latexes of styrene mediated by the two different RAFT agents and the subsequent block copolymers via each addition method. $Z_{\text{average}}$ (nm) is the mean diameter based upon the intensity of scattered light. (All entries refer to the polymers synthesized and discussed in Section 5.3.1, Table 5.2.) .....	109

*Indexes and lists*

---

Table 5.5 Particle size analysis of the seed latexes of styrene mediated by the two different RAFT agents and the subsequent block copolymers via each addition method.  
 $Z_{\text{average}}$  (nm) is the mean diameter based upon the intensity of scattered light. .... 110

Table 5.6 Particle size analysis of the seed latexes of PMMA mediated by the two different RAFT agents and the subsequent block copolymers via each addition method.  
 $Z_{\text{average}}$  (nm) is the mean diameter based upon the intensity of scattered light. .... 113

## *List of Acronyms*

2D-LC	Two-dimensional liquid chromatography
ACN	Acetonitrile
AIBN	2,2-Azobis(isobutyronitrile)
ATRP	Atom transfer radical polymerization
CCD	Chemical composition distribution
CDB	Cumyl dithiobenzoate
CMC	Critical micelle concentration
CP	Critical point
CSIRO	Commonwealth Scientific and Industrial Research Organization
CTAB	Cetyl trimethylammonium bromide
CVADTB	Cyanovaleric acid dithiobenzoate
CVATTB	Cyanovaleric acid trithiocarbonate
DDI	Distilled deionized water
DKI	Deutsches Kunststoff-Institut
DLS	Dynamic light scattering
DMSO	Dimethyl sulfoxide
DRI	Differential refractive index
EtOAc	Ethyl acetate
HPLC	High performance liquid chromatography
IR	Infra red
LAC	Liquid adsorption chromatography
LC	Liquid chromatography
LC-CC	Liquid chromatography at critical conditions
MADIX	Macromolecular design by interchange of xanthates
MEK	Methylethylketone
MMA	Methyl methacrylate
MMD	Molar mass distribution
MWD	Molecular weight distribution
NMR	Nuclear magnetic resonance

*Indexes and lists*

---

PDI	Polydispersity index
PMMA	Poly(methyl methacrylate)
PMMA-b-PS	Poly(methyl methacrylate)-block-polystyrene
PS	Polystyrene
PS-b-PMMA	Polystyrene-block-poly(methyl methacrylate)
RI	Refractive index
RAFT	Reversible addition fragmentation transfer
SDS	Sodium dodecyl sulfate
Sty	Styrene
SEC	Size exclusion chromatography
TEM	Transmission electron microscopy
THF	Tetrahydrofuran
UV	Ultra violet
UV/Vis	Ultra violet/Visible
VAc	Vinyl acetate

## *List of Symbols*

$\Delta H$	Difference in enthalpy
$\Delta S$	Difference in entropy
$f_I$	Initiator efficiency
$k_d$	Decomposition rate coefficient for the initiator
$k_p$	Propagation rate coefficient
$k_t$	Termination rate coefficient
$R_p$	The rate of polymerization
$(x_n)$	Number average degree of polymerization
$[I]_0$	Initial concentration of initiator
$[M]$	Monomer concentration
$[M]_0$	Initial concentration of monomer
$[RAFT]_0$	Initial concentration of RAFT agent
$\bar{M}_n$	Number average molar mass
$\bar{M}_n, \textit{theoretical}$	Calculated number average molar mass
$\bar{M}_n, \textit{SEC}$	Number average molar mass obtained from SEC analysis
$\bar{M}_w$	Weight average molar mass
$\bar{M}_w/\bar{M}_n$	Polydispersity index
$\bar{n}$	The average number of radicals per particle,
$N$	The number of latex particles per unit volume,
$N_A$	The Avogadro constant
$x$	Fractional Conversion
$Z_{\textit{average}}$	The mean diameter based upon the intensity of scattered light

# *Chapter 1: Introduction and Aims*

## **Abstract**

This introductory chapter comprise over a brief overview of the dissertation to allow the reader to understand the context of each chapter. In addition, the general aims of the research are presented here.

## 1.1 General Introduction

Polymerization involves the chemical combination of many small units known as monomers. Polymers vary in structure by being linear, branched or cross-linked in three-dimensional networks, and some have less common shapes resembling combs, stars or ladders. Homopolymers consist of only one type of repeating unit, whereas copolymers are made up of two or more different monomer units that can be arranged in either random or alternating sequences. It is well known that the physicochemical properties and biological behaviour of polymeric systems depend on the microstructural characteristics of their macromolecular chains that are constructed during the polymerization process by any of the established mechanisms of reaction.<sup>1</sup> A particular polymerization method, mechanism and process will yield a polymer with molecular architecture and set of physical properties that differ from those obtained by another polymerization method, mechanism and process.

Polymer formation involves either chain or step reactions. In chain polymerization, once a chain is initiated, monomer molecules add in rapid succession to the reactive end group of the growing chain until it terminates and become unreactive. The most common mechanisms of chain polymerization are anionic, cationic and radical. Of the three, free radical polymerization dominates in the commercial industry; it has been widely used to produce synthetic materials. Conventional free radical polymerization has however been enhanced by the discovery of methods or techniques allowing living radical polymerization. In recent years, the focus of polymer chemistry has moved away from the bulk synthesis of high molecular weight materials to now targeting the synthesis of specialty materials via the introduction of specific functionalities of polymer backbones or chain ends. Among the various polymerization processes that have been reported to yield such products, living radical polymerization appears to be one of the most promising for high scale applications.<sup>2</sup> The synthesis of functional polymers with predictable molecular weight and narrow molecular weight distribution can easily be achieved under conditions similar to those of free radical polymerization.<sup>3,4</sup>

The reversible addition-fragmentation chain-transfer (RAFT)<sup>5,6</sup> process, in particular, allows the preparation of complex macromolecular architectures. This technique can be applied to most monomers that can be polymerized by free radical polymerization and it does not require stringent reaction conditions.<sup>7-9</sup> The use of the RAFT process in emulsion is important commercially as it combines its own desirable features with those of emulsions.<sup>10,11</sup> The emulsion system offers certain

## Chapter One: Introduction and Aims

---

advantages over most other polymerization systems, which include higher polymerization rates, higher conversion of monomer, great heat dissipation and low solvent content. The recent rapid increase in the use of polymeric dispersions in industry is due to environmental concerns and regulations to substitute solvent-based systems with water borne products, as well as to the fact that polymeric dispersions have unique properties that meet a wide range of market needs.

Through the utilization and combination of the aforementioned processes, fascinating complex macromolecules can be produced. Prior to determining the applications of the resulting novel polymeric materials, the materials must be characterized. Hence the investigation and development of suitable characterization techniques are required. Liquid chromatography (LC) has proven to be a powerful tool for the molecular characterization of polymers that often have multiple variations of distribution.<sup>12-15</sup>

### 1.2 Aims

1. To synthesize two inherently different RAFT agents, 4-cyano-4-((thiobenzoyl)sulfonyl)pentanoic acid (cyanovaleric acid dithiobenzoate) and S-4-cyanopentanoic acid-S'-benzyltrithiocarbonate.
2. To apply the RAFT reagents in the "living" free radical polymerization of styrene and methyl methacrylate via the RAFT process in both homogeneous and heterogeneous media.
3. To carry out block copolymerization by the addition of new monomer to the already existing RAFT end-capped chains in two polymerization sequences, polystyrene-*block*-poly (methyl methacrylate) (PS-*b*-PMMA) and poly(methyl methacrylate)-*block*-polystyrene (PMMA-*b*-PS).
4. To conduct chromatographic analysis on the Sty/PMMA block copolymers via liquid chromatography at critical conditions (LC-CC), and via its online coupling with size-exclusion chromatography (SEC).

## *Chapter One: Introduction and Aims*

---

### **1.3 Thesis Layout**

#### **Chapter 1- Introduction and aims**

A brief general introduction to concepts relevant to the current study and the aims and outline of the thesis are presented.

#### **Chapter 2- Historical and theoretical background**

This chapter entails a concise discussion of the historical background and provides theoretical background to the processes and analytical techniques utilized in this study.

#### **Chapter 3- RAFT agents “made easy”**

The synthetic routes used to prepare the RAFT agents implemented in this study are described. A facile approach to preparing trithiocarbonates was successfully applied to produce a RAFT agent featuring an innovative stabilizing and leaving group combination.

#### **Chapter 4- The living character of CVADTB and CVATTB in homogeneous polymerization**

The mediation behaviour of two RAFT agents, cyanovaleric acid dithiobenzoate and cyanovaleric acid benzyl trithiocarbonate, were investigated by using them in performing solution polymerizations of the model monomers styrene and methyl methacrylate at 80°C and 100°C respectively. Rate effects, the predictability of the molecular weights of the polymers, the polydispersities of the polymers and the ability of the RAFT agents to allow block copolymer formation were compared.

#### **Chapter 5- RAFT mediated miniemulsion polymerizations**

The mediation behaviour of the synthesized RAFT agents in heterogeneous media is presented. Results include the RAFT mediated miniemulsion polymerization of styrene and methyl methacrylate, respectively, followed by a second stage addition of a new monomer for block copolymer formation. The effect of using different types of monomer additions, namely shot, feed and pre-swelling additions was studied. Results of characterization using SEC, TEM and particle size analysis are included.

#### **Chapter 6- Chromatographic investigation of block copolymers via hyphenated techniques**

This chapter addresses the analysis of the block copolymers synthesized in Chapters 4 and 5 via liquid chromatography. Different chromatographic modes were used to investigate the differences

*Chapter One: Introduction and Aims*

---

in heterogeneity of the polymers due to the different approaches of second monomer addition in the sequential block copolymer syntheses.

**Chapter 7- Conclusions and Recommendations**

A summary of the main conclusions presented in preceding chapters and mention on recommendations for future research is included.

## 1.4 References

- (1) Brandrup, J.; Immergut, E. H.; Grulke, E. A. *Polymer Handbook*; John Wiley and Sons, Inc: New York, **1999**.
- (2) Matyjaszewski, K.; Davis, T. P. *Handbook of Radical Polymerization*; John Wiley and Sons, Inc: Hoboken, **2002**.
- (3) Moad, G.; Solomon, D. H. *The Chemistry of Free Radical Polymerization*, 1st Ed.; Elsevier Science Ltd: Oxford, **1995**.
- (4) Moad, G.; Solomon, D. H. *The Chemistry of Free Radical Polymerization*, 2nd Ed.; Elsevier Science Ltd: Oxford, **2006**.
- (5) Le, T. P.; Moad, G.; Rizzardo, E.; Thang, S. H.; In PCT. Int. Appl.; wo98/01478; **1998**
- (6) Chiefari, J.; Chong, Y. K. B.; Ercole, F.; Krstina, J.; Jeffery, J.; Le, T. P. T.; Mayadunne, R. T. A.; Meijs, G. F.; Moad, C. L.; Moad, G.; Rizzardo, E.; Thang, S. H. *Macromolecules* **1998**, *31*, 5559-5562.
- (7) Rizzardo, E.; Chen, M.; Chong, B. Y. K.; Moad, G.; Skidmore, M.; Thang, S. H. *Macromol Symp* **2007**, *2*, 104-116.
- (8) Moad, G.; Rizzardo, E.; Thang, S. H. *Aust J Chem* **2006**, *59*, 669-692.
- (9) Zard, S. Z. *Aust J Chem* **2006**, *59*, 663-668.
- (10) Save, M.; Guillaneuf, Y.; Gilbert, R. G. *Aust J Chem* **2006**, *59*, 693-711.
- (11) McLeary, J. B.; Klumperman, B. *Soft Matter* **2006**, *2*, 45-53.
- (12) Pasch, H.; Trathnigg, B. *HPLC of Polymers*; Springer: Berlin, **1997**.
- (13) Berek, D. *Prog Polym Sci* **2000**, *25*, 873-908.
- (14) Van der Horst, A.; Schoenmakers, P. J. *J Chromatogr A* **2003**, *1000*, 693-709.
- (15) Macko, T.; Hunkeler, D. *Adv Polym Sci* **2006**, *163*, 61-136.
- (16) Weber, W. G.; McLeary, J. B.; Sanderson, R. D. *Tetrahedron Lett* **2006**, *47*, 4771-4774.

## ***Chapter 2: Historical and Theoretical Background***

### **Abstract**

This chapter provides a concise overview of the theoretical aspects that pertain to the synthesis processes and analytical techniques utilized in this study. An introduction to free radical polymerization and the movement towards “living” radical polymerization, in specific the RAFT process, is presented. The basic framework of emulsion polymerization and its derivative, miniemulsions, is discussed. Finally, the use of liquid chromatography as a characterization technique for copolymers, in terms of molar mass and chemical composition, is described.

## **2.1. Radical Polymerization**

### **2.1.1 The nature of radical chain polymerization**

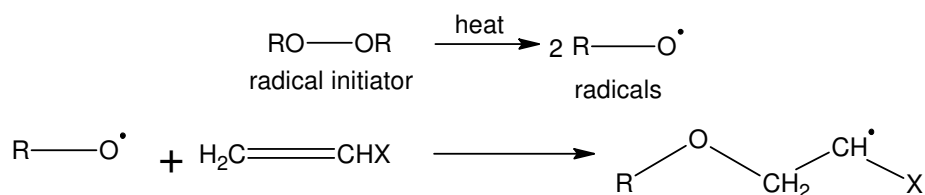
Chain polymerization entails the formation of polymer chains by the reaction of monomer molecules with reactive end-groups on the growing chains. Once produced, a radical, cationic or anionic active centre adds many monomer units in a chain reaction mechanism and the chains grow rapidly to a very large size. As a relatively inexpensive process, radical chain polymerization is one of the most widely used polymerization techniques.<sup>1</sup> It can be performed in both homogeneous and heterogeneous systems and has several advantages over other chain polymerization mechanisms that involve an anionic or cationic reactive center. In comparison to ionic or coordination polymerizations it is robust and can tolerate higher impurity levels of water and stabilizers and even traces of oxygen. In addition it accommodates a large monomer range. To facilitate polymerization, radical generation is necessary. As the active species, radicals continuously add monomer units (propagation) until the reaction is terminated through radical-radical reactions. The end result is dead polymer chains, which cannot be re-initiated. Initiation and termination reactions occur simultaneously throughout the polymerization process. Due to the short-lived propagating radicals, the chains do not grow at the same rate. The absence of control over the incorporation of monomer into the polymeric chain implies that many macromolecular properties, in particular the molecular weight and its distribution, chemical composition and chain architecture cannot be influenced sufficiently, which restricts the versatility of the free radical process.

### **2.1.2 The mechanism and radical kinetics**

During the initiation step of radical polymerization the initiator breaks homolytically to yield two radicals. The yield of primary radicals produced is usually not 100% and their conversion to initiating radicals depends on a variety of factors, as they may undergo rearrangement or fragmentation to give secondary radical species or interact with solvent or species other than the monomer. Ideally, each radical should add to an alkene monomer, converting it into an active radical species, which continuously add a new monomer subunit and marks the onset of chain propagation.

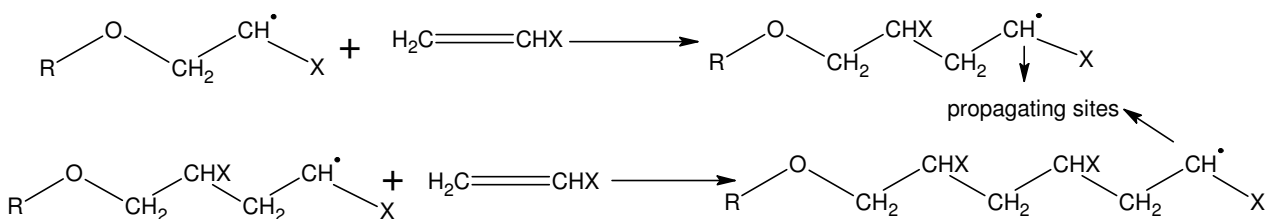
## Chapter Two: Historical and Theoretical Background

Chain-initiating steps:



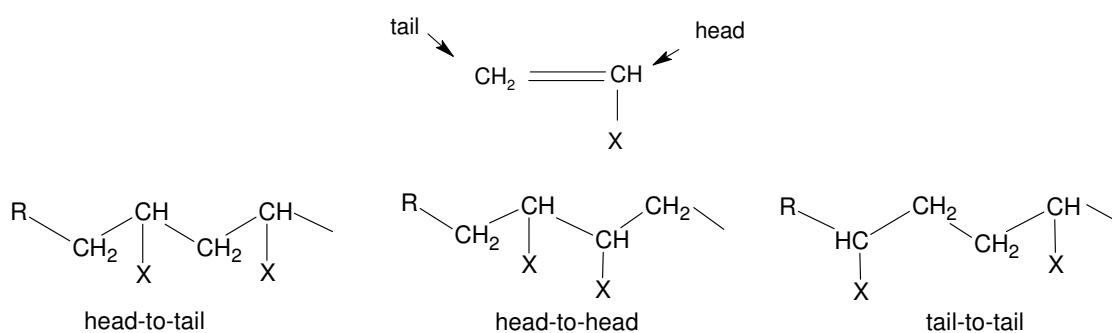
Scheme 2.1 Homolytic cleavage of the initiator and the chain initiating steps

Chain-propagating steps:



Scheme 2.2 Chain propagation by the addition of monomer units

Chain-growth polymerization of substituted ethylenes exhibits an overwhelmingly predominance for head-to-tail placement, where the head of one monomer is attached to the tail of another. This phenomenon is strictly dependent on the substituents present. The rates of addition of propagating radicals to monomer are affected by polar, resonance and steric factors resulting from the substituents bound to the reacting carbon-carbon double bond and the radical center.<sup>2</sup> Attack of monomer at the methylene carbon atom is less sterically hindered and yields a free radical site that is more stable because the substituent group, for example X in Scheme 2.3, stabilizes the free-radical site by steric hindrance and in many cases also by mesomeric stabilization.



Scheme 2.3 Possibilities of monomer insertion linkages

*Chapter Two: Historical and Theoretical Background*

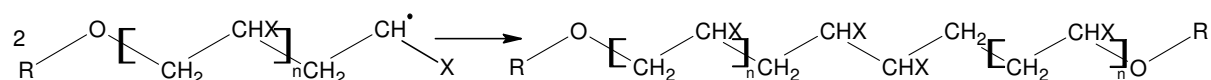
---

In general, propagation proceeds in a highly regioselective manner to yield a polymer chain consisting of head-to-tail linkages. An occasional head-to-head linkage can be expected; the proportion of which depends on the substituent group. If the substituent is small and offers little or no mesomeric stabilization then a high proportion of head-to-head linkages results.

The propagation process is repeated until the propagating sites are lost due to termination. Termination involves the bimolecular reaction between two radical species to produce dead polymer. Although primary radical termination, the reaction between a primary radical and a propagating species, may also contribute to the loss of propagating radicals, combination and disproportionation are the two most common reactions. The coupling of two radicals is far less energetic, forming head-to-head linkages in the polymer backbone and yielding chain ends consisting of initiator fragments. Disproportionation entails the abstraction of a hydrogen atom in the beta position to the radical center from one growing chain to another. In the event two polymer molecules are formed: one with a saturated chain end and one with an unsaturated chain end, both however have initiator-fragments at the other end.

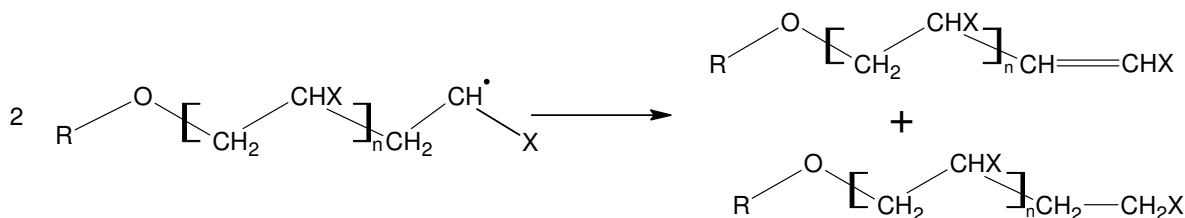
Methods of chain termination:

Chain combination:



Scheme 2.4 Termination of chains via combination

Disproportionation:



Scheme 2.5 Termination of chains via disproportionation

*Chapter Two: Historical and Theoretical Background*

The mode of termination is therefore important as it clearly affects the molecular architecture of the polymer formed and thereby some of its properties. Depending on the monomer and polymerization conditions, both termination reactions contribute, but to different extents. For example, in the polymerization of styrene, the chain radicals terminate principally via combination, whereas for methyl methacrylate, termination occurs predominantly by disproportionation at temperatures above 60°C.<sup>3</sup> Termination is perhaps the most intricate of the basic reactions in free-radical polymerization as it represents uninterrupted events of polymer radicals undergoing translational diffusion to come into relative proximity of one another, chain ends approaching one another by segmental diffusion, and finally the chemical reaction taking place. Supplementary reactions known to terminate the growth of a chain radical can be collectively termed as chain transfer reactions.

Chain transfer is achieved by the reaction of a propagating radical with a non-radical species to produce a dead polymer chain and a new radical normally capable of initiating a new chain.



Scheme 2.6 Chain transfer to a non-radical species

It can occur to all substances present in the polymerization system, therefore the hypothetical molecule AB (scheme 2.6) can be an additive, solvent, monomer, polymer, initiator or an impurity. The significance of these transfer reactions is dependent on the particular propagating radicals involved, the reaction medium and the polymerization conditions. In specific cases an additive can be employed to effectively reduce the molecular weight or to introduce designated end groups to the polymer chains. In the case of chain transfer to polymer the process can occur intermolecularly or intramolecularly. Intramolecular chain transfer is known as back-biting and results in the formation of short-chain branching, whereas intermolecular chain transfer leads to long-chain branching. Together the two types of reactions bring changes in the skeletal structure and molar mass distribution, which inevitably have major effects on the bulk polymer properties.<sup>4</sup>

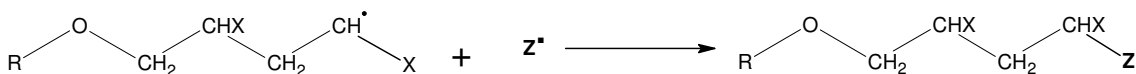
Inhibition and retardation are two more examples of the effect of chain transfer during free radical polymerization. The polymerization of monomers is suppressed due to the reaction of certain substances with the initiating and/or propagating radicals, converting them to either non-radical species or radicals of reactivity too low to continue propagation. Inhibitors tend to prevent

*Chapter Two: Historical and Theoretical Background*

---

polymerization from occurring until they are consumed, whereas retarders reduce the rate of polymerization.

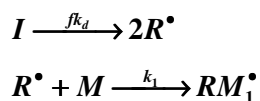
Inhibition:



Scheme 2.7 Inhibition

The kinetics of the sequence of events during polymerization can be summarized by the following primary processes:

**Initiation**



Scheme 2.8 Initiation

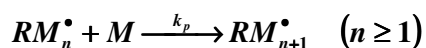
*I* denotes an initiator that decomposes with rate coefficient  $k_d$  to give primary free radicals  $R^{\bullet}$ , which add to one monomer *M* with rate coefficient  $k_1$  to give the new propagating radical  $RM_1^{\bullet}$ . The formation of primary free radicals proceeds at a rate that is much slower than the rate at which they react with monomer. Thus the first step of initiation is rate-determining and controls  $R_i$ , which is the rate of formation of chain radicals, which can be described by equation 2.1:

$$R_i = f \times \frac{d[R^{\bullet}]}{dt} = 2fk_d[I] \tag{2.1}$$

The initiator efficiency *f*, is the fraction of primary free radicals  $R^{\bullet}$  that are successful in initiating polymerization and its value is typically within the range of 0.3-0.8 due to side reactions.

Chapter Two: Historical and Theoretical Background

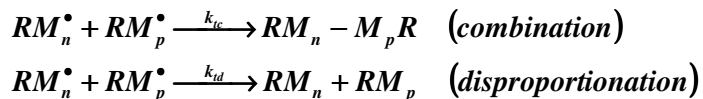
---

**Propagation**Scheme 2.9 Propagation

The rate at which monomer is consumed is known as the rate of polymerization,  $R_p$ . On the basis of the assumption that the rate coefficient for propagation,  $k_p$ , is independent of the length of the growing chain and that the amount of monomer consumed in the initiation stage is negligible compared to that consumed by the growing chains in propagation, the equation for  $R_p$  can be given by:

$$R_p = k_p [M^\bullet][M] \quad (2.2)$$

In order to obtain an expression for  $[M^\bullet]$ , the balance between initiation and termination of chain radicals must be considered.

**Termination**Scheme 2.10 Termination

Assuming that chain transfer reactions are followed by rapid reinitiation and chain transfer has no effect on  $[M^\bullet]$ , the rate of change of  $[M^\bullet]$  with time is given by

$$\frac{d[M^\bullet]}{dt} = R_i - 2k_t [M^\bullet]^2 \quad (2.3)$$

*Chapter Two: Historical and Theoretical Background*

---

$k_t$  is the overall rate coefficient for termination and is defined by:

$$k_t = k_{tc} + k_{td} \quad (2.4)$$

where  $k_{tc}$  is the rate coefficient for combination and  $k_{td}$  is the rate coefficient for disproportionation. During polymerization a stage is quickly attained where initiation and termination rates balance each other out. The net rate of change in  $[M\bullet]$  is then zero and the reaction is said to be under *steady-state conditions*, thereby implying that  $d[M\bullet]/dt = 0$  in equation 3. This yields the following equation for the steady-state concentration of chain radicals:

$$[M\bullet] = \left( \frac{R_i}{2k_t} \right)^{1/2} \quad (2.5)$$

If this equation is substituted into equation 2, a general expression for the rate of polymerization can be obtained.

$$R_p = k_p \left( \frac{R_i}{2k_t} \right)^{1/2} [M] \quad (2.6)$$

The substitution of equation 1 into equation 6, gives the following:

$$R_p = k_p \left( \frac{fk_d}{k_t} \right)^{1/2} [M][I]^{1/2} \quad (2.7)$$

**Chain transfer**

Scheme 2.11 Chain transfer

*Chapter Two: Historical and Theoretical Background*

---

Chain transfer affects the reactivity of radical centers, thereby affecting the molecular weight distribution in a polymerization. The Mayo-equation, equation 2.8, can be used for the reciprocal of  $x_n$ , which is the number average degree of polymerization:

$$\frac{1}{x_n} = \frac{1}{(x_n)_0} + C_M + C_I \frac{[I]}{[M]} + C_S \frac{[S]}{[M]} \quad (2.8)$$

in which

$$(x_n)_0 = \frac{2^{1/2} k_p [M]}{(1+q)(R_i k_t)^{1/2}} \quad (2.9)$$

and

$$C_M = \frac{k_{trM}}{k_p} \quad ; \quad C_I = \frac{k_{trI}}{k_p} \quad ; \quad C_S = \frac{k_{trS}}{k_p}$$

$(x_n)_0$  is the number-average degree of polymerization in the absence of chain transfer,  $q = k_{td}/k_t$  is the fraction of termination reactions that proceed by disproportionation ( $0 \leq q \leq 1$ ), and the quantities  $C_M$ ,  $C_I$  and  $C_S$  are known as the transfer constants for chain transfer to monomer, initiator and solvent, defined by their transfer coefficients respectively. In general, the transfer constant with respect to a chain transfer agent can be denoted as  $C_T$  where:

$$C_T = \frac{k_{trT}}{k_p} \quad (2.10)$$

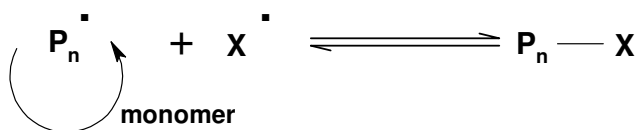
## **2.2. Living Radical Polymerization**

### **2.2.1 Overview**

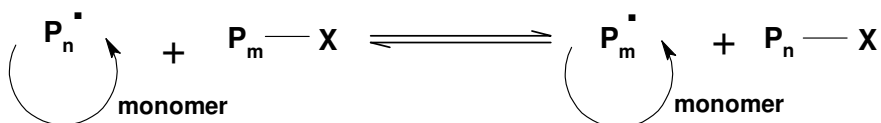
The use of synthetic polymers in commercial applications has created a continuously growing demand for new materials that challenge the research scope of the polymer industry. Polymers with complex, well-defined architectures and nano-structured morphologies are the order of the day and, due to the limitations of free radical polymerization with respect to degree of control over molecular weight, molecular weight distribution and architecture, a demand for “living” polymerization was created.

The road to living polymerization originated in 1956 through the first discovery and definition thereof by Michael Szwarc.<sup>5</sup> His article introduced the living anionic polymerization technique and is widely regarded as the birth of a number of subsequent techniques which enabled the preparation of novel structures. The basis of his theory involved the elimination of transfer and termination reactions from chain growth polymerizations; offering polymers of controlled composition, architecture and molecular weight distribution, providing routes to narrow dispersity end-functional polymers, high purity block copolymers, star polymers and other more complex architectures. Ionic, coordination or group transfer mechanisms are the traditional methods where all chains are initiated in the beginning of polymerization and continue until all monomer is consumed. Subsequent addition of fresh monomer leads to continued chain growth and in the case where the second monomer differs from first, for example, block copolymers are formed. The successes of these methods are largely dependent on the special polymerization conditions required which limits their practical use.

Conventional free radical polymerization can be distinguished from the other chain growth polymerization methods with regards to its versatility and ease of polymerization. The emergence of techniques implementing living character while retaining these advantages, has provided a new set of tools that allow the synthesis of polymers with pre-defined molecular weights based on monomer and initiator concentrations, narrow polydispersity indexes and end-group functionality, giving unique control over the process and the polymer product.

*Chapter Two: Historical and Theoretical Background*Scheme 2.12 Reversible deactivation

Living character is made possible by suppressing the tendency of radical-radical termination taking place in the system. This is achieved by adding reactants that react with the propagating radicals by reversible deactivation (Scheme 2.12) or reversible chain transfer (Scheme 2.13) to give dormant species. A fast equilibration between active and dormant chains ensures that all chains have equal probability to grow.

Scheme 2.13 Reversible chain transfer

The main techniques constituting living radical polymerization are Atom Transfer Radical Polymerization (ATRP),<sup>6</sup> Nitroxide Mediated Polymerization (NMP)<sup>7</sup> and Reversible-Addition Fragmentation Transfer (RAFT).<sup>7,8</sup> NMP was developed by the CSIRO group in the early 1980s and is currently well established for use in the synthesis of low polydispersity homopolymers and blocks copolymers of styrene and acrylates. Despite developments to broaden its applications, it is still very much restricted to a specific range of monomers. Although ATRP is more versatile, it requires unconventional initiating systems and compatibility of the process with the polymerization media is often problematic.<sup>7</sup> RAFT is the most recent method, yet arguably the most convenient and versatile.

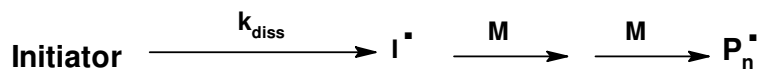
*Chapter Two: Historical and Theoretical Background***2.2.2 Reversible-addition fragmentation transfer (RAFT)****2.2.2.1 History of RAFT**

The use of reversible chain transfer in radical polymerizations giving characteristics of living polymerizations was first illustrated in 1995 by two research groups. Krstina *et al*<sup>9</sup> introduced the use of macromonomers and methacrylic monomers to give narrow polydispersity block copolymers, while Matyjaszewski *et al*<sup>10</sup> showed that controlled radical polymerization can be achieved by implementing alkyl iodides. The mechanism of the reversible chain transfer step can be divided into two classes: homolytic substitution or addition-fragmentation. Reversible addition-fragmentation transfer is the most well known process of its class and has become associated with radical polymerizations carried out in the presence of thiocarbonyl thio compounds.

The RAFT process was discovered in Australia by the CSIRO group and the first patent appeared in 1998.<sup>11,12</sup> Parallel studies were done by Charlot and coworkers at Rhodia in France, involving xanthate esters which they coined as MADIX (Macromolecular Design by Interchange of Xanthates).<sup>13</sup> Numerous applications of xanthate addition fragmentation chemistry in organic synthesis have subsequently been described in papers and reviews by the same group.<sup>14-18</sup> According to the review on RAFT by Moad *et al*<sup>19</sup> in 1995, the RAFT patent of Le *et al*<sup>11</sup> was the 9<sup>th</sup> most cited in the field of chemistry and related science in 2003 and the most cited of those published within the last ten years. The latest update in September 2007, indicates that the first paper on RAFT polymerization received more than 952 citations.<sup>12</sup>

**2.2.2.2 The RAFT mechanism**

The essential feature of the RAFT process is a sequence of addition-fragmentation equilibria. As in conventional free radical polymerization, initiation and radical-radical termination is ever present. At the onset stages of the polymerization, primary radicals  $[I \bullet]$  from the initiator decomposition reaction will either react with monomer units, giving oligomeric propagating chains of  $n$  degree of polymerization ( $P_n \bullet$ ), or with the S=C moiety of the RAFT agent.

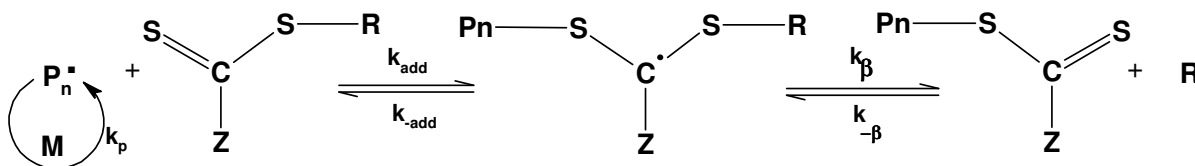
**Initiator decomposition and formation of oligomeric, propagating radicals:**

Scheme 2.14 Initiator decomposition and formation of oligomeric, propagating radicals

## Chapter Two: Historical and Theoretical Background

The addition reaction of the small carbon-centred radicals to the RAFT agent is in most cases rapid and not rate determining. The first rate-determining step is the reaction of the propagating radical ( $P_n^\bullet$ ) with the RAFT agent to form an intermediate radical. Fragmentation of the formed intermediate species can be either into the two original reactant species, or into a temporarily dormant polymeric RAFT agent and a radical ( $R^\bullet$ ) originating from the initial RAFT agent. The next step is the re-initiation of polymerization by the reaction of radical ( $R^\bullet$ ) with monomer to form a new propagating radical ( $P_m^\bullet$ ).

### Initial reaction of oligomeric radical with RAFT agent:



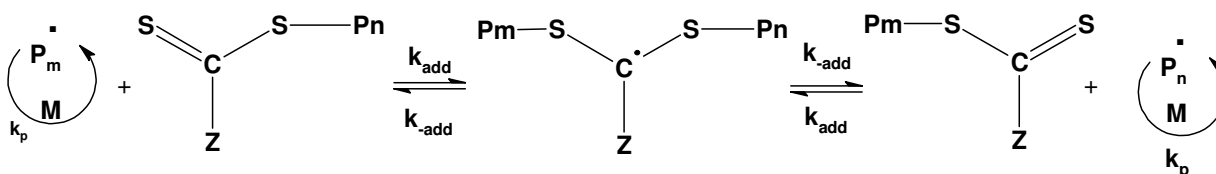
Scheme 2.15 Initial reaction of oligomeric radical with RAFT agent

### Reinitiation:



Scheme 2.16 Reinitiation

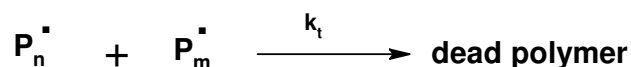
### Establishment of equilibrium between active and dormant species in the RAFT process:



Scheme 2.17 Establishment of equilibrium between active and dormant species in the RAFT process

*Chapter Two: Historical and Theoretical Background*

There is approximately equal probability for the intermediate radical to either fragment back into its starting species or into a dormant polymeric radical. The rapid equilibrium between the active propagating radicals ( $(P_n \bullet)$  and  $(P_m \bullet)$ ) and the dormant polymeric thiocarbonyl thio compounds, provides equal probability for all chains to grow and allows for the production of polymers with narrow molecular weight distributions. When the polymerization is complete or has ceased, most of chains retain the thiocarbonyl thio end group.

**Termination:**

Scheme 2.18 Termination to give dead polymer

It is important to realise that the equilibria shown take place between the entire populations of propagating radicals and dormant chains, rather than the pair-wise reaction between a specific radical and a specific dormant chain. To enable a stepwise growth of the polymer chains with low chain length polydispersities, the addition rate of the propagating polymeric radicals to the thiocarbonyl double bond must be fast compared to that of propagation, and termination must be suppressed by keeping the propagating radical concentration low.

**2.2.2.3 The choice of RAFT agents**

Several factors influence the efficiency of the RAFT agent and therefore the proper choice of transfer agent for a specific system to give optimal results is essential. For the RAFT agents to show good living polymerisation characteristics they should have a reactive C=S double bond (a high  $k_{add}$ ) (Scheme 2.15). There should be rapid fragmentation of the intermediate radicals (a high  $k_{\beta}$ , weak S-R bond), side reactions should be minimized (Scheme 2.15) and fragmentation should occur in favour of the products ( $k_{\beta} \geq k_{-add}$ ). The rate of fragmentation can be enhanced by the presence of electron-withdrawing groups and radical-stabilizing groups on the R-substituent. Steric factors, radical stability, and polar factors are important in determining the leaving group ability of R. The more stable, more electrophilic, more bulky radicals are better leaving groups. The leaving group ability decreases in the series where R is tertiary >>> secondary > primary. To ensure that fragmentation occurs in the desired direction, R should be a good homolytic leaving group, relative

*Chapter Two: Historical and Theoretical Background*

to  $P_n$ . The leaving ability of R should also be balanced with the ability of the expelled radical ( $R\bullet$ ) to re-initiate polymerization. In some cases it could be an excellent leaving group but a poor re-initiating group. If it has difficulty in adding to monomer then inhibition and retardation of polymerization might occur. Conversion of the transfer agent will be slow and a broad molar mass distribution will be obtained.

The activation group Z strongly influences the rate of addition to the thiocarbonyl double bond (C=S) bond. The trend in the relative effectiveness of RAFT agents with different Z groups is rationalized in terms of interaction of Z with the C=S bond to activate or deactivate that group towards free-radical addition. Addition is faster when Z = aryl, alkyl (dithioesters) or S-alkyl (trithiocarbonates), and lower when Z = O-alkyl (xanthates) or N, N-dialkyl (dithiocarbamates). Several papers report on the effects of R and Z on the effectiveness and transfer coefficients of RAFT agents. Figure 2.1<sup>19</sup> provides a summary of how to select the appropriate RAFT agent for particular monomers since the success of the transfer agent depends on monomer polymerized in conjunction with the properties of the leaving group R and stabilizing group Z.

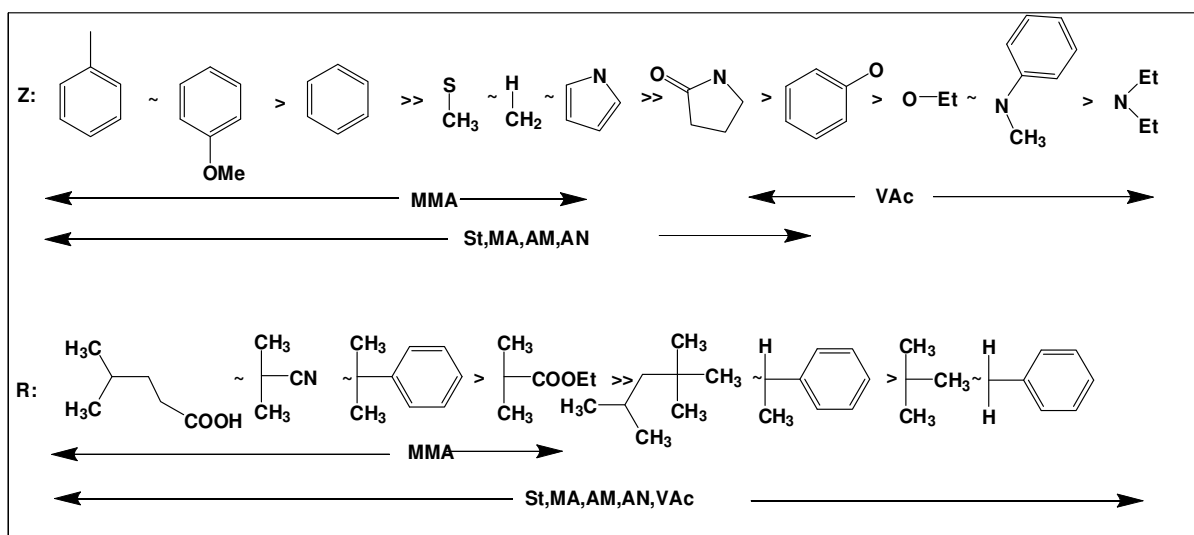


Figure 2.1 Guidelines for the selection of RAFT agents for various polymerizations. For Z, addition rates decrease and fragmentation increases from left to right. For R, fragmentation rates decrease from left to right.

Generally, transfer coefficients decrease in the series dithiobenzoates > trithiocarbonates  $\approx$  dithioalkanoates > dithiocarbonates (xanthates) and dithiocarbamates. Electron withdrawing substituents on Z can enhance the activity of RAFT agents to modify the above order.

## *Chapter Two: Historical and Theoretical Background*

---

### **2.2.2.4 Block copolymers via RAFT**

By definition block copolymers are polymer chains constructed from two or more segments of differing composition through covalent bonding. The simplest case is an AB diblock, which consist of two segments, but higher-order  $(AB)_n$  multi-blocks or more exotic types including radial or star-blocks and graft copolymers with block copolymer arms are also possible. Block copolymers are found in areas as diverse as biomaterials, drug delivery, nanocomposites and electronics. They feature in many applications as a result of the multifaceted role played by these species and can either serve as surfactants, thermoplastic elastomers, compatibilizers, viscosity modifiers, or dispersants, to stabilize colloidal suspensions, and other compounds. In general, there are four known processes by which block copolymers can be synthesized via the RAFT process:<sup>20</sup>

1. The sequential addition of monomers to a living chain end
2. Batch copolymerization of monomers with different activity ratios to form a gradient block copolymer
3. The use of a functional polymer prepared by another process as an initiator (NMP, ATRP) or transfer agent (RAFT)
4. The joining of pre-prepared blocks in a post-polymerization coupling reaction.

Traditionally block copolymers were synthesized via techniques which included anionic and cationic polymerization (classified as classical living techniques) as well as (non-living) end-group functionalization and Ziegler-Natta catalysts. Due to their limitations, the much preferred “living” free radical polymerization has been increasingly employed and all the methodologies (NMP, ATRP and RAFT) have been adapted for block copolymer synthesis. This has led to a large increase in the availability of block copolymers and “living” free radical polymerization is currently one of the most active fields of research in polymer chemistry.

The most direct method for synthesizing block copolymers involves the sequential addition of two monomers in a polymerization reaction. The living radical methods simplify matters because the product of polymerization is a dormant polymer that is stable enough to be isolated and purified before being used in another polymerization process. To enable successful block formation, the following important points should be considered:

1. It is essential to preserve the end functionality of the starting block and prevent excessive concentration of dead blocks. The polymerization of the first monomer should have ceased before

*Chapter Two: Historical and Theoretical Background*

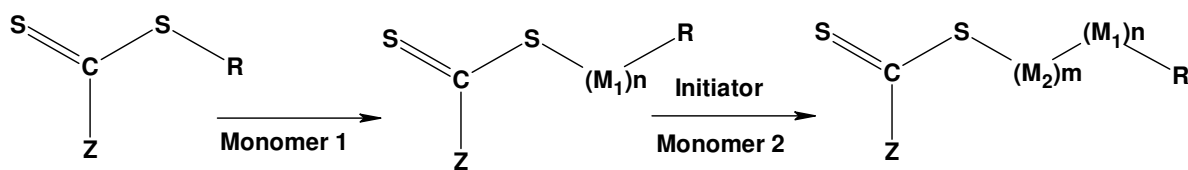
its total consumption to limit the termination of chains that will continue to occur in the absence of monomer.

2. The rate of cross-propagation is very important as in any sequential polymerization. Efficient cross-propagation is dependent on the rate constant of cross-addition ( $k_{a,b}$ ) and to the rate constant of propagation ( $k_{p,b}$ ) of the second monomer (monomer B) as well as the equilibrium constants ( $K_a$ ,  $K_b$ ) between active and dormant species for the two kinds of monomer units. Even if the reactivity ratios of monomers and the rate constants of propagation are known, but the equilibrium constants are not necessarily available in literature, further difficulties have to be overcome with the syntheses.

3. Even though polymerization orders can be reversed, it does not guarantee that the purities of the blocks obtained in the individual sequences will be similar.

4. Choice of starting block is important and it should be chosen on the basis of its relative quality as a leaving group.

With regards to synthesizing the first block followed by the second block, NMP and ATRP have limitations concerning their experimental conditions (temperature, monomer conversion, use of additives, etc.). Therefore synthesizing blocks via the RAFT process has gained popularity.



Scheme 2.19 Sequential block copolymer synthesis via the RAFT process

In the presence of a RAFT agent, the first block consists of a thiocarbonylthio moiety at the chain ends. This polymeric RAFT agent can react further upon the addition of fresh initiator and new monomer.

In RAFT-mediated polymerization, the order of construction of the blocks of a block copolymer can be very important.<sup>21</sup> The propagating radical of the first block should provide a better homolytic leaving group with respect to that of the second block. An efficient crossover requires that the rate

## *Chapter Two: Historical and Theoretical Background*

---

of transfer to the terminal dithioesters carried out by a given precursor be higher than the rate of transfer to the dithioesters generated at the end of the growing second block.<sup>12,22</sup> It is also important that the initiator concentration is much lower than that of the transfer agent, because the proportion of dead homopolymers is directly related to the concentration of the initiator consumed.

### **2.3. Homogeneous Systems**

Homogenous media are uncomplicated, and allow the study of the effects of different components such as monomer, solvent and initiator or chain transfer agent, without the problems related to a multiphase process. The homogeneous processes can be divided into bulk and solution polymerization. Bulk polymerization offers the simplest process with minimum contamination of the pure monomer. The characteristics associated with radical chain polymerization, such as its highly exothermic nature, high activation energies involved and tendency towards the gel effect, combine to make it difficult to control. Careful temperature control is required as heat dissipation becomes problematic. Strong and elaborate stirring equipment might be needed since the viscosity of the reaction system increases rapidly at relatively low conversion. Local hot spots may occur, resulting in discoloration of polymer product and a broadened molecular weight distribution due to chain transfer to polymer. The heat dissipation and viscosity problems can be circumvented by carrying out the polymerizations to low conversions, along with separation and recycling of the unreacted monomer. In the case of solution polymerization, the presence of a solvent overcomes many of the disadvantages of the bulk process. Transfer of the heat of polymerization, stirring and thermal control become much easier in comparison to a bulk system since the viscosity of the reaction mixture is decreased. However, the presence of solvent might present new difficulties. Unless chosen with appropriate consideration, chain transfer to solvent can become a problem and the purity of polymer may be affected if solvent removal is difficult.

### **2.4. Heterogeneous Systems**

An alternative to solution or bulk polymerization is the entire domain of dispersed-phase polymerization. In this class of processes, the liquid monomer is dispersed in a second, continuous phase. Heterogeneous systems are more complex than comparable homogeneous systems, because the chemical reactions are directly dependent on the ability of the reactants to physically interact, while materials are in a state of subdivision. Polymerizations carried out in multiphase systems include emulsion, precipitation, suspension and dispersion polymerization. The variety of systems

## *Chapter Two: Historical and Theoretical Background*

---

differ from each other in terms of the initial state of the polymerization mixture, the mechanism of particle formation, the size of the final polymer particles and the kinetics of polymerization.<sup>23,24</sup> Environmental and health concerns and regulations have created a rapid increase in the use of polymeric dispersions which substitute solvent-based systems with water borne products. If the continuous phase is water, the high thermal conductivity provides a very effective heat transfer medium. The high specific heat and large latent heat of vaporization provide a large safety margin and, in addition, water is plentiful, non-toxic and inexpensive. Importantly, the polymerization technique involved in any process can have a profound impact on factors such as overall kinetics and molecular microstructure such as molar mass, chemical composition distribution and branching. In radical polymerization in heterogeneous systems the partitioning of monomers, initiator, radicals, transfer agents and other species must be considered, especially in the case of “living” free radical polymerization, where they all play an important role. For the purpose of this study, radical polymerization in emulsion will be discussed.

### **2.5. The Basic Framework of Radical Emulsion Polymerization Mechanism and Kinetics**

Emulsion polymerization can be defined as a colloidal dispersion of polymer nanoparticles ( $10^1$ - $10^3$  nm in diameter) in a continuous aqueous medium. The main ingredients include one or more monomers, water and a free-radical initiator (most often water-soluble), with the options of an added surfactant and/or small pre-formed particles as seed.<sup>23,25</sup> It is a rather complex process because nucleation, growth and stabilization of polymer particles are controlled by the free radical polymerization mechanisms in combination with various colloidal phenomena.

The reaction system is characterized by the emulsified monomer droplets (1-10 $\mu$ m in diameter,  $10^{12}$ - $10^{14}$  dm<sup>-3</sup>) dispersed in the continuous aqueous phase with the aid of an oil-in-water surfactant at the onset of polymerization. Monomers must have minimum water solubility in relation to diffusion as well as radical entry. Emulsion polymerizations of styrene,<sup>26-28</sup> butadiene,<sup>29,30</sup> vinyl acetate,<sup>31-34</sup> acrylates and methacrylates,<sup>34-36</sup> acrylic acid<sup>37-39</sup> and vinyl chloride<sup>40</sup> are well documented. Monomer-swollen micelles (5-10nm in diameter,  $10^{19}$ - $10^{21}$  dm<sup>-3</sup>) will also exist in the reaction system provided the concentration of the surfactant is above its critical micelle concentration (cmc). Only a small fraction of the relatively hydrophobic monomer is present in the micelles or dissolved in the aqueous phase as most of the monomer molecules dwell in the giant

## *Chapter Two: Historical and Theoretical Background*

---

monomer reservoirs (i.e. monomer droplets). The polymerization is initiated by the addition of initiator; and typical water-soluble initiators are the potassium, sodium and ammonia salts of persulfate. During the progress of polymerization an extremely large oil-water interfacial area is generated as particle nuclei form and grow in size. An effective stabilizer such as ionic and non-ionic surfactants and/or protective colloid (e.g. hydroxyethyl cellulose and polyvinyl alcohol), which can be physically adsorbed or chemically incorporated onto the particle surface, is required to prevent the interactive latex particles from coagulating. Satisfactory colloidal stability can be achieved via the electrostatic stabilization mechanism,<sup>41-43</sup> the steric stabilization mechanism,<sup>44-46</sup> or both.<sup>47-49</sup>

The most striking feature of the emulsion process is the isolation of radicals among the discrete monomer-swollen polymer particles. In effect, the probability of bimolecular termination of free radicals is greatly reduced, resulting in a faster polymerization rate and higher molecular weight polymers. Although the nucleation period is quite short, generation of particle nuclei during the early stages of the polymerization plays a crucial role in determining the final latex particle size and particle size distribution, which in turn have a significant influence on the quality of latex products.

### **2.5.1 The different intervals in emulsion polymerization**

Emulsion polymerization can be divided into three intervals: the particle formation stage, termed Interval I, and the particle growth stages, Intervals II and III.

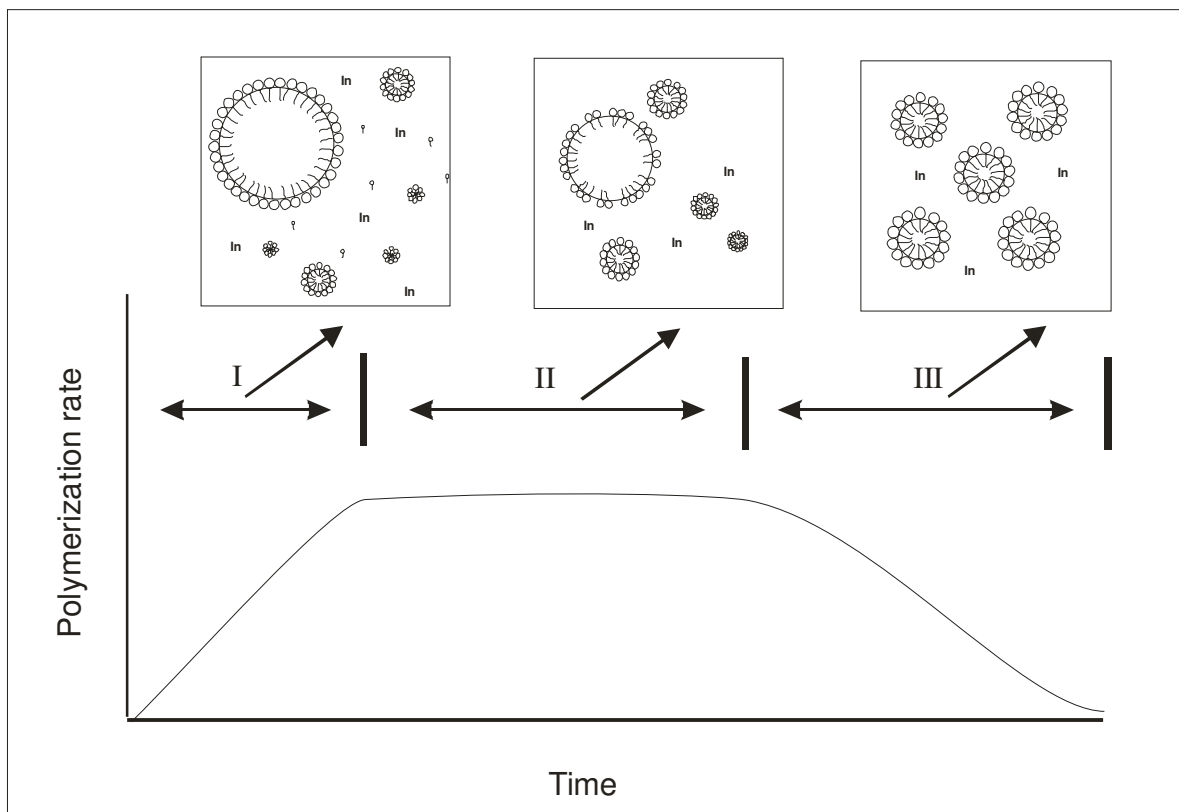
*Chapter Two: Historical and Theoretical Background*

Figure 2.2 The three regions involved in a conventional batch emulsion polymerization and their kinetics. (Adapted from Qui et al<sup>50</sup>)

### Interval I

The micelle nucleation model was originally postulated by Harkins<sup>51-53</sup> and further developed by Smith and Ewart.<sup>54-56</sup> Free radicals generated in the aqueous phase first polymerize with dissolved monomer molecules to yield oligomeric radicals with an increased hydrophobicity. At a certain critical chain length they show a strong tendency to enter the monomer-swollen micelles and continue to add to the residing monomer molecules. The monomer-swollen micelles are successfully transformed into particle nuclei, which continuously grow by acquiring the reactant species from neighboring monomer droplets and monomer-swollen micelles. The particle nucleation stage (interval I) ends immediately after the exhaustion of micelles.

Although the particle nucleation period is relatively short (up to about 10-20% monomer conversion), it controls the particle size and particle size distribution of latex products. Mechanisms other than micelle nucleation are responsible for the particle formation process when the surfactant concentration is below the cmc. Researches such as Priest<sup>57</sup> and Roe<sup>58</sup> have proposed the homogeneous nucleation mechanism for the formation of particle nuclei in the continuous aqueous phase. The oligomeric radicals originating from waterborne radicals become water-insoluble when a

## *Chapter Two: Historical and Theoretical Background*

---

critical chain length is reached; they coil up and form particle nuclei in the water phase. This is followed by formation of stable primary particles via the limited flocculation of the relatively unstable particle nuclei and adsorption of surfactant molecules on their particle surfaces. A third mechanism is possible when the droplet size is reduced to the submicron range and monomer droplets can compete with micelles in capturing free radicals. This concept will be discussed in the section describing the miniemulsion polymerization technique (Section 2.6.2).

### **Interval II**

After the particle nucleation process is completed the number of latex particles per unit volume of water remains relatively constant towards the end of polymerization. The propagation reaction of free radicals with monomer molecules takes place primarily in monomer-swollen particles. Monomer droplets serve as reservoirs to supply the growing particles with monomer and surfactant species. The majority of monomer is consumed in this particle growth stage; monomer conversion ranges from about 10-20 to 60%. Transport of monomer, free radicals and surfactant to the growing particles and partition of these reagents among the continuous aqueous phase, emulsified monomer droplets (monomer reservoir), monomer-swollen particles (primary reaction loci) and oil-water interface are the key factors that govern the particle growth stage. The particle growth stage (interval II) ends when monomer droplets disappear in the polymerization system.

### **Interval III**

In interval III, latex particles become monomer-starved and the concentration of monomer in the reaction loci continues to decrease toward the end of polymerization. The polymerization rate thus decreases during interval III. It may also however increase rapidly with increasing monomer conversion. This is attributed to the greatly reduced bimolecular termination reaction between two polymeric radicals within the very viscous particle provided that polymerization is carried out at a temperature below the glass transition temperature of the monomer-starved polymer solution. This phenomenon is termed the gel effect.<sup>59</sup>

### **2.5.2 Phase transfer events in emulsion polymerization**

The transport of free radicals between the continuous aqueous phase and particles determines the average number of free radicals per particle during polymerization. The radicals generated in the aqueous phase can be absorbed by the particles during interval II.

## Chapter Two: Historical and Theoretical Background

*Entry* is the process whereby radicals (oligomeric) move from the aqueous phase into the particle phase. For example, a dormant particle is activated in the propagation reaction immediately after the capture of one free radical from the aqueous phase. In addition to the main propagation reaction, one free radical may undergo a bimolecular termination reaction with another free radical if there are two or more free radicals in the particle. *Exit* is the process by which radicals desorb from the particles into the aqueous phase. It occurs through the chain transfer reaction of a polymeric radical to monomer or chain transfer agent (if present) inside the particle. The molecular diffusion of this free radical from the interior of the particle, across the particle-water interface, and then into the aqueous phase may occur. The desorbed radical may also have the chance to be absorbed again by another particle and reinitiate the propagation reaction therein. The process of exit is complicated by the simultaneous process of re-entry and a number of distinct fates that may befall an exited free radical as illustrated in Figure 2.3.

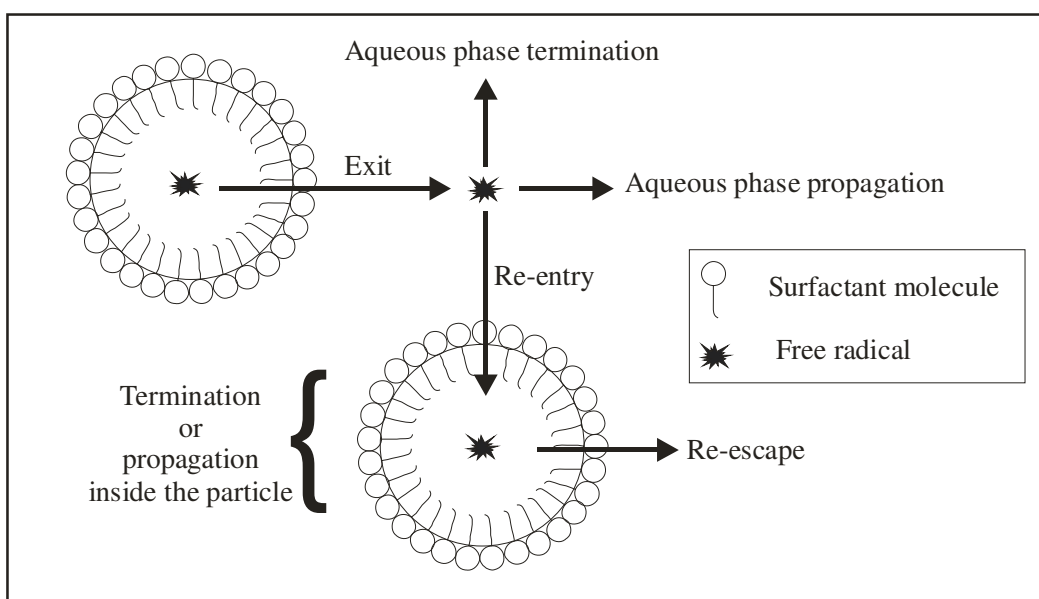


Figure 2.3 The possible fates of exited free radicals.

1. Absorption of radicals from the water phase into particles
2. Desorption of radicals from particles
3. Bimolecular termination of radicals in the particles.

*Chapter Two: Historical and Theoretical Background*

---

The abovementioned fates of the radicals determine the value of the average number of radicals per particle  $\bar{n}$ , which is a key parameter in determining both the rate and molar mass profiles during the course of polymerization. The rate of polymerization is given by equation 2.11

$$R_p = k_p [M] \bar{n} N / N_A \quad (2.11)$$

where  $k_p$  is the rate coefficient of propagation,  $[M]$  the monomer concentration in the particles,  $\bar{n}$  the average number of radicals per particle,  $N$  the number of latex particles per unit volume,  $R_p$  the rate of polymerization and  $N_A$  the Avogadro constant. Smith and Ewart<sup>55,56</sup> outlined three limiting cases:

**CASE 1:  $\bar{n} \ll 0.5$** 

This situation is the result of faster desorption than absorption of radicals by particles. Consequently, a particle contains one radical at a time at most; which is typical for monomers with high water solubility.

**CASE 2:  $\bar{n} = 0.5$** 

The rate of radical exit from the particles is insignificant. Termination is instantaneous when a second radical enters a particle already containing a radical; therefore particles have either zero or one propagating chain at any point in time. This system is referred to as zero one and is typical of styrene and butadiene emulsion polymerization. The time interval between entries varies in a random fashion. When a radical enters a particle, this particle immediately starts to polymerize at a steady-state rate. As soon as a second radical enters, this rate abruptly falls to zero. Cases 1 and 2 are known as the zero-one systems.

**CASE 3:  $\bar{n} \gg 0.5$** 

This situation occurs when bimolecular termination is no longer instantaneous on entry of a second radical in an active particle. The rate of termination within particles is small relative to the entry rate and the particle volume is relatively large. This system behaves like a bulk system; there are no effects of compartmentalization and more than one radical can exist per particle.

## **2.6. Miniemulsion Polymerization**

Miniemulsion polymerization can be regarded as a derivative of emulsion polymerization with the unique feature of avoiding the transport issues present in the conventional system. The concept aims at producing a latex which is a 1:1 copy of the original droplets, thus achieving direct control over the number of particles and avoiding complex nucleation steps. Droplet sizes are reduced to submicron size (50-500nm) using a strong shear force such as ultrasonication, making it possible for them to compete for radical entry and becoming the primary loci of polymerization. A miniemulsion polymerization system consists of monomer, water, surfactant, initiator and a hydrophobe and is simplified to two phases throughout the polymerization process by compartmentalization. Miniemulsion began with the publication of a single paper, originating from discussions between Ugelstad and Vanderhoff, speculating the possibility of nucleation and polymerization in very fine monomer droplets during emulsion polymerization.<sup>60</sup> Unlike emulsion polymerization, miniemulsions can be used to produce composite particles since additives that are not capable of aqueous phase transport, such as pigments and water insoluble materials, can be added to monomer prior to dispersion. Research on miniemulsion polymerization has been conducted for styrene, butyl acrylate, methyl methacrylate, vinyl acetate, vinyl 2-ethylhexanoate, as well as a number of copolymerization systems.<sup>25</sup>

### **2.6.1 Preparation of miniemulsion by ultrasound homogenization**

The process of miniemulsion formation requires mixing of all the components of the emulsion followed by a preshearing step in which the droplet size is mechanically reduced to provide an emulsion with large droplets and a wide droplet size distribution. Subsequently, ultrasonic homogenization is carried out via a fission-fusion process in such a manner that a narrow distribution of small droplet sizes is formed. After the application of the homogenization process, the system will relax to a homogenized state that is stabilized against particle growth, at which point the system can be polymerized. For a miniemulsion to be formed, a significant amount of energy is required to predisperse the system to a theoretical minimum particle size for each specific surfactant concentration. The precise time required to reach the minimum particle size needs to be predetermined for each experimental setup, as machine differences as well as other environmental variables play a role.

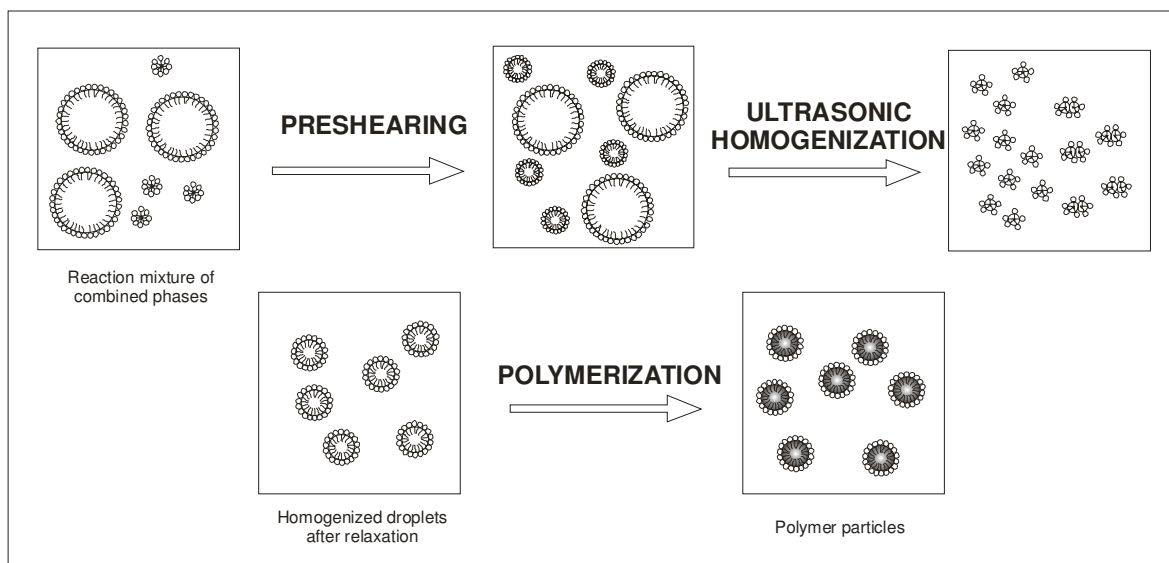
*Chapter Two: Historical and Theoretical Background*

Figure 2.4 The preparation steps involved in creating a miniemulsion latex. (Adapted from Antonetti and Landfester.<sup>61</sup>)

### 2.6.2 Mechanism and kinetics of miniemulsion polymerization

The reaction kinetics of miniemulsion systems are much simpler compared to conventional emulsion polymerization. The monomer diffusion to the reaction sites is of no kinetic importance since the monomer concentration is at a maximum at the loci. The important feature is that the reaction proceeds by polymerization of the monomer in the small droplets, so there is no true interval II.

#### 2.6.2.1 Mechanism of particle nucleation

Particle nucleation refers to all three mechanisms: micellar, homogeneous and droplet, all of which may compete and coexist in the same system, although one will often dominate. Hansen and Ugelstad<sup>62</sup> have presented probabilities for each of these mechanisms, in the presence of all three. In miniemulsion polymerizations, ideally every droplet is nucleated and transformed into a polymer particle, each behaving as an individual nanoreactor. This fundamental difference between micellar and homogeneous nucleation results in different kinetics from a conventional emulsion polymerization as studied for styrene by Bechthold *et al.*<sup>63</sup> A particle formation stage is observed at the onset of polymerization, accompanied by an increase in polymerization rate,  $R_p$ , and the average number of radicals per particle,  $\bar{n}$  (Interval I). After the rate reaches a maximum and  $\bar{n}$  reaches a value 0.5, this period is followed immediately by interval III, with a steadily decreasing rate and constant value of  $\bar{n} = 0.5$ . During this stage, polymerization follows first-order kinetics with respect

## *Chapter Two: Historical and Theoretical Background*

---

to monomer, as in bulk, solution and suspension polymerization. A final stage with increasing  $R_p$  and  $\bar{n}$  is finally observed, typical of the gel effect.

Micellar nucleation can be avoided as most miniemulsion polymerizations are below their cmc. Depending on the monomer, homogeneous nucleation is still possible in miniemulsions, but can be limited by adjusting kinetic parameters to favour the capture of oligoradicals before they reach critical size. Droplet nucleation undoubtedly takes place in conventional emulsion polymerization, but it is generally considered to be insignificant.

### **2.6.2.2 Stability of miniemulsions**

To ensure that the predominant particle formation mechanism is droplet nucleation, both high shear and a surfactant/costabilizer system is necessary. High shear is provided by a sonicator or a mechanical homogenizer, to break up the emulsion into submicron monomer droplets, while the surfactant is necessary to retard droplet coalescence caused by Brownian motion, creaming or settling. The costabilizer prevents Ostwald ripening by retarding monomer diffusion from the smaller to the larger droplets.

#### **2.6.2.2. (a) Effect of a surfactant**

Once the monomer droplet size is reduced by shear, the droplets will be able to compete successfully for aqueous phase radicals with any remaining micelles. In addition, a large increase in interfacial area caused by the reduction in droplet size will result, which will require a monolayer of surfactant to remain stable. The necessary surfactant will be provided by the break-up of existing surfactant micelles. Therefore, not only do the small droplets compete effectively for micelles, their presence causes the destruction of the micelles, leaving droplet nucleation as the dominant particle nucleation process.

#### **2.6.2.2. (b) Effect of a hydrophobe**

Enhanced stabilization arises from the addition of a 'cosurfactant' or an ultra-hydrophobe. The latter should be highly insoluble in the aqueous phase and highly soluble in the monomer droplets. Typical examples include hexadecanol and hexadecane. The function of the long-chain alcohol can be two-fold. The first is limiting the coalescence by forming a barrier at the surface of droplets by combination with the surfactant and/or second, preventing the diffusion of monomer molecules from small to large particles, namely Ostwald ripening. The ultra-hydrophobe behaves exclusively according to the second mechanism. The presence of a few percent of added polymer has been shown to enhance nucleation and produce a latex particle from every monomer droplet.<sup>64</sup> Therefore

## *Chapter Two: Historical and Theoretical Background*

---

the choice of a suitable hydrophobe is a key issue for a successful miniemulsion polymerization. Several researchers have used polymers, chain transfer agents and comonomers as substitutes.<sup>65-67</sup>

### **2.7. Characterization of Polymers with Complex Architectures by Liquid Chromatography**

#### **2.7.1 Overview**

Chromatography comprises a broad range of physical methods that facilitate the separation of complex mixtures with great precision by being able to purify almost any soluble or volatile substance if the correct adsorbent material, carrier fluid and operating conditions are employed. In any chemical or bio-processing industry, the need to separate and purify a product from a complex mixture is a necessary and important step in the production line. For a better understanding of tailor-made products and their structure in the polymer industry, specialised analytical methods are required. Liquid chromatography (LC) is a powerful tool for the molecular characterization of complex polymers that feature several simultaneous distributions in molecular characteristics such as molecular weight, chain architecture, chemical composition and functionality.<sup>68-70</sup>

By definition, LC covers all chromatographic techniques in which the mobile phase is a liquid<sup>71</sup> and can be broadly divided into three different modes: the size exclusion chromatography (SEC) mode, the interaction mode and the critical mode. SEC is most commonly applied for separation based on the size (hydrodynamic volume) of molecules in solution and the extent to which they are excluded from porous particles.<sup>71</sup> The molecular weight (MW) and molecular weight distribution (MWD) can be obtained using a calibration curve that transfers the logarithm of the molar mass to the retention time or volume, or using on-line molar mass detectors such as light scattering or viscometry. Its popularity in molecular characterization of polymers stems from the wide applicability, high speed and ease of use. It has however an intrinsic limitation in that it cannot distinguish between heterogeneity in composition, chain architecture, microstructure and functionality. For that purpose the second mode of analysis is the method of choice.

Interactive LC is based on molecular interactions between the polymer molecules and the mobile and stationary phases in the column.<sup>72</sup> To achieve the desired separation, the composition of the mobile phase can be varied. Gradient elution is often needed to elute a variety of polymer molecules

## *Chapter Two: Historical and Theoretical Background*

---

within a reasonable time, because the molecular interactions vary significantly with the size and structure of the polymer molecules.

The third chromatographic mode is LC at critical conditions (LC-CC).<sup>73,74</sup> Using this method it is possible to analyse specific sequences in segmented copolymers (such as single blocks in block copolymers) irrespective of the total polymer composition.<sup>75-80</sup> During this specific mode of isocratic LC, retention is independent of molar mass and solely influenced by the chemical composition or functionality of the molecules. These so-called critical conditions are hard to achieve and maintain, but they are extremely useful for separating polymer molecules according to the number of functional groups present.

### **2.7.2 Critical point of adsorption**

At the critical conditions of a selected homopolymer, the enthalpic interaction of the polymeric solutes is exactly compensated by the entropic size exclusion effect and the related chains elute from the LC column at the same retention volume, independently of molecular weight. At the critical point of adsorption the polymers are regarded as “chromatographically invisible”. This concept of “invisibility” was developed by Entelis *et al*<sup>81</sup> as a method for the determination of the functionality type distribution of telechelic oligomers and polymers. Soon after, this interesting feature was widely utilized in the characterization of block copolymers and their functionality.<sup>76,82,83</sup> The relation of the LC-CC mode to that of SEC and liquid adsorption chromatography (LAC) is usually illustrated by the schematic representation shown in Figure 2.5.

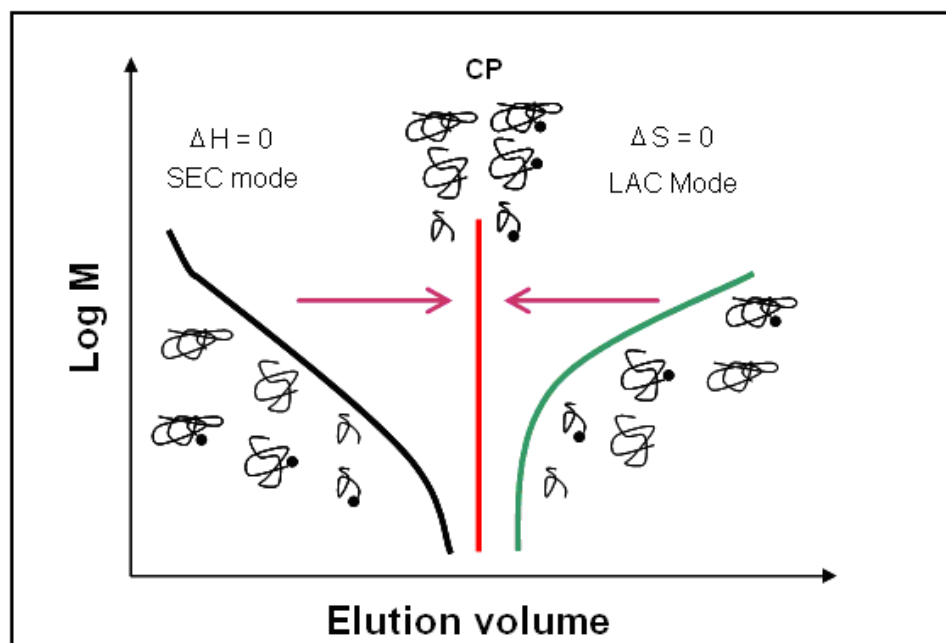


Figure 2.5 A schematic representation of the different chromatographic modes found in liquid chromatography brought about by change in the eluent composition or analysis temperature. (Kind courtesy of Deutsches Kunststoff- Institut (DKI))

The determination of the critical point (CP) for any polymer is the most time consuming and labour intensive process in critical chromatography and is done with a series of different standards. Different isocratic modes of solvent/non-solvent mixtures are used as eluent for the separation of the standards, which are dissolved in the same isocratic solvent mixtures. Despite the controversy as to the precision of the method, there is a consensus that LC-CC can estimate individual block length reasonably.<sup>84,85</sup>

### 2.7.3 Two-dimensional chromatography

A very efficient approach to analyzing the molecular heterogeneity of complex polymers is by combining different mechanisms of their chromatographic separations with each other or with a selective detector. As complex polymers feature simultaneous distributions (functionality type, chemical composition and/or molecular weight) that are mutually dependent, a two-dimensional separation is required to characterize each distribution independently. Two-dimensional liquid chromatography (2D-LC) systems have been used for many years to separate and characterize synthetic polymers, biomolecules and complex mixtures.<sup>86</sup> Erni and Frei<sup>87</sup> were the first to explore the on-line approach, which is currently referred to as “comprehensive” 2D-LC. Work done by several research groups has contributed greatly to the development of 2D-LC.<sup>82,88-91</sup> A typical experimental configuration of 2D-LC in polymer analysis has incorporated LC-CC as the first

## *Chapter Two: Historical and Theoretical Background*

---

dimension to separate in terms of the molecular characteristics (composition or functionality). The chemically homogeneous fractions are then subsequently transferred to SEC as the second dimension to separate according to molecular weight.<sup>76,88,89,92</sup> SEC has been a preferred choice for the second dimension separation since it is a universal technique to separate polymers according to molar mass. The SEC retention can be greatly affected by molecular characteristics other than molecular weight, but once homogeneity of the sample is achieved a more meaningful correlation with molecular weight can be made. Furthermore, the development of new types of columns, allows SEC separation to be carried out within minutes.<sup>79</sup>

### **2.7.3.1 “Comprehensive” 2D-LC setup**

In a comprehensive 2D-LC setup, a multiple port (8 as used in the current study) switching valve equipped with two loops is used in a symmetrical configuration. While one loop is being filled with the first dimension elute, the fraction that has previously been collected in the second loop is analysed in the second dimension. The collection time of each fraction in the first dimension separation has to be equal or longer than the analysis time in the second dimension separation. As a consequence, the analysis time in the second dimension and the loop volume together determine the (maximum) flow rate for the first dimension separation. The total analysis time is essentially the product of the analysis time of the second dimension separation and the number of fractions collected from the first dimension separation. To limit the total analysis time and to conserve the chromatographic separation (resolution) efficiency obtained in the first dimension, it is very important that the second dimension separation be kept fast. In order to obtain a truly comprehensive coupled separation, the flow rate of the first dimension separation cannot be very high. Figure 2.6 shows a typical “comprehensive” chromatographic system with its individual analytical components.

## Chapter Two: Historical and Theoretical Background

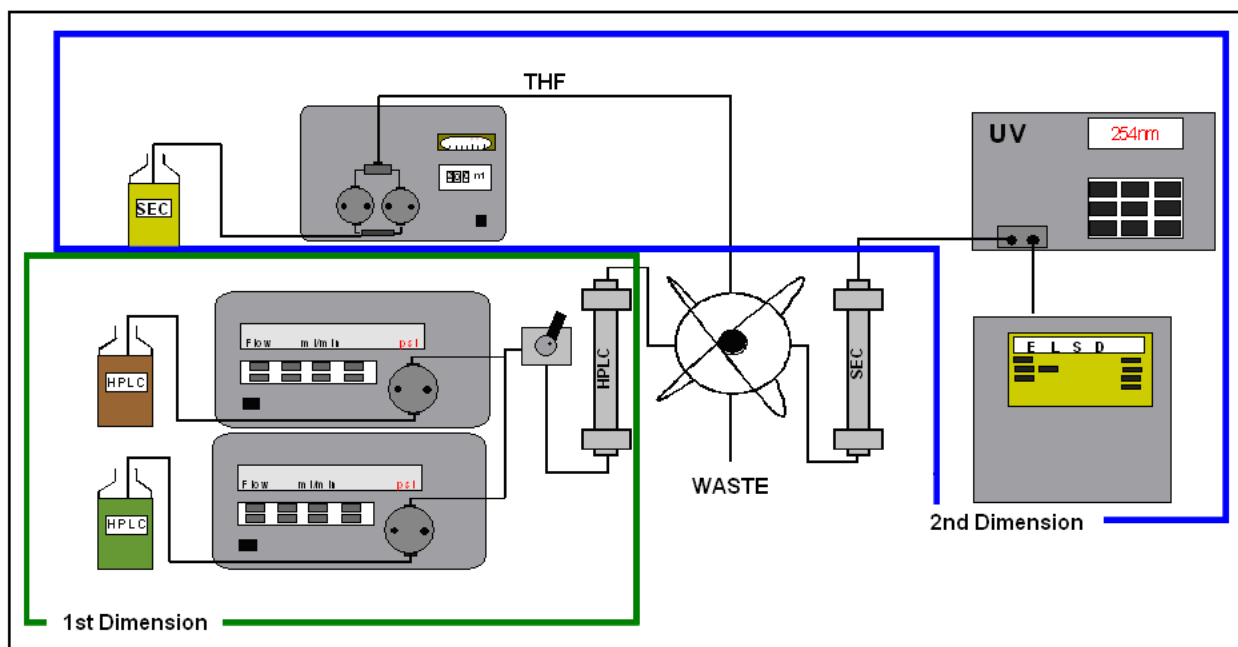


Figure 2.6 Schematic representation of a typical online 2D-chromatography system. (With kind courtesy of DKI). The first dimension represents separation with regard to chemical composition, while the second dimension involves separation with regard to hydrodynamic volume.

It illustrates how fractions collected from the first dimension, after separation with regard to chemical composition, are transferred to the second dimension to undergo SEC analysis for separation based on hydrodynamic volume. The increased demand for chromatographic materials that are able to achieve fast, reproducible and well-resolved separations of large quantities of structure analogues is a challenge. The chromatographic triangle represents the most important criteria in chromatography, namely resolution, speed and loadability.<sup>93</sup> Optimizing any of these parameters could come at the expense of others. A fast separation, for example, may result in bad resolution and loadability, and *vice versa*. Variable parameters are column dimensions (length, inner diameter), mobile phase (type and flow rate), column temperature (starting temp., temp. program) stationary phase (type, particle size, pore size, phase volume ratio).

In the present study, the use of comprehensive 2D-LC (specifically LC x SEC) to determine the chemical composition distribution (CCD) and molar mass distribution (MMD) of block copolymers of PS and PMMA synthesized via the RAFT process in solution and miniemulsion systems will be demonstrated.

*Chapter Two: Historical and Theory*

---

**2.8. References**

- (1) Otsu, T. *J Polym Sci Part A: Polym Chem* **2000**, *38*, 2121-2136.
- (2) Matyjaszewski, K.; Davis, T. P. *Handbook of Radical Polymerization*; John Wiley and Sons, Inc: Hoboken, **2002**; pp 846-847.
- (3) Lovell, P. A.; El-Aasser, M. S. *Emulsion polymerization and emulsion polymers*; John Wiley and Sons, Inc: Chichester, **1999**; p 11.
- (4) Lovell, P. A.; El-Aasser, M. S. *Emulsion polymerization and emulsion polymers*; John Wiley and Sons, Inc: Chichester, **1999**; pp 12-13.
- (5) Szwarc, M. *J Polym Sci Part A: Polym Chem* **1998**, *36*, 9-15.
- (6) Wang, J.-S.; Matyjaszewski, K. *Macromolecules* **1995**, *28*, 7572-7573.
- (7) Braunecker, W. A.; Matyjaszewski, K. *Prog Polym Sci* **2007**.
- (8) Moad, G.; Rizzardo, E.; Thang, S. H. *Aust J Chem* **2006**, *59*, 669-692.
- (9) Krstina, J.; Moad, G.; Rizzardo, E.; Winzor, C. L. *Macromolecules* **1995**, *28*, 5381-5386.
- (10) Matyjaszewski, K.; Gaynor, S.; Wang, J.-S. *Macromolecules* **1995**, *28*, 2093-2095.
- (11) Le, T. P.; Moad, G.; Rizzardo, E.; Thang, S. H.; In PCT. Int. Appl.; wo98/01478; **1998**
- (12) Chiefari, J.; Chong, Y. K. B.; Ercole, F.; Krstina, J.; Jeffery, J.; Le, T. P. T.; Mayadunne, R. T. A.; Meijs, G. F.; Moad, C. L.; Moad, G.; Rizzardo, E.; Thang, S. H. *Macromolecules* **1998**, *31*, 5559-5562.
- (13) Charmot, D.; Corpart, P.; Adam, H.; Zard, S. Z.; Biadatti, B. G. *Macromolecular Symposium* **2000**, *150*, 23-32.
- (14) Zard, S. Z. *Aust J Chem* **2006**, *59*, 663-668.
- (15) Perrier, S.; Takolpuckdee, P. *J Polym Sci Part A: Polym Chem* **2005**, *43*, 5347-5393.
- (16) Bernard, J.; Favier, A.; Zhang, L.; Nilasaroya, A.; Davis, T. P.; Barner-Kowollik, C.; Stenzel, M. H. *Macromolecules* **2005**, *38*, 5475-5484.
- (17) Smulders, W.; Monteiro, M. J. *Macromolecules* **2004**, *37*, 4474-4483.
- (18) Thang, S. H.; Chong, Y. K. B.; Mayadunne, R. T. A.; Moad, G.; Rizzardo, E. *Tetrahedron Lett* **1999**, *40*, 2435-2438.
- (19) Moad, G.; Rizzardo, E.; Thang, S. H. *Aust J Chem* **2005**, *58*, 379-410.
- (20) Moad, G.; Solomon, D. H. *The Chemistry of Free Radical Polymerization, Second fully revised edition*, 2nd Ed.; Elsevier Science Ltd: Oxford, **2006**; pp 541-543.
- (21) Chong, Y. K. B.; Krstina, J.; Le, T. P. T.; Moad, G.; Postma, A.; Rizzardo, E.; Thang, S. H. *Macromolecules* **2003**, *36*, 2256-2272.
- (22) Rizzardo, E.; Chiefari, J.; Chong, Y. K.; Ercole, F.; Krstina, J.; Jeffrey, J.; Mayadunne, R. T. A.; Meijs, G. F.; Moad, C.; Moad, G.; Thang, S. H. *Macromol Symp* **1999**, *143*, 291-307.
- (23) Gilbert, R. G. *Emulsion Polymerization: A Mechanistic Approach*; Academic Press: London, **1995**.
- (24) Arshady, R. *Colloid Polym Sci* **1992**, *270*, 717-732.
- (25) Lovell, P. A.; El-Aasser, M. S. *Emulsion polymerization and emulsion polymers*; John Wiley and Sons, Inc: Chichester, **1999**.
- (26) Friis, N.; Hamielec, A. E. *J Polym Sci Polym Chem Ed* **1973**, *11*, 3321-3325.
- (27) James, D. R.; Sundberg, D. C. *J Polym Sci Polym Chem Ed* **1980**, *18*, 903-911.
- (28) Miller, C. M.; Clay, P. A.; Gilbert, R. G.; El-Aasser, M. S. *J Polym Sci Part A: Polym Chem* **1997**, *35*, 989-1006.
- (29) Vandezande, G. A.; Rudin, A. *Two-Stage Emulsion Polymerization of Acrylonitrile and Butadiene*, 1st Ed.; Daniels, E. S., Ed.: Canada, **1992**; Vol. 462, pp 255-271.
- (30) Mahdavian, A.-R.; Abdollahi, M. *Polymer* **2004**, *45*, 3233-3239.
- (31) Vandezande, G. A.; Smith, O. W.; Basset, D. R. In *Emulsion Polymer Performance*; Union Carbide Corporation: Cary, North Carolina pp 1-46.

*Chapter Two: Historical and Theory*

---

- (32) Nomura, M.; Harada, M.; Nakagawara, K.; Eguchi, W.; Nagata, S. *J Chem Eng Japan* **1971**, *4*, 48-54.
- (33) Lange, D. M.; Poehlein, G. W.; Hayashi, S.; Komatsu, A.; Hirai, T. *J Polym Sci Part A: Polym Chem* **1991**, *29*, 785-792.
- (34) Kong, X. Z.; Pichot, C.; Guillot, J.; Cavaille, J. Y. *Polym Latexes* **1992**, *492*, 163-187.
- (35) De Wet-Roos, D.; Knoetze, J. H.; Cooray, B.; Sanderson, R. D. *J App Polym Sci* **1999**, *71*, 1347-1360.
- (36) Kong, X. Z.; Pichot, C.; Guillot, J. *Colloid Polym Sci* **1987**, *265*, 791-802.
- (37) Unzue, M. J.; Schoonbrood, H. A. S.; Asua, J. M.; Goñi, A. M.; Sherrington, D. C.; Stähler, K.; Goebel, K.-H.; Taler, K.; Sjöberg, M.; Holmberg, K. *J App Polym Sci* **1997**, *66*, 1803-1820.
- (38) Chu, F.; Graillat, C.; Guyot, A. *J App Polym Sci* **1998**, *70*, 2667-2677.
- (39) Ito, K.; Sabao, K.; Kawaguchi, H. *Macromolecular Symposium* **1995**, *91*, 65-72.
- (40) Vindevoghel, P.; Nagues, P.; Guyot, A. *J App Polym Sci* **1994**, *52*, 1879 - 1889.
- (41) Capek, I. *Adv Colloid Interface Sci* **2004**, *112*, 1-29.
- (42) Weiss, J.; McClements, D. J. *Langmuir* **2000**, *16*, 2145-2150.
- (43) Parker, A. P.; Reynolds, P. A.; Lewis, A. L.; Hughes, L. *Colloids Surf., A: Physicochem Eng Asp* **2005**, *268*, 162-174.
- (44) March, G. C.; Napper, D. H. *J Colloid Interface Sci* **1977**, *61*, 383-387.
- (45) Capek, I.; Chudej, J.; Janickova, S. *J Polym Sci Part A: Polym Chem* **2003**, *41*, 804-820.
- (46) Chambon, P.; Chemtob, A.; Cloutet, E.; Cramail, H.; Gibanel, S.; Gnanou, Y.; Heroguez, V.; Quemener, D.; Radhakrishnan, B. *Polym Int* **2006**, *55*, 1146-1154.
- (47) Thickett, S. C.; Gilbert, R. G. *Macromolecules* **2006**.
- (48) Save, M.; Manguian, M.; Chassenieux, C.; Charleux, B. *Macromolecules* **2004**, *38*, 280-289.
- (49) Vorwerk, L.; Gilbert, R. G. *Macromolecules* **2000**, *33*, 6693-6703.
- (50) Qiu, J.; Charleux, B.; Matyjaszewski, K. *Prog Polym Sci* **2001**, *26*, 2083.
- (51) Harkins, W. D. *J Chem Phys* **1945**, *13*, 381-382.
- (52) Harkins, W. D. *J Chem Phys* **1946**, *14*, 46-49.
- (53) Harkins, W. D. *J Am Chem Soc* **1947**, *69*, 1428-1441.
- (54) Smith, W. V.; Ewart, R. H. *J Chem Phys* **1946**, *16*, 592-599.
- (55) Smith, W. V. *J Am Chem Soc* **1949**, *71*, 4077-4082.
- (56) Smith, W. V. *J Am Chem Soc* **1948**, *70*, 3695-3702.
- (57) Priest, W. J. *J Phys Chem* **1952**, *56*, 1077-1083.
- (58) Roe, C. P. *Ind Eng Chem* **1968**, *60*, 20-33.
- (59) Russell, G. T.; Gilbert, R. G.; Napper, D. H. *Macromolecules* **1992**, *25*, 2459-2469.
- (60) Ugelstad, J.; El-Aasser, M. S.; Vanderhoff, J. W. *Polym Lett* **1973**, *11*, 503-513.
- (61) Antonietti, M.; Landfester, K. *Prog Polym Sci* **2002**, *27*, 689-757.
- (62) Hansen, F. K.; Ugelstad, J. *J Polym Sci Polym Chem Ed* **1978**, *16*, 1953-1979.
- (63) Bechthold, N.; Landfester, K. *Macromolecules* **2000**, *33*, 4682-4689.
- (64) Miller, C. M.; Sudol, E. D.; Silebi, C.; El-Aasser, M. S. *Macromolecules* **1995**, *28*, 2754-2764.
- (65) Aizpurua, I.; Amalvy, J. I.; Barandiaran, M. J. *Colloids Surf., A: Physicochem Eng Asp* **2000**, 59-66.
- (66) Quintero, C.; Mendon, S. K.; Smith, O. W.; Thames, S. F. *Polym Prepr* **2004**, *45*, 1110-1111.
- (67) Tiarks, F.; Landfester, K.; Antonietti, M. *Langmuir* **2001**, *17*, 908-918.
- (68) Fukuda, T. *J Polym Sci Part A: Polym Chem* **2004**, *42*, 4743-4755.
- (69) Park, I.; Park, S.; Cho, D.; Chang, T.; Kim, E.; Lee, K.; Kim, Y. J. *Macromolecules* **2003**, *36*, 8539-8543.
- (70) Han, X.; Fan, J.; He, J.; Xu, J.; Fan, D.; Yang, Y. *Macromolecules* **2007**, *40*, 5618-5624.

*Chapter Two: Historical and Theory*

---

- (71) Heftmann, E. *Chromatography Part A: Fundamentals and Techniques*, 5th Ed.; Elsevier: Amsterdam, **1992**; Vol. 51A.
- (72) Chang, T. *Adv Polym Sci* **2003**, *163*, 1-60.
- (73) Gorbunov, A. A.; Skvortsov, A. M. *Adv Colloid Interface Sci* **1995**, *62*, 31-108.
- (74) Macko, T.; Hunkeler, D. *Adv Polym Sci* **2006**, *163*, 61-136.
- (75) Gorbunov, A.; Trathnigg, B. *J Chromatogr A* **2002**, *955*, 9-17.
- (76) Pasch, H.; Trathnigg, B. *HPLC of Polymers*; Springer: Berlin, **1997**.
- (77) Pasch, H. *Adv Polym Sci* **2000**, *150*, 1-66.
- (78) Pasch, H. *Macromol Symp* **2002**, *178*, 25-37.
- (79) Pasch, H.; Kilz, P. *Macromol Rapid Comm* **2003**, *24*, 104-108.
- (80) Pasch, H. *Macromol Symp* **2001**, *174*, 403-412.
- (81) Entelis, S. G.; Evreinov, V. V.; Gorschkov, A. *Adv Polym Sci* **1986**, *76*, 129-175.
- (82) Pasch, H. *Adv Polym Sci* **1997**, *128*, 1-45.
- (83) Guttman, C. M.; Di Marzio, E. A.; Douglas, J. F. *Macromolecules* **1996**, *29*, 5723-5733.
- (84) Lee, W.; Cho, D.; Chang, T.; Hanley, K. J.; Lodge, T. P. *Macromolecules* **2001**, *34*, 2353-2358.
- (85) Lee, W.; Park, S.; Chang, T. *Anal Chem* **2001**, *73*, 3884-3889.
- (86) Murphy, R. E.; Schure, M. R.; Foley, J. P. *Anal Chem* **1998**, *70*, 4353-4360.
- (87) Erni, F.; Frei, R. W. *J Chromatogr* **1978**, *149*, 561.
- (88) Gerber, J.; Radke, W. *Polymer* **2005**, *46*, 9224-9229.
- (89) Adrian, J.; Esser, E.; Hellman, G.; Pasch, H. *Polymer* **2000**, *41*, 2439-2449.
- (90) Ikegami, T.; Hara, T.; Kimura, H.; Kobayashi, H.; Hosoya, K.; Cabrera, K.; Tanaka, N. *J Chromatogr A* **2006**, *1106*, 112-117.
- (91) Im, K.; Kim, Y.; Chang, T.; Lee, K.; Choi, N. *J Chromatogr A* **2006**, *1103*, 235-242.
- (92) Van der Horst, A.; Schoenmakers, P. J. *J Chromatogr A* **2003**, *1000*, 693-709.
- (93) Grynbaum, M. D.; Meyer, C.; Putzbach, K.; Rehbein, J.; Albert, K. *J Chromatogr A* **2006**.

## ***Chapter 3: RAFT Agents***

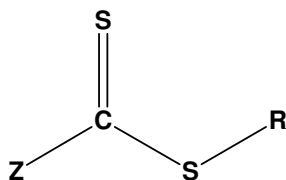
### ***“Made Easy”***

#### **Abstract**

The synthetic routes of the RAFT agents implemented in this study are presented. A novel approach to trithiocarbonates was successfully implemented to produce a RAFT agent showcasing an R-group with potentially excellent leaving capabilities. Purities of the final RAFT agents were checked via  $^1\text{H}$  and  $^{13}\text{C}$  NMR and characterization was done by UV analysis.

### 3.1 Introduction

The RAFT agents and their preparation discussed by Le *et al*<sup>1</sup> make up only the foundation of RAFT agent synthesis, as novel and improved reagents has become an important part of the RAFT process research.<sup>2-5</sup> Traditionally, the most important techniques commonly used for RAFT agent synthesis have included the use of Grignard synthesis<sup>6,7</sup>, transesterification<sup>8</sup> and nucleophilic addition.<sup>4,9,10</sup> The two RAFT agents implemented in this study are typical examples of how research ensures continued development and advancement.



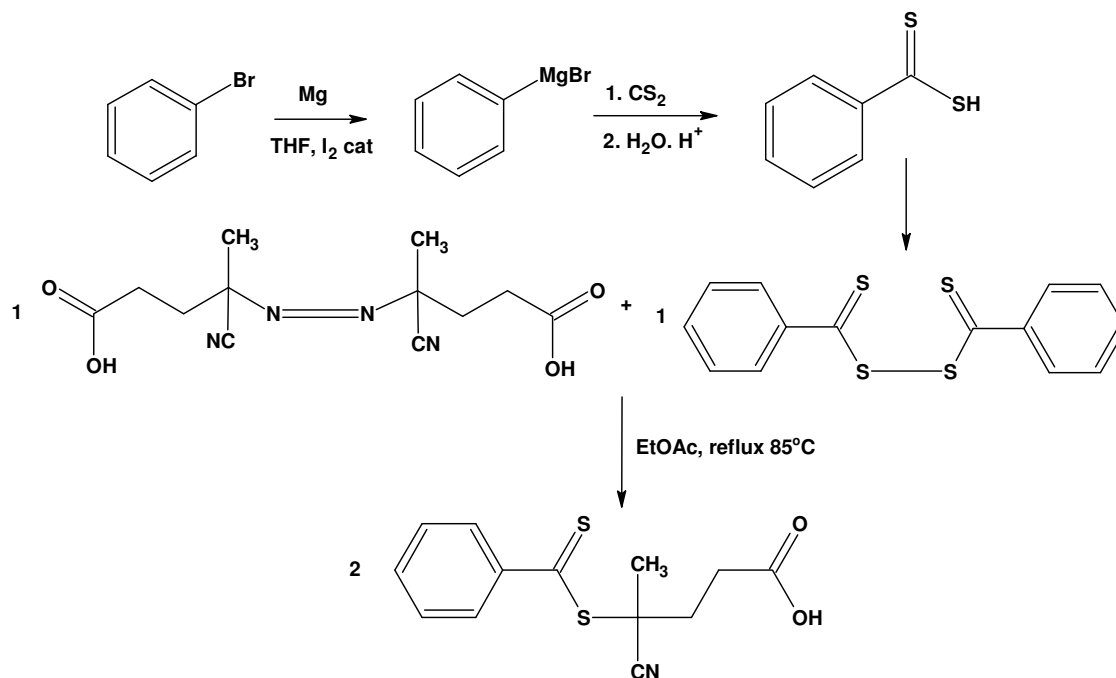
Scheme 3.1 General RAFT agent structure

The first reagent, 4-cyano-4-((thiobenzoyl)sulfonyl) pentanoic acid (cyanovaleric acid dithiobenzoate) (CVADTB), can be classified as a “traditional” RAFT agent. It is well documented<sup>1,11-13</sup> and used extensively as one of the first effective dithioesters that was available. The methodology of its preparation described in this work is not exclusive, but clearly suffers several drawbacks. Although the procedures are robust and reproducible, dithioesters prepared via Grignard synthesis are limited in terms of scale, product loss occurs due to the formation of unstable intermediates and it has the reputation for generating unpleasant odours in the process.

Trithiocarbonates have proven to be interesting RAFT agents to work with as they are capable of being monofunctional or difunctional.<sup>14,15</sup> Their syntheses require shorter reaction times, less stringent conditions and their purification is less complicated than dithiobenzoates. The second RAFT agent used in this study, represents the breaking of a new dawn in terms of RAFT agent synthesis. Recently, Weber *et al*<sup>16</sup> suggested a novel procedure for the synthesis of bis(thiocarbonyl)disulfides. The route entails an elimination mechanism rather than the more common oxidation by iodine systems to prepare disulfides. In effect, it opens the pathway to prepare RAFT agents with exciting leaving and stabilizing group combinations. The S-4-cyanopentanoic acid-S'-benzyltrithiocarbonate synthesized and used in this work is a typical example of how a bis(thiocarbonyl)disulfide can be utilized to produce an efficient trithiocarbonate RAFT agent of high purity and yield in an easy manner. This specific reagent plays a key role in this study, as its implementation in RAFT mediated polymerization has, to date, not been reported.

## 3.2 Experimental

### 3.2.1 Cyanovaleric acid dithiobenzoate



Scheme 3.2 The preparation of cyanovaleric acid dithiobenzoate

#### Materials

Bromobenzene 99% (Aldrich), carbon disulfide (CS<sub>2</sub>) 99.5% (Aldrich), diethyl ether 99.5% (Merck), dimethyl sulfoxide (DMSO) 99% (Merck), absolute ethanol 95% (Merck), ethyl acetate CP, heptane CP (ACE), HCl 32% (ACE), iodine 99% (Aldrich), magnesium 98% (Aldrich), pentane CP, THF distilled from LiAlH<sub>4</sub>, 4,4'-azo-bis(4-cyanovaleric acid) 75% (Sigma-Aldrich).

#### Procedure

##### a) Grignard synthesis

Magnesium turnings (2.9166g, 0.12mol) were weighed off and placed in a reaction vessel along with a crystal of iodine, a few milliliters of dry THF and a stirrer bar. Bromobenzene (18.8411g, 0.12mol) and THF (90.8538g, 1.26mol) were placed in two separate dropping funnels. 10% of the bromobenzene and THF were added and the mixture was heated using a heating gun to start the reaction. The onset of the reaction was indicated by a colour change from brown to colourless. The temperature was kept below 40°C using an ice bath. The remaining solvent and bromo-compound

### Chapter Three: RAFT Agent Synthesis

---

were slowly added drop-wise. The mixture was allowed to cool after completion of the reaction. The reaction mixture had a metallic green colour. Carbon disulfide (CS<sub>2</sub>) (9.1372g, 0.12mol) was slowly added to the Grignard mixture via the dropping funnel. During addition the colour turned reddish brown. The product was poured into a beaker of crushed ice and stirred until all the ice melted. 33% HCl was used to acidify the mixture to yield the dithio-acid. The HCl was slowly dripped into the mixture using a drip pipette, until a colour change to bright pink was observed. The dithio-acid was extracted with diethyl ether and the water layer was washed twice (300mL). The ether was removed by rotary evaporation under reduced pressure.

#### **b) Formation of bis(phenylthiocarbonyl)disulfide**

Catalytic quantities of iodine and twice the molar ratio of DMSO (14.7642g, 0.1889mol) to dithiobenzoic acid (14.5741g, 0.09447mol) were added to a reaction vessel in a medium of absolute ethanol. The excess DMSO ensured that the reaction proceeded more rapidly at room temperature. Cooling with an icebath speeded up crystallization of the product. The reaction mixture was refluxed overnight. The product was filtered off to yield a fine pink powder which were dried under vacuum. The yield of bis(thiocarbonyl)disulfide obtained was approximately 42% (6.0478g).

The NMR spectroscopy data were as follows: <sup>1</sup>H NMR (400MHz, CDCl<sub>3</sub>) δ (ppm): 7.4 (m, 4H, H<sub>meta</sub>); 7.6 (dd, 2H, H<sub>para</sub>); 8.1 (dd, 4H, H<sub>ortho</sub>) <sup>13</sup>C NMR (75MHz, CDCl<sub>3</sub>) δ (ppm): 219.58 (C=S); 143.69, 133.15, 128.65, 127.56 (C<sub>aromatic</sub>). The trace amounts of acid were difficult to remove. The purity of the product was estimated to be greater than 98%.

#### **c) Formation of cyanovaleric acid dithiobenzoate**

The final step in the synthesis of the desired RAFT agent was carried out according to the method of Le *et al.*<sup>1,11</sup> Bis(thiobenzoyl)disulfide (6.0478g, 0.0197 mol) and 4,4'-azo-bis(4-cyanovaleric acid) (5.5303g, 0.0197 mol) were refluxed in a medium of ethyl acetate at 85<sup>o</sup>C for 24 hours. Afterwards, the ethyl acetate was removed by rotary evaporation. The product was purified by column chromatography on silica as stationary phase to give a yield of 7.389g (70%) The eluent system used was a mixture of 3:3:4 pentane: heptane: ethyl acetate. A drop of chloroform was added to promote crystallization and the product was dried under vacuum.

The NMR data were as follows: <sup>1</sup>H NMR spectroscopy (400MHz, CDCl<sub>3</sub>) δ (ppm): 1.9 (s, 3H, H<sub>methyl</sub>); 2.4-2.7 (m, 4H, H<sub>methylene</sub>); 7.4 (m, 2H, H<sub>meta</sub>); 7.57 (dd, 1H, H<sub>para</sub>); 7.9 (dd, 2H, H<sub>ortho</sub>). <sup>13</sup>C NMR (75MHz, CDCl<sub>3</sub>) δ (ppm): 222.15 (C=S); 176.65 (C<sub>acid</sub>); 144.46, 133.04, 128.56, 126.65 (C<sub>aromatic</sub>); 118.36 (C≡N); 45.59 (C<sub>quat.</sub>); 33.03, 29.48 (C<sub>methylene.</sub>); 24.14 (C<sub>methyl</sub>). The estimated purity was >98%. UV (in THF, nm) 302.68.

## Chapter Three: RAFT Agent Synthesis

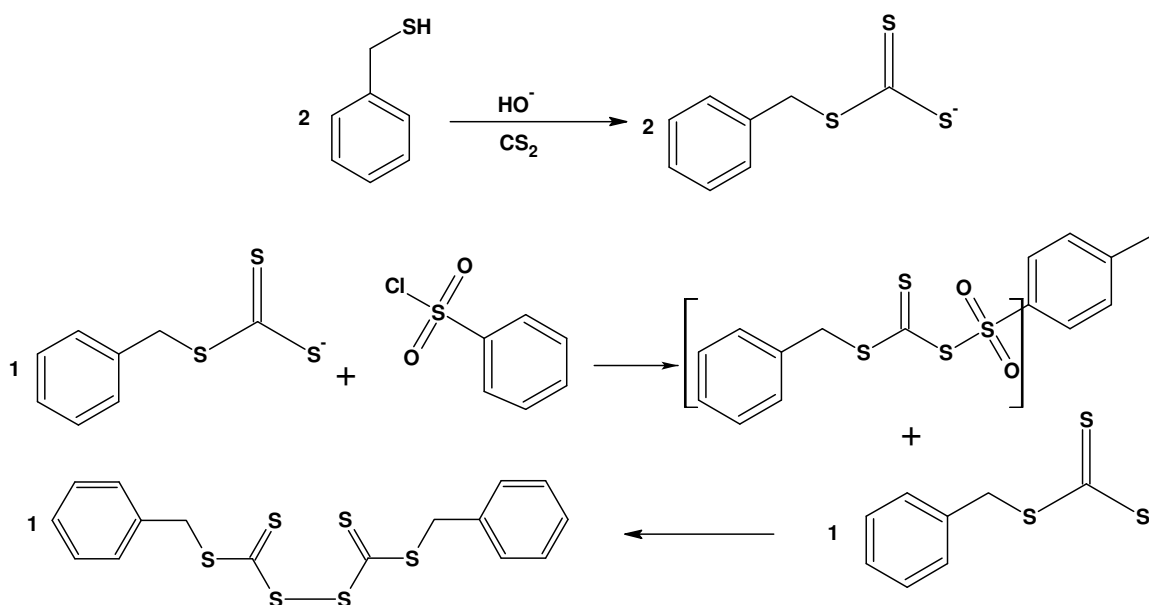
## 3.2.2 Cyanovaleric acid benzyl trithiocarbonate

## Materials

Benzyl mercaptan 99% (Sigma-Aldrich), potassium hydroxide (ACE), Aliquat 336 (Fluka), carbon disulfide (CS<sub>2</sub>) 99.5% (Sigma-Aldrich), *p*-tosyl chloride (Sigma-Aldrich), dichloromethane CP (ACE), NaHCO<sub>3</sub> (aqueous) (Merck), sodium chloride solution (Merck), magnesium sulfate (ACE), pentane CP (ACE), acetone CP (ACE), 4,4'-azo-bis(4-cyanovaleric acid) +99% (Sigma-Aldrich), ethyl acetate CP (ACE), hexane CP (ACE).

## Procedure

## a) Preparation of bis(benzylsulfanyl thiocarbonyl) disulfide



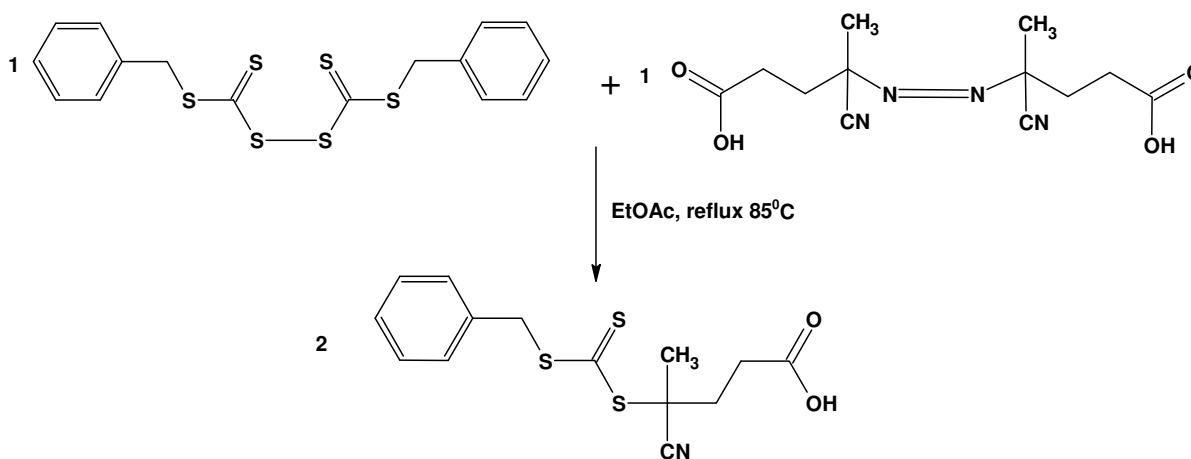
Scheme 3.3 The preparation of bis(benzylsulfanyl thiocarbonyl) disulfide

The bis(benzylsulfanyl thiocarbonyl) disulfide was prepared and purified according to the method of Weber *et al.*<sup>16</sup> Benzyl mercaptan (12.4g, 100mmol) was added dropwise to a solution of potassium hydroxide (7.3g, 130mmol) in 30mL water, followed by 0.2g of Aliquat 336 and carbon disulfide (7.6g, 100mmol) in one portion. *p*-Tosyl chloride (9.6g, 50mmol) and 0.2g Aliquat 336 were dissolved in 100mL of dichloromethane, then stirred and cooled to -5°C. The trithiocarbonate solution was added dropwise over 1h to the *p*-tosyl chloride solution. Stirring was continued for

*Chapter Three: RAFT Agent Synthesis*

another 30 min at  $-5^{\circ}\text{C}$  and then for a further hour at room temperature where after the layers separated. The aqueous layer was extracted with dichloromethane (2x30mL). The combined organic phases were successfully washed with aqueous  $\text{NaHCO}_3$  and water, and then dried over magnesium sulfate. The solvent was removed under vacuum and the yellow solid was washed with pentane and recrystallized from acetone. The resulting crystals were washed with pentane and dried under vacuum. The yield obtained for the yellow recrystallized product was 80% (16.0g).

The NMR data were as follows:  $^1\text{H}$  NMR (300MHz,  $\text{CDCl}_3$ )  $\delta$  (ppm): 7.32-7.29 (m, 10H, Ar); 4.50(s, 4H,  $\text{CH}_2$ ).  $^{13}\text{C}$  NMR (75MHz,  $\text{CDCl}_3$ )  $\delta$  (ppm): 220.75 (C=S), 134.07, 129.51, 128.98, 128.29, 42.96.

**b) Formation of cyanovaleric acid benzyl trithiocarbonate**

Scheme 3.4 The preparation of cyanovaleric acid benzyl trithiocarbonate

The bis(benzylsulfanyl thiocarbonyl) disulfide (6.00g, 0.015mol) and 4,4'-azo-bis(4-cyanovaleric acid) (4.2181g, 0.015mol) were refluxed in ethyl acetate at  $85^{\circ}\text{C}$  for 10 hours, after which the solvent was removed by rotary evaporation. The crude product was purified by column chromatography using the 4:1 hexane to ethyl acetate as eluent. The obtained crystals were dried under vacuum and gave a yield of 4.2914g (88%).

The NMR data were as follows:  $^1\text{H}$  NMR (400MHz,  $\text{CDCl}_3$ )  $\delta$  (ppm): 1.8 (s, 3H,  $\text{H}_{\text{methyl}}$ ); 2.3-2.6 (m, 4H,  $\text{H}_{\text{methylene}}$ ); 4.5 (s, 2H,  $\text{H}_{\text{methylene}}$ ); 7.3 (m, 5H,  $\text{H}_{\text{aromatic}}$ ).  $^{13}\text{C}$  NMR (75MHz,  $\text{CDCl}_3$ )  $\delta$  (ppm): 216.32 (C=S); 172.05(C=O, acid); 134.31, 129.48, 128.98, 128.18 (C=C, aromatic); 118.88 (C $\equiv$ N); 55.4 (C-S); 46.33 ( $\text{CH}_2\text{S}$ ); 41.45, 33.43 ( $\text{C}_{\text{methylene}}$ ); 24.66 ( $\text{C}_{\text{methyl}}$ ). The estimated purity was 99%. UV (in THF, nm) 303.54.

### **3.3 Conclusions**

The syntheses of the two RAFT agents, 4-cyano-4-((thiobenzoyl)sulfonyl) pentanoic acid (cyanovaleric acid dithiobenzoate) and S-4-cyanopentanoic acid-S'-benzyltrithiocarbonate, were successfully carried out. The preparation of the respective targeted disulfides for the dithioester and trithiocarbonate, followed distinctly different routes. Preparation of the trithiocarbonate was much faster and less complicated.

The novel trithiocarbonate RAFT agent S-4-cyanopentanoic acid-S'-benzyltrithiocarbonate is an excellent example of the type of RAFT agent that can be produced through the development of facile synthesis routes.

### 3.4 References

- (1) Le, T. P.; Moad, G.; Rizzardo, E.; Thang, S. H.; In PCT. Int. Appl.; wo98/01478; **1998**
- (2) Thang, S. H.; Chong, B. Y. K.; Mayadunne, R. T. A.; Moad, G.; Rizzardo, E. *Tetrahedron Lett* **1999**, *40*, 2435-2438.
- (3) Donovan, M. S.; Lowe, A. B.; Sumerlin, B. S.; McCormick, C. L. *Macromolecules* **2002**, *35*, 4123-4132.
- (4) Lai, J. T.; Filla, D.; Shea, R. *Macromolecules* **2002**, *35*, 6754-6756.
- (5) Takolpuckdee, P.; Mars, C. A.; Perrier, S.; Archibald, S. J. *Macromolecules* **2004**, *38*, 1057-1060.
- (6) Ramadas, S. R.; Srinivasan, P. S.; Ramachandran, J.; Sastry, V. V. S. *Synthesis* **1983**, 605-622.
- (7) Ramadas, K.; Srinivasan, N. *Synth Commun* **1995**, *25*, 227-234.
- (8) Buttè, A.; Storti, G.; Morbidelli, M. *Macromolecules* **2001**, *34*, 5885-5896.
- (9) Adamy, M.; Van Herk, A. M.; Destarac, M.; Monteiro, M. J. *Macromolecules* **2003**, *36*, 2293-2301.
- (10) Destarac, M.; Charmot, D.; Franck, X.; Zard, S. Z. *Macromol Rapid Comm* **2000**, *21*, 1035-1039.
- (11) Chiefari, J.; Chong, B. Y. K.; Ercole, F.; Krstina, J.; Le, T. P. T.; Mayadunne, R. T. A.; Meijs, G. F.; Moad, C.; Moad, G.; Rizzardo, E.; Thang, S. H. *Macromolecules* **1998**, *31*, 5559-5562.
- (12) Thomas, D. B.; Convertine, A. J.; Hester, R. D.; Lowe, A. B.; McCormick, C. L. *Macromolecules* **2004**, *37*, 1735-1741.
- (13) Thomas, D. B.; Convertine, A. J.; Myrick, L. J.; Scales, C. W.; Smith, A. E.; Lowe, A. B.; Vasilieva, Y. A.; Ayres, N.; McCormick, C. L. *Macromolecules* **2004**, *37*, 8941-8950.
- (14) Mayadunne, R. T. A.; Rizzardo, E.; Chiefari, J.; Chong, Y. K.; Moad, G.; Thang, S. H. *Macromolecules* **1999**, *32*, 6877-6980.
- (15) Wang, R.; McCormick, C. L.; Lowe, A. B. *Macromolecules* **2005**, *38*, 9518-9525.
- (16) Weber, W. G.; McLeary, J. B.; Sanderson, R. D. *Tetrahedron Lett* **2006**, *47*, 4771-4774.

## ***Chapter 4: The Living Character of CVADTB and CVATTB in Homogeneous Polymerization***

### **Abstract**

The mediation behaviour of two RAFT agents, cyanovaleric acid dithiobenzoate and cyanovaleric acid benzyl trithiocarbonate, were investigated by performing solution polymerizations of the model monomers styrene and methyl methacrylate at 80°C and 100°C respectively. The efficiency of the RAFT agents was compared in terms of rate effects, the predictability of the molecular weights of the polymers, the polydispersities of the polymers and their ability to allow block copolymer formation via sequential addition of monomers.

## 4.1 Introduction

The starting point of our investigation involved the use of cyanovaleric acid dithiobenzoate (CVADTB) as RAFT agent.<sup>1-5</sup> Dithiobenzoates are known for their retardation behaviour from previous studies<sup>6-9</sup> and for this reason we sought an improvement in polymerization by means of RAFT agent choice. When employing dithiobenzoates, inhibition and rate retardation are commonly observed, with the extent of both of these effects depending on the particular monomer system under investigation.<sup>10,11</sup> It has generally been accepted that the relative stability and thus the average lifetime of the intermediate RAFT radicals are of key importance for rate retardation and inhibition effects in RAFT polymerization. We aimed to synthesize and apply a trithiocarbonate RAFT agent with tailored properties for comparison purposes. A similar R-group to CVADTB would cancel out reinitiation differences for both styrene and MMA monomers, while a different stabilizing group, e.g. altering the Z-group from phenyl to S-benzyl, should increase the fragmentation rate and result in faster establishment of the RAFT equilibrium. The radical in the RAFT intermediate is changed from being in a disulfur benzylic position to a less stable disulfur alkyl position.

CVATTB was exactly the RAFT agent needed and the facile route of Weber *et al*<sup>12</sup> for the preparation of the disulfide intermediate provided an elementary synthetic path for the preparation of this RAFT agent as shown in chapter 3. The efficacy of dithiobenzoate derivatives in promoting living polymerization of MMA depends strongly on the nature of the leaving group radical.<sup>13</sup> Chong *et al*<sup>14</sup> reported that the tertiary cyanoalkyl gave substantially narrower PDIs under the given reaction conditions than a number of other common initiating radicals. The authors also illustrated that for styrene a much wider range of R groups are effective.

A simplified experimental polymerization system was needed to carry out the study in such a way as to minimize the variables and allow direct comparison of the RAFT agents. The disadvantages of bulk polymerization, especially in the case of methyl methacrylate which is susceptible to autoacceleration at higher temperatures,<sup>15</sup> were overcome by solution polymerization. The objective of the work described in this chapter was to investigate the mediation behaviour of the two different RAFT agents, CVADTB and CVATTB in solution polymerization with regards to the polymerization rate, living character and their ability to facilitate successful block copolymerization.

## 4.2 Experimental

### 4.2.1 Materials/Reagents

The crude monomers, styrene (>99.7%, Protea Chemicals), and methyl methacrylate (>99.9%, Lucite International), were washed with a solution of 0.3 M potassium hydroxide (85% KOH, ACE) to remove inhibitors/stabilizers and then distilled under reduced pressure. The purified monomers were stored for short periods over molecular sieves in a refrigerator until use. Crude azobis (isobutyronitrile) (AIBN) (Riedel de Haen), was recrystallized from methanol, filtered off and refrigerated. Ethyl acetate (CP) (Merck) and toluene (CP) (Merck) were purified by standard distillation procedures before use.

### 4.2.2 RAFT agents used

The syntheses of the two RAFT agents used, 4-cyano-4-((thiobenzoyl)sulfonyl) pentanoic acid (cyanovaleric acid dithiobenzoate) (CVADTB) (**1**) and S-4-cyanopentanoic acid-S'-benzyltrithiocarbonate (**2**) (CVATTB) are described in Chapter 3 (section 3.2.).

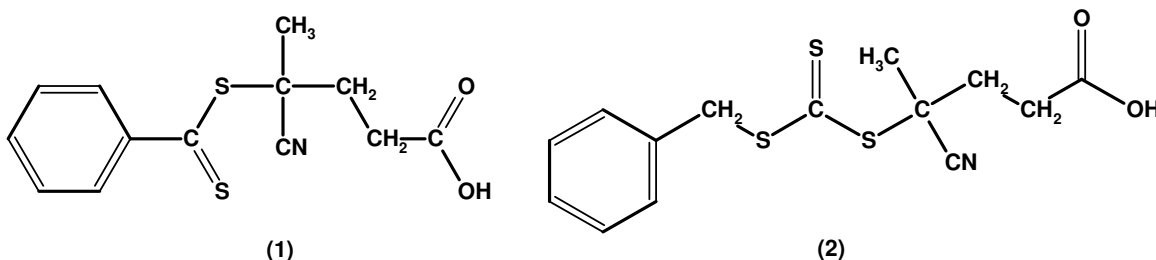


Figure 4.1 Chemical structures of RAFT agents 4-cyano-4-((thiobenzoyl)sulfonyl) pentanoic acid (cyanovaleric acid dithiobenzoate) (CVADTB) (**1**) and S-4-cyanopentanoic acid-S'-benzyltrithiocarbonate (CVATTB) (**2**).

### 4.2.3 Polymerizations

#### 4.2.3.1 RAFT mediated solution polymerization of styrene and methyl methacrylate.

The solution polymerizations of methyl methacrylate in ethyl acetate and styrene in toluene were carried out under nitrogen atmosphere at 80°C and 100°C respectively. The monomer, solvent, initiator and RAFT agent were weighed off and mixed together in a three neck round bottom flask. The solution was degassed under continuous stirring and after the oil-bath reached the targeted temperature; the reaction vessel was lowered into the bath and polymerization was allowed to proceed. On completion of the reaction the reaction mixture was cooled and stirred with methanol to facilitate precipitation. The product was filtered off, dried under vacuum and labeled. The

*Chapter Four: Homogeneous RAFT Polymerizations*

reaction conditions of the polymerizations to prepare the starting block polymers of styrene and methyl methacrylate respectively are shown in Table 4.1.

*Table 4.1: Experimental details of the RAFT mediated solution polymerizations of styrene (Sty) and methyl methacrylate (MMA) with RAFT agents CVADTB and CVATTB.*

<b>Reaction number</b>	<b>Monomer (mol x 10<sup>-3</sup>)</b>	<b>RAFT agent</b>	<b>RAFT (mol x 10<sup>-4</sup>)</b>	<b>AIBN (mol x 10<sup>-5</sup>)</b>	<b>Solvent (g)</b>	<b>Reaction temperature (°C)</b>	<b>Reaction time (h)</b>
Sty06	3.412	CVADTB	6.267	7.856	35.52	100	24
Sty07	3.410	CVATTB	6.087	6.089	35.66	100	24
Sty08	3.411	CVATTB	6.099	10.100	35.65	100	24
MMA03	249.7	CVADTB	4.560	3.057	25.00	80	4.5
MMA05	341.0	CVADTB	6.114	6.577	34.14	80	5.5
MMA07	341.0	CVATTB	6.117	6.637	34.14	80	8

\*Sty polymerizations were carried out in toluene while the MMA polymerizations were carried out in EtOAc.

#### **4.2.3.2 Block copolymer polymerizations**

A calculated mass of the dried and purified starting block polymer was placed in a reactor together with solvent and dissolved under continuous nitrogen purging. The reactor was placed in a preheated oilbath at the desired temperature and the reaction commenced immediately after the addition of fresh monomer and initiator via either “shot” or “feed” addition. “Shot” addition involves the addition of monomer and initiator in one shot while “feed” addition involves the addition via a feed pump system, at a specified rate, which in turn depends on the monomer concentration to be added and the total reaction time anticipated to complete the polymerization. The total polymerization time was based on the polymerization rate behaviour of the second monomer to be added under identical reaction conditions. Feed additions were performed with the use of a Metrohm 711 Liquino and 700 Dosino (Swiss Lab). On completion of the reaction the reaction mixture was cooled and stirred with methanol to precipitate the polymer out. The product was filtered off and dried.

## Chapter Four: Homogeneous RAFT Polymerizations

---

### 4.2.4 Kinetic analysis

Samples were taken at time intervals throughout the polymerizations for gravimetric analysis to follow the conversion of monomer to polymer. Samples were removed via a septum by needle, placed into sample pans and left to dry. All sample sets were further dried in a vacuum oven at appropriate temperatures to ensure removal of solvent and monomer traces.

### 4.2.5 SEC analysis

Molecular weights were determined using Size Exclusion Chromatography (SEC) of the kinetic analysis samples. The SEC instrument consisted of a Waters 1515 isocratic HPLC pump, a Waters 717plus auto-sampler, Waters 600E system controller (run by Breeze Version 3.30 SPA) and a Waters 610 fluid unit. A Waters 2414 differential refractometer was used at 30°C in series with a Waters 2487 dual wavelength absorbance UV/Vis detector operating at variable wavelengths. Tetrahydrofuran (THF, HPLC grade, stabilized with 0.125% BHT) sparged with IR-grade helium was used as eluent at flow rates of 1 ml min<sup>-1</sup>. The column oven was kept at 30°C and the injection volume was 100  $\mu$ l. Two PLgel (Polymer Laboratories) 5  $\mu$ m Mixed-C (300x7.5 mm) columns and a pre-column (PLgel 5  $\mu$ m Guard, 50x7.5 mm) were used. Calibration was done using narrow polystyrene standards ranging from 800 to 2x10<sup>6</sup> g. mol<sup>-1</sup>. All molecular weights were reported as polystyrene equivalents.

## 4.3 Results and Discussion

### 4.3.1 Styrene and methyl methacrylate polymers

The results of the final polymers obtained are summarized in Table 4.2 for the reactions carried out with CVADTB and CVATTB for both Sty and MMA. The repeated reactions showed final conversion values that were relatively close and all polymers had polydispersities that were well below the literature benchmark<sup>5</sup> of 1.5 except MMA03 (Table 4.2). The two monomers were polymerized in two different solvents at two different temperatures. The temperatures were chosen in such a fashion as to obtain reasonable conversions within practical time periods. MMA has a higher propagation rate constant than Sty and for this reason was polymerized at a lower temperature.

## Chapter Four: Homogeneous RAFT Polymerizations

Table 4.2: Final polymers produced by the RAFT mediated homogeneous polymerization of styrene and methyl methacrylate with RAFT agents CVADTB and CVATTB. The data is representative of the reactions run tabulated in Table 4.1

Polymer	RAFT agent	Conversion (%)	$\bar{M}_n$ , theoretical	$\bar{M}_n$ , SEC	$\bar{M}_w/\bar{M}_n$
Sty06	CVADTB	46.33	22623	25526	1.32
Sty07	CVATTB	40.10	20627	18474	1.19
Sty08	CVATTB	38.27	18419	17027	1.24
MMA03	CVADTB	76.10	22883	16300	1.67
MMA05	CVADTB	74.90	53977	30537	1.21
MMA07	CVATTB	53.82	26029	25953	1.12

## 4.3.1.1 Rates of reaction

The relationships between the rate of monomer consumption and reaction time profiles are illustrated in Figure 4.2 for the Sty polymerizations in the presence of CVADTB and CVATTB at similar initial RAFT agent concentrations (Table 4.1).

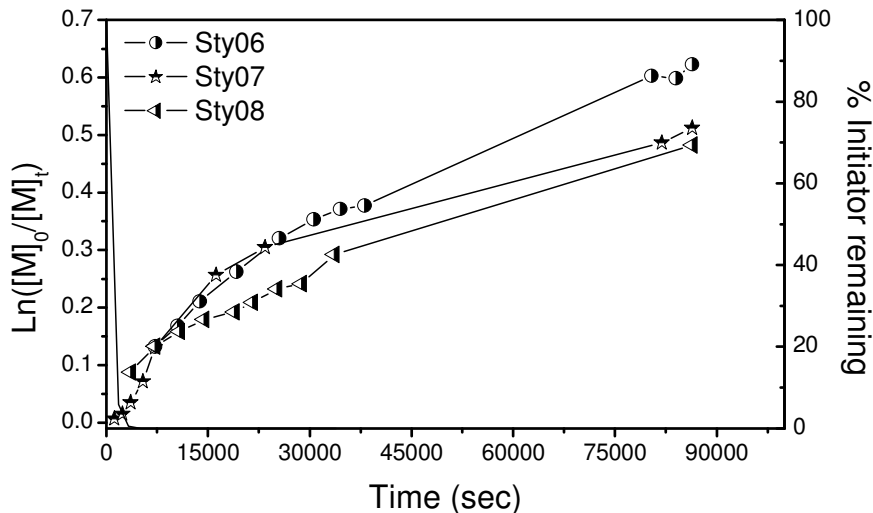


Figure 4.2 A comparison of the first-order kinetics of the polystyrene polymerizations using the two different RAFT agents synthesized in this study. See Table 4.2

The differences between the rates of polymerization at this temperature are not significant enough to be able to conclude that the RAFT agents provided different polymerization behaviour. No clear linear relationship exists between the rate of polymerization and time and there is no clear induction period in the polymerizations. In the conventional radical polymerization of styrene the Diels-Alder

## Chapter Four: Homogeneous RAFT Polymerizations

---

dimerization and the successive styrene-assisted homolysis of the cyclo-adduct is the general pathway of radical generation, therefore the rate of thermal initiation of styrene in bulk is likely to be third-order in monomer concentration.<sup>16</sup> It should be noted that the initiator is consumed after approximately 1 hour. It can be observed that the rate of polymerization is fairly slow for all three of the reactions, as the  $k_p$  for styrene is relatively low in relation to methyl methacrylate.<sup>17</sup> In support of the behaviour of CVADTB, it has been established that, although its use is popular, when using dithiobenzoates as mediating agents, rate retardation can occur. Moad *et al*<sup>7</sup> reported that the rate of polymerization is decreased with increasing initial RAFT agent concentration. Carrying out the styrene polymerizations at 100°C could have made the effect less severe, as temperature has shown to have a significant effect in the relative amount of retardation experienced in RAFT mediated polymerization.<sup>13,18</sup> In principle, by applying high temperature, the fragmentation of the intermediate RAFT radical into the dithioester moiety and the propagating radical, may be enhanced compared to the addition reaction. The concentration of intermediate radicals is reduced and thus rate retardation is suppressed. Studies by Arita *et al*<sup>19</sup> showed that cumyl dithiobenzoate (CDB) mediated Sty polymerizations between 120°C and 180°C proceeded with molecular weights increasing with monomer conversion and yielded polymer with polydispersities well below 1.5. In short, the results of this study showed a minimal difference in the mediation behaviour in terms of rate effects in the Sty polymerization runs.

Despite the fact that the MMA runs were conducted at a lower temperature, their reaction rates were still faster for both RAFT agents than the rates of the Sty runs and reaction times were consequently much shorter. The reason for this is largely related to the fact that the  $k_p$  for MMA is higher than that of Sty as well as the low degree of retardation that is observed in RAFT mediated polymerizations of methacrylates.<sup>20</sup> In addition, the stabilization of the propagating radical by the alpha methyl group ensures that methacrylates experience less retardation than styrenics, making the fragmentation rates higher. The polymerization of MMA in solution mediated by the two different RAFT agents at 80°C shows two different effects (Figure 4.3).

## Chapter Four: Homogeneous RAFT Polymerizations

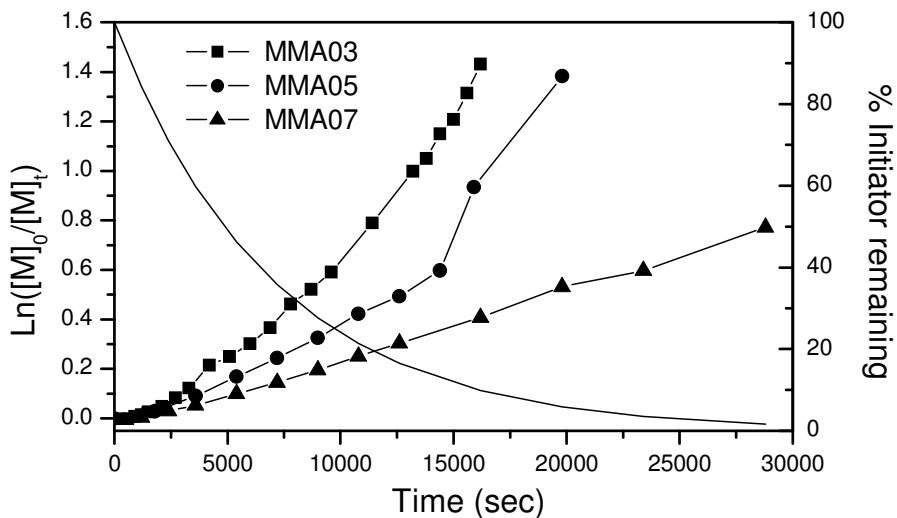


Figure 4.3 A comparison of the first-order kinetics of the poly(methyl methacrylate) polymerizations using the two different RAFT agents synthesized in this study (See Table 4.2 for details).

The trithiocarbonate mediated polymerization clearly shows a linear rate of polymerization which is indicative of controlled polymerization. The two reactions mediated by the dithiobenzoate transfer agent show an increasing rate with time. This behaviour is typically caused by an artifact such as the loss of monomer from the polymerization system. It is unlikely that at this temperature and concentration that any significant auto-acceleration effect will be observed.

For the purposes of this study it is difficult to draw strong conclusions about the retardation of the reactions from these polymerizations. It seems unlikely that the rate of polymerization of the reaction mediated by the trithiocarbonate is much higher than that of the dithiobenzoate. In both the polymerizations of Sty and MMA in solution the conditions are such that the RAFT agent itself does not cause substantial changes in the rate of polymerization.

#### 4.3.1.2 Molecular weight distributions

In Figures 4.4 and 4.6 the mediation behaviour of the two RAFT agents in terms of their ability to provide controlled polymerization is compared. The theoretically derived number average molecular weights are used as a reference to determine the relative degree of predictability and the polydispersity index is used as a guide to determine the differences in the degree of control. The theoretical values were obtained using equation (4.1).

## Chapter Four: Homogeneous RAFT Polymerizations

$$\bar{M}_n = M_{\text{RAFT}} + \frac{x[M]_0 M_{\text{monomer}}}{[\text{RAFT}]_0 + Cf [I]_0 (1 - e^{-k_d t})} \quad (4.1)$$

where  $\bar{M}_n$  is the number average molar mass;  $M_{\text{monomer}}$  is the monomer molar mass;  $M_{\text{RAFT}}$  the molar mass of the RAFT agent;  $[M]_0$  and  $[\text{RAFT}]_0$  are the initial concentrations of the monomer and RAFT agent and  $x$  is the fractional conversion. The term  $Cf [I]_0 (1 - e^{-k_d t})$  represents the initiator derived chains where  $C$  is a constant that represents the proportion of termination occurring via combination or disproportionation in the system (which create either one or two chains respectively),  $f$  is the initiator efficiency,  $[I]_0$  is the initial initiator concentration,  $k_d$  the rate coefficient of dissociation and  $t$  the time in seconds.

Figure 4.4 was examined in the context of Figure 4.2. For both the reactions presented, the polydispersity of the polymer produced is well defined, narrow and consistent. It indicates that there is a very strong correlation between the predicted molecular weight using Equation (4.1) and the SEC number average molecular weight for the reaction in which CVATTB was used.

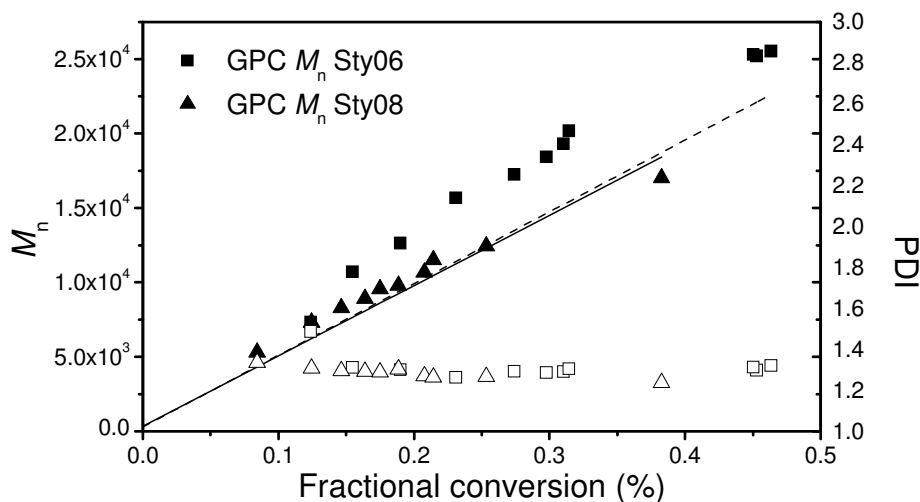
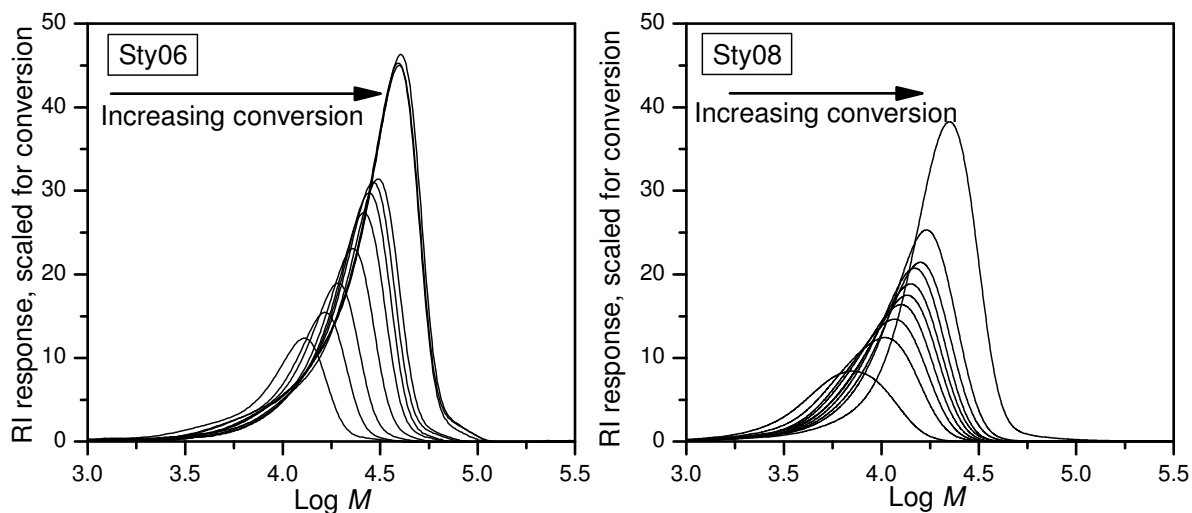


Figure 4.4 The molecular weight and polydispersity index of the polystyrene polymerizations as a function of conversion. The dashed (Sty06, CVADTB) and solid (Sty08, CVATTB) lines are the theoretically derived molecular weights for the respective data sets.

The correlation in the reaction in which CVADTB was used is good but does not completely correspond to the predicted values. The deviation is to higher molecular weight with conversion. This is consistent with either a loss of RAFT agent functionality or some other process that leads to the formation of higher molecular weight material in the reaction leading to a positive skewing of

*Chapter Four: Homogeneous RAFT Polymerizations*

the SEC determination. The related molecular weight distributions of Sty06 and Sty08 after 24 hours are shown in Figure 4.5, which clearly illustrates the growth of the polystyrene chains.



*Figure 4.5 Size-exclusion chromatograms of two of the polystyrene polymerizations as a function of increasing conversion. See Table 4.2. Sty06 (CVADTB) exhibits a high molecular weight shoulder at higher conversions; a phenomenon that is absent in Sty08 (CVATTB).*

As the PS conversion increases above 30% the molecular weights start to increase more dramatically. Skewing of molecular weight distributions occurs with increasing conversion, which is more pronounced for Sty06. At higher conversions, termination reactions began to play a larger role, leading to a loss of RAFT agent functionality and the formation of dead polymer. Polystyrene terminates via combination, which could explain the obvious skewing of the curves and the positive deviation of molecular weight from the predicted values in Figure 4.4. In contrast to Sty06, Sty08 has no additional “dead” polymer peak at high monomer conversions. This can be attributed to the better mode of control over the polymerization by CVATTB in comparison to CVADTB. The polymerization mediated by the trithiocarbonate exhibited a linear growth of  $\bar{M}_n$  conversion with excellent correlation to the predicted values obtained from Equation 4.1, and the polydispersity values were lower compared to that found by Sty06.

## Chapter Four: Homogeneous RAFT Polymerizations

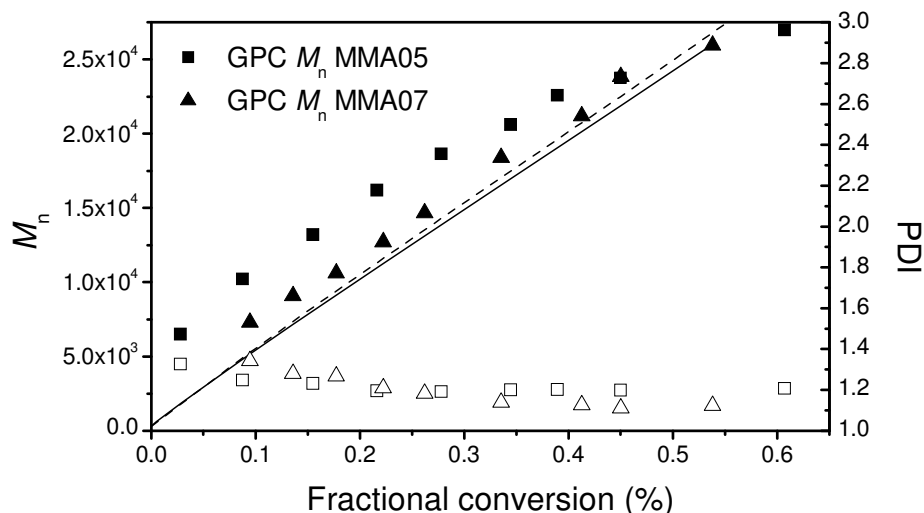


Figure 4.6 The molecular weight and polydispersity index of the poly(methyl methacrylate) polymerizations as a function of conversion. The dashed (MMA05) and solid (MMA07) lines are the theoretically derived molecular weights.

In Figure 4.6 it is observed that the polydispersity index decreases with conversion, which is consistent with what is reported in the literature for this type of polymerization.<sup>5,21</sup> The correlation between predicted and experimental molecular weight remains excellent, but it is clear that the trithiocarbonate mediated reaction provides better control. The dithiobenzoate reaction shows a positive deviation from the theoretically predicted values from early in the reaction – this is consistent with a decreased RAFT agent concentration. The values do however approach the predicted values at higher concentrations. Referring back to Figure 4.3, it seems likely that deviation is consistent with the apparent acceleration observed in the rate of polymerization, i.e. this is suggestive of an artifact in the polymerization rather than a true approach to the theoretical prediction. For the purposes of this study however, it is sufficient to be able to see that the control provided by the RAFT agent in the polymerization is predictable and within a narrow band of the predicted value.

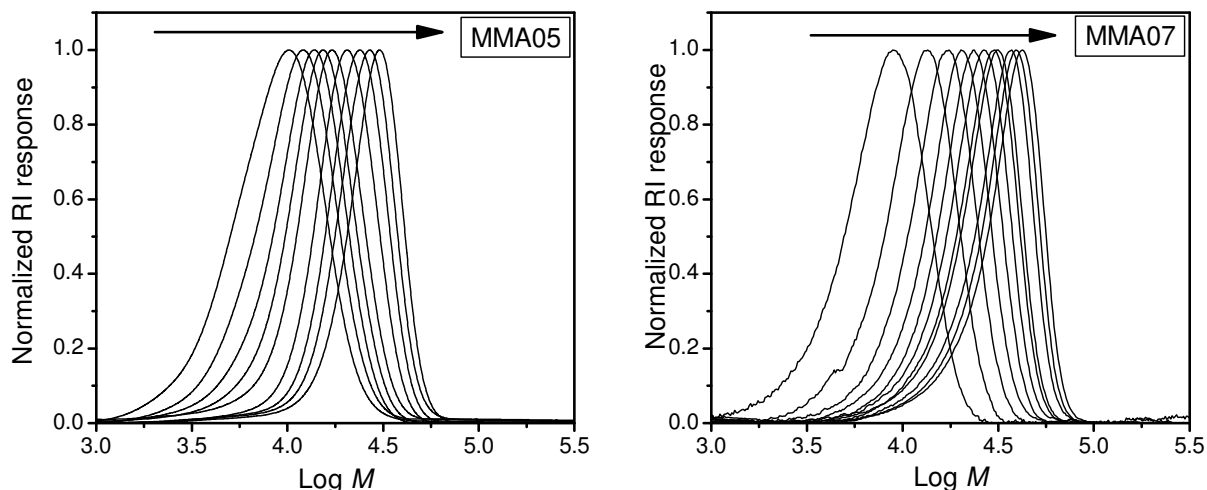
*Chapter Four: Homogeneous RAFT Polymerizations*

Figure 4.7 Size-exclusion chromatograms of two of the poly(methyl methacrylate) polymerizations as a function of increasing conversion (See Table 4.2.).

The growth of the PMMA homopolymers is controlled, the distribution appears to be largely monomodal and it becomes narrower with increasing molecular weight. There is no clear evidence of high or low molecular weight shoulders although there is some indication of tailing to the low molecular weight side of the distribution, which is consistent with the termination that can be expected by normal free radical termination mechanisms within a RAFT mediated polymerization.

Both RAFT agents are thus very capable of controlling the homopolymerization of both monomers used under the polymerization conditions chosen for this study.

#### 4.3.1.3 UV-RI overlays

The evidence for the presence of the RAFT moiety, which is responsible for the living character of the polymer chains, can be clarified using ultra violet (UV) analysis. This is made possible through the dual detection available during SEC analysis. The styrene monomer unit absorbs at a wavelength of 254nm while the RAFT moiety is known to absorb in a wavelength range of 280-350nm. The UV detector was set at 254nm and 320 nm, to discriminate between the two different functionality types. As indicated in Chapter 3, the thiocarbonyl thio moiety of both of the RAFT agents absorbs strongly at the aforementioned wavelength.

The use of UV RI (refractive index) overlays in SEC comparisons needs to be done with care. In the systems studied, a number of different factors need to be considered. Firstly, the detectors are in series, meaning that an elution time adjustment needs to be made to the signals to ensure that the correct points are being compared. The respective UV signals are however obtained at the same

*Chapter Four: Homogeneous RAFT Polymerizations*

---

elution time. Secondly, the nature of the signals being compared need to be examined. UV detection is a function of chromophores whereas refractive index signals are a function of mass. This means that in the case of RI responses the signal intensity is a function of chain length as well as the number of chains. Carrying out UV analysis at 254nm, the dominant chromophore is that of the styrene rings on the polystyrene chains. As there is a ring on each repeat unit, the intensity of the signal is a function of the chain length as well as the number of chains. This means that the UV signal at 254nm and the RI signal can directly be compared. When examining the UV signal at 320nm however, the dominant chromophore is the thiocarbonyl thio end group. This means that there is only one group per chain and the signal is now only a function of the number of chains and not the length of the chains. Overlay comparisons of the two signals indicate which fraction of the total chain distribution has the RAFT terminal moiety.

In Figure 4.8 the UV-RI overlays of the final samples of the RAFT mediated PS polymers are shown. The UV detection presented corresponds to the analysis carried out at 320nm. At lower molecular weight, the UV signal observed is very strong for both Sty06 and Sty08, due to the fact that the chains are much smaller, resulting in a high concentration of RAFT agent per mass of chain. One of the factors affecting the UV signal is the dilution effect due to an increase in molecular weight, which results in a weaker signal at high molecular weight. There is however still a marked difference between the responses of Sty06 and Sty08 at higher molecular weight. The RI response of Sty06 has a definite shoulder at the high molecular weight end. This small peak is clearly absent in the UV response, confirming that there are chains present which do not contain the thiocarbonyl thio chromophore. This supports the statement made earlier in Section 4.3.1.2, namely that this high molecular weight polymer consists of “dead” chains, formed due to loss of RAFT agent and radical-radical termination reactions. The UV response of Sty08 overlays perfectly with the RI signal throughout the distribution and suggests that most, if not all of the chains were end-capped with the RAFT moiety.

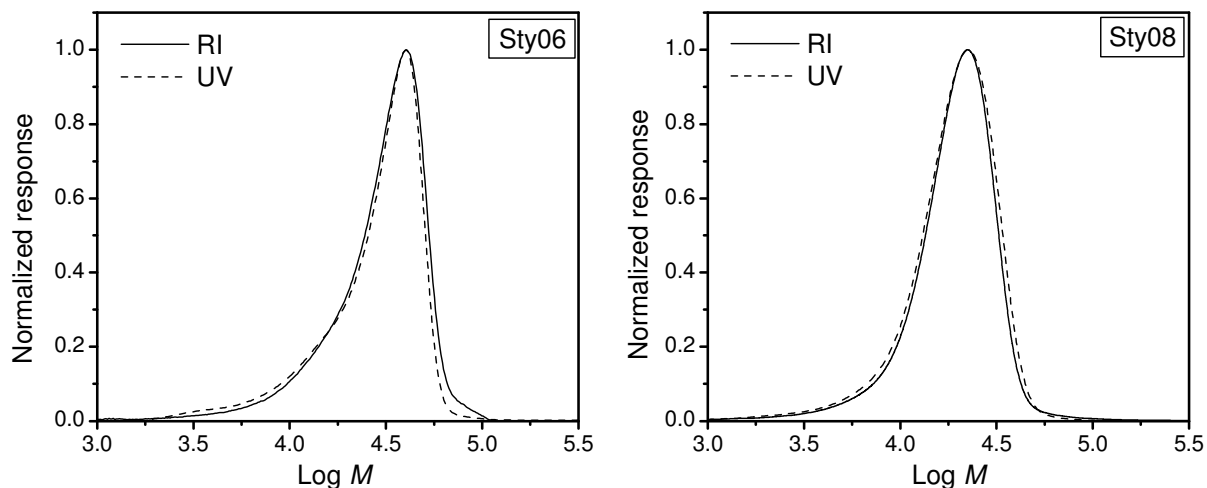
*Chapter Four: Homogeneous RAFT Polymerizations*

Figure 4.8 UV-RI overlays of the final styrene polymers end-capped with the respective RAFT agents (See Table 4.2). The UV determinations for both reactions were done at a wavelength of 320nm.

The effect of an increased UV response at the low molecular weight end is more hyphenated in Fig 4.9. Analysis of the PMMA polymers by SEC with ultraviolet (UV) detection at 320nm shows the main peak to be unimodal in MMA05 and MMA07. Both entries show a close to perfect overlay of the UV with RI responses. The loss of intensity in the UV response for both polymers at high molecular weight is significantly less than in the case of the PS polymers.

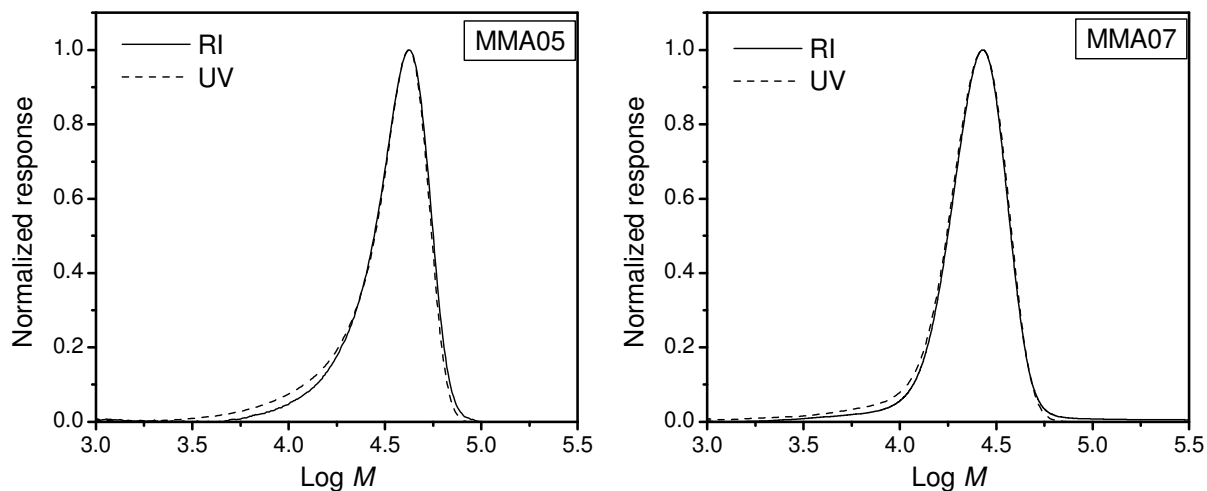


Figure 4.9 UV-RI overlays of the final poly(methyl methacrylate) polymers end-capped with the respective RAFT agents (See Table 4.2). The UV determinations for both reactions were done at a wavelength of 320nm.

The presence and amount of dead chains in a RAFT mediated polymerization system is important because it can influence the living character of a polymer as well as its transformation into a block

*Chapter Four: Homogeneous RAFT Polymerizations*

copolymer. In this part of the study it was essential that the active RAFT group be retained at the polymer chain end in order for this polymer to be the starting block for further block copolymerization. It is in fact the main requirement for chain extension to block copolymers and therefore adequate characterization was imperative.

**4.3.2 Chain extension of starting blocks**

Of the four known processes mentioned by Moad *et al*<sup>22</sup> by which block copolymers can be synthesized, we decided on the use of a functional polymer prepared by the RAFT process and then utilizing the product in a simple manner, which involved the sequential addition of monomers to the existing material. The final polymers of Sty06, Sty07, MMA05 and MMA07 mentioned in Table 4.2, were isolated and purified before chain extension. The preservation of the end functionality of the starting block was checked via UV-RI analysis and the results were discussed in Section 4.3.1.3. The preservation of the RAFT end-functionality of the polymer chains indicated that the starting blocks fulfilled the requirements of control/livingness in the sense defined by Matyjaszewski.<sup>23</sup>

*Table 4.3: Experimental details of the block copolymerization of the RAFT end-capped PS and PMMA polymers.*

Starting Polymer	Polymer-RAFT (mol x 10 <sup>-3</sup> )	$\bar{M}_{n,SEC}$	$\bar{M}_w/\bar{M}_n$	Monomer added	Monomer (mol x 10 <sup>-3</sup> )	Addition reaction	AIBN (mol x 10 <sup>-5</sup> )	Feeding rate (ml/min)	Time (h)	Reaction temperature (°C)
PS06- CVADTB	0.2370	16877	1.14	MMA	69.92	Shot	9.683	-	6	80
					70.92	Feed	6.089	0.025	6	80
PS07- CVATTB	0.2165	18474	1.19		89.99	Shot	11.080	-	6	80
					89.89	Feed	6.089	0.032	6	80
PMMA05- CVADTB	0.2290	22096	1.13	Sty	120.3	Shot	8.404	-	10	100
					120.02	Feed	6.089	0.023	10	100
PMMA07- CVATTB	0.1927	25953	1.12		120.02	Shot	7.125	-	10	100
					120.01	Feed	6.089	0.023	10	100

## Chapter Four: Homogeneous RAFT Polymerizations

---

For the next part of the study, it was expected that these polymeric RAFT agents would react further upon the addition of fresh initiator and a second monomer. We set out to investigate the following three issues:

(1) A comparison of the block sequences. The polystyrene and poly(methyl methacrylate) polymers end-functionalized with CVADTB and CVATTB (as described in the previous section), were chain extended with Sty and MMA respectively. Even though polymerization orders can be reversed, it does not guarantee that the purities of the blocks obtained will be similar. The sequence of monomer addition needs careful consideration. To assist the formation of narrow-polydispersity AB block copolymers, the first formed polymeric thiocarbonyl-thiol compound should have a high transfer constant to the monomer in the subsequent polymerization.<sup>3</sup> Keeping in mind that if  $k_p$  is the propagation rate coefficient and  $k_{tr}$  is the transfer rate coefficient, then the chain transfer coefficient  $C_{tr}$  is equal to  $k_{tr}/k_p$ . Goto *et al*<sup>8</sup> illustrated that for a smooth copolymerization, of monomer B to polymer A, the exchange rate constant  $k_{ex}(BA)$  must be large enough. From their kinetic analysis regarding MMA/Sty/dithiobenzoate systems,  $C_{ex}(MMA) = 140$  and  $C_{ex}(Sty) \approx 6000$ , where  $C_{ex}(MMA)$  and  $C_{ex}(Sty)$  are the chain transfer coefficients for MMA and Sty respectively. Thus the PS radical can readily add to PMMA-RAFT end-capped chains, while the opposite sequence did not proceed as smoothly.<sup>24</sup>

Choice of starting block is therefore important and should be chosen on basis of the relative quality as leaving group. The first block should provide the better (or equivalent) homolytic leaving group since in the fragmentation step the propagating radical from the second monomer must displace the propagating radical from the first (greater stability of the re-initiating radical). For example, in the case of a methacrylate-styrenic block, the methacrylate segment should be prepared first.

(2) A comparison of the efficiencies of the RAFT agents for block formation. Within the scope of each block sequence, the difference between the abilities of the RAFT agents to promote block formation was investigated. The transfer agents differ in the stability of the intermediate radical being formed in the process due to their respective stabilizing groups. To facilitate the comparison of the block formation ability of the materials in these specific cases (Section 4.3.2), it was decided that mathematical compensation for the differences in the UV absorption of the thio-carbonyl thio species and the refractive index chromatographs would be carried out. As stated previously, RAFT agent functional chains will contain only a single chromophore, leading to a signal that is diluted as

## *Chapter Four: Homogeneous RAFT Polymerizations*

---

a function of molar mass. In most cases comparison of the signals keeping this factor in mind is sufficient to discriminate between effects, but where broader distributions or mixed distributions are present, as in the case of these chain extensions, it may be difficult to discriminate between different effects. To overcome the potential problem, multiplication of the 320nm UV trace with the molar mass, prior to normalization, was carried out to ensure that a more correct chromatographic comparison could be conducted.

(3) A comparison of shot addition vs. feed addition. Two different methods of monomer addition were carried out to investigate whether there was any variation or improvement in the block purity obtained.

Analysis of the block copolymers was done by SEC, which is by far the most common and often the only method of assessment. Despite the fact that simple inspection of a SEC trace could make quantitative assessment problematical, it is a very useful tool to indicate whether block formation occurred within a system and how successful the synthesis was. The distributions obtained indicate the growth of the chains of the original polymer used as the first block.

### **4.3.2.1 PS-*b*-PMMA**

The first block sequence to be examined is the sequence which literature suggests should provide poorer results (see Chapter 2, Section 2.2.2.4). The use of PS homopolymer for chain extension with MMA is reported to provide a lower degree of efficiency due to the nature of the two leaving groups involved. The results of the styrene polymers end-capped with RAFT agents CVADTB (1) and CVATTB (2) are presented under the two potential routes in which monomer addition occurred.

#### ***a) Shot additions***

The first route was to add all the monomer and fresh initiator in a single shot. The reaction only commenced once the oilbath reached its targeted temperature of 80°C. In RAFT mediated polymerization, the radical source introduced to the system to trigger the reaction also leads to the formation of uncontrolled homopolymer as side product. Importantly, a low concentration of AIBN was used to maintain a high ratio of living chains to dead/uncontrolled chains.

## Chapter Four: Homogeneous RAFT Polymerizations

*(i) CVADTB*

The dithiobenzoate mediated Sty06 in Section 4.3.1 was chain extended using the conditions tabulated in Table 4.3. The results obtained from SEC analysis gave the following final values:

$$\bar{M}_{n,SEC} = 31\,360 \text{ and a } \bar{M}_w/\bar{M}_n = 1.26.$$

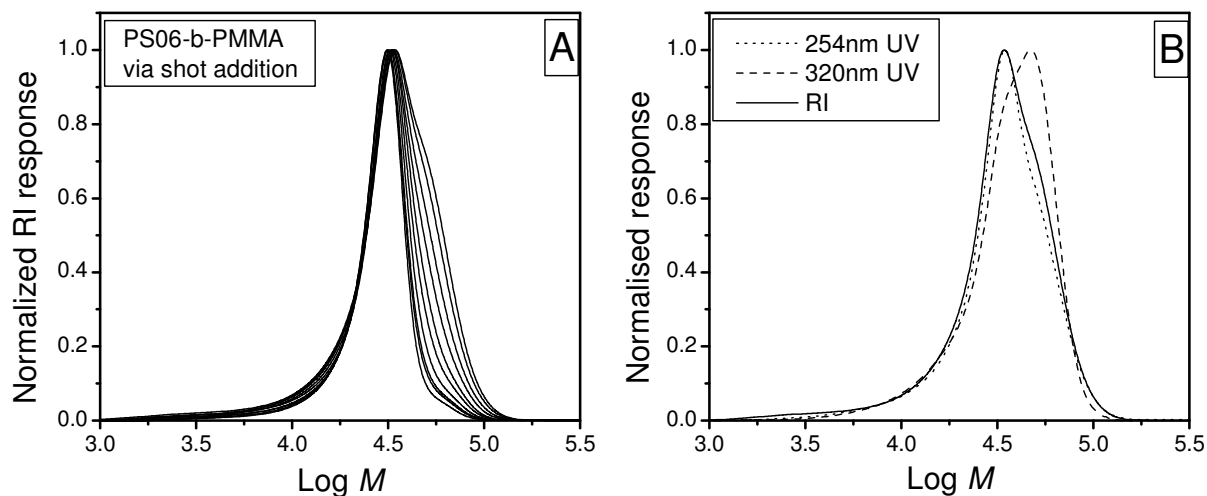


Figure 4.10 A: Size-exclusion chromatograms of the block formation of Sty06 mediated by dithiobenzoate CVADTB extended with PMMA via shot addition of monomer. See Table 4.3 for experimental details. B: The UV-RI response overlays of the final sample of the block copolymerization reaction of the same polymer in A. The dotted line represents UV absorbance at 254nm, while the dashed line represents UV absorbance at 320nm.

Figure 4.10 plot A, shows that there is indeed chain extension occurring, yet the polymer clearly consists of more than one species. The peak maximum values indicate that there is an increase in molecular weight occurring throughout the polymerization. In conjunction with the shift on the Log  $M$  axis to higher values, the narrow peak also increases in width with time. This supports the increase in polydispersity with time in the reaction, however the low molecular weights suggests that control is not lost. The broadening phenomenon leads to what appears to be the making of a second distribution. Plot B illustrates the UV-RI overlays of the final sample of the polymerization. The 254nm UV absorbance corresponds to the styrene (dotted line) and the 320nm (dashed line) absorbance represents that of the RAFT agent functionality. It appears that Sty is present throughout the distribution as the dotted line overlays exceptionally well with the RI response. There is only a small loss of absorbance at the high molecular weight bump, as pointed out earlier, whereas in the same area there is an increased response of the 320nm signal. This suggests that at the high molecular weight end the amount of styrene is reduced. This is indicative of the PS-b-PMMA being present, as the RAFT moiety is still absorbing strongly. The 320nm UV absorbance then tails off to

## Chapter Four: Homogeneous RAFT Polymerizations

give a reduced response to that of the RI towards the baseline at high molecular weight, showing that terminated styrene is part of the distribution. At the low molecular weight end, the slight loss of both UV absorbancies indicates that it is very likely that uncontrolled PMMA also formed in the process.

### (ii) CVATTB

The trithiocarbonate mediated Sty07 in Section 4.3.1 was chain extended using the conditions given in Table 4.3. From SEC analysis  $\bar{M}_{n,SEC} = 24209$  and a  $\bar{M}_w/\bar{M}_n = 1.37$ .

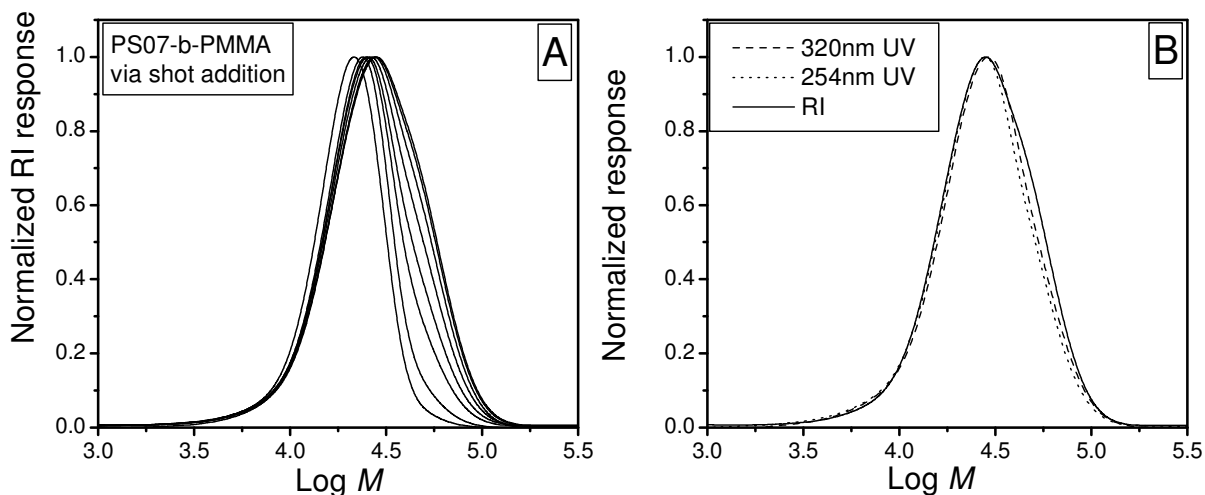


Figure 4.11 A: Size-exclusion chromatograms of the block formation of Sty07 mediated by the trithiocarbonate CVATTB chain extended with PMMA via shot addition of monomer. See Table 4.3 for experimental details. B: The UV-RI response overlays of the final sample in the block copolymerization reaction of the same polymer in A. The dotted line represents UV absorbance at 254nm; while the dashed line represents UV absorbance at 320nm.

The behaviour of the chain extension of the trithiocarbonate mediated polystyrene is similar to that of the dithiobenzoate mediated polystyrene. There is clearly an increase in the molecular weight of the polymer with time as the shift in log M to higher values are more pronounced than in Figure 4.10. Once again there is a simultaneous increase in the polydispersity of the material. It seems possible that the original homopolymer polystyrene has not been completely consumed during the reaction; however it is not possible to be definitive on this point from the SEC results. In Figure 4.11 B, the UV responses overlay quite nicely with the RI although there is still a loss of intensity at the higher molecular weight for both absorbance wavelengths. This time the tendency seems to be higher molecular weight PMMA forming in the system. The loss of intensity in UV response need not be a result of uncontrolled polymerization but possibly the result of termination leading to the loss of the RAFT end group. PMMA terminates by disproportionation predominantly, creating

## Chapter Four: Homogeneous RAFT Polymerizations

---

macromonomers which might lead to branches and higher molecular weight. The peak seems to be shifting with conversion though it is difficult to be sure on this point. It may just be lifting as the controlled peak shifts to higher molar mass.

### ***b) Feed additions***

The second possible route for the addition of monomer to a reaction mixture is the use of a feed system to control the amount of free monomer available within the reaction at any time. Feed addition of monomer should lead to improved living character or control of the reaction as the system will be monomer starved and the exchange reaction occurring in the RAFT process will be enhanced in comparison to propagation reaction occurring simultaneously.

It has been reported that the quality of block copolymers produced using the less preferred monomer addition sequence is improved when a feed system is used.<sup>21</sup>

The reaction commenced in a similar fashion to that of the shot addition. The rate of addition depended on the amount of monomer to be added for the block formation, determined by the targeted final molecular mass of the block copolymer. Another important factor that played a role was the time over which the polymerization had to take place. This was based on the rates obtained from the homogeneous polymerization of the monomer (in this case MMA) as described in Section 4.3.1.1.

### ***(i) CVADTB***

In the same fashion as in the shot addition (Section 4.3.2.1a), Sty06 was chain extended in a feed system with MMA. The results from SEC analysis were the following:  $\bar{M}_{n,SEC} = 27120$  and a  $\bar{M}_w/\bar{M}_n = 1.21$ . Figure 4.12 shows that here are three distributions of polymer.

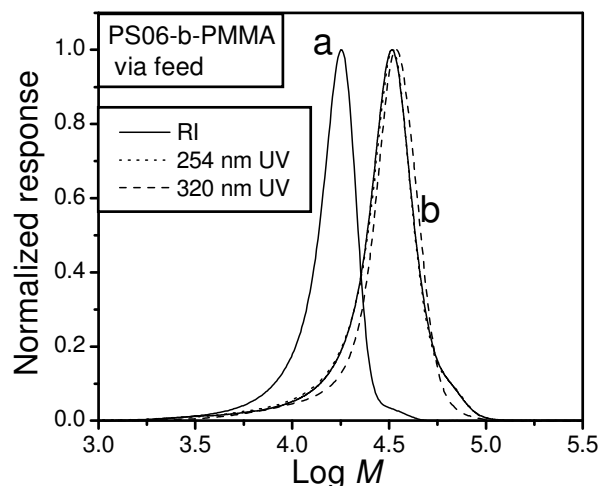


Figure 4.12 Size-exclusion chromatograms of the block formation of Sty06 mediated by the CVADTB extended with PMMA via a monomer feed system (b). See Table 4.3 for experimental details. The UV-response overlays of the block copolymer are presented: the dotted line represents UV absorbance at 254nm, while the dashed line represents UV absorbance at 320nm. The RI response of the starting block material (a) is also included.

The first distribution is the slight low molecular weight fraction present as tailing, which could possibly be unactivated, yet RAFT end-capped styrene starting material, as it does consist of a 254nm and 320nm UV response. Another possibility is the formation of PMMA homopolymer in the system by the addition of the second monomer. The primary living peak which is being chain extended with time represents the second distribution (plot (b) in Figure 4.10) and the third peak, is a high molecular weight shoulder that is consistent with a termination by combination, as commonly observed in PS polymerization. The cause of the third distribution can be due to the termination behaviour of the initial block material either by itself or in combination with the block polymer being formed—the latter would then lead to a triblock copolymer. There is clear evidence of living behaviour in this polymerization and much improved control when compared to the shot addition method.

#### (ii) CVATTB

The second chain extension is that of the trithiocarbonate mediated Sty07. Plot (a) in Figure 4.13 represents the molecular weight distribution of the RAFT end-capped PS starting block. SEC analysis showed the following values:  $\bar{M}_{n,SEC} = 22118$  and a  $\bar{M}_w/\bar{M}_n = 1.27$ .

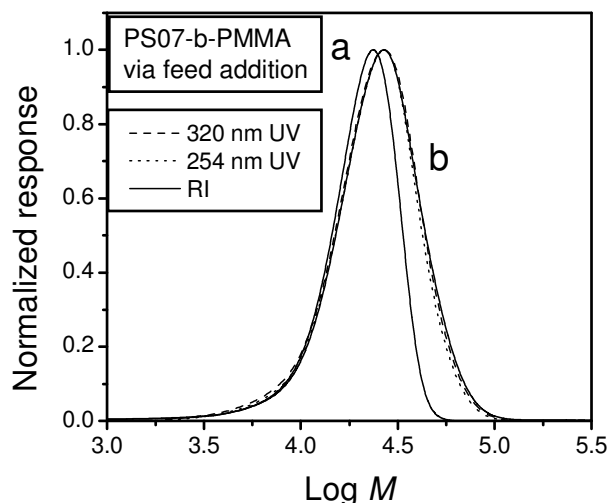


Figure 4.13 Size-exclusion chromatograms of the block formation of Sty07 mediated by CVATTB extended with PMMA via a monomer feed system. See Table 4.3 for experimental details. The UV-response overlays of the block copolymer are presented: the dotted line represents UV absorbance at 254nm, while the dashed line represents UV absorbance at 320nm. The RI response of the starting block material (a) is also included.

The quality of the block polymer produced when the trithiocarbonate mediated polystyrene is chain extended using MMA via a feed addition system is excellent. There is little evidence of either low molecular or high molecular weight shoulders in the system and the overlays of the UV signal at 320 nm suggest that the RAFT agent is homogeneously incorporated within the distribution.

#### 4.3.2.2 PMMA-b-PS

The preferred monomer addition sequence in the formation of Sty/MMA block copolymers is that of adding Sty as a second monomer to a homopolymer of MMA.

##### *a) Shot addition*

Addition of the monomer in a single shot to the reaction mixture resulted in an immediate improvement in block formation. The following results were obtained for the copolymers synthesized from the starting blocks mediated by CVADTB and CVATTB.

##### *(i) CVADTB*

Several distributions of polymer can be identified in the chain extension of the PMMA mediated by the dithiobenzoate RAFT agent with Sty via a shot addition, as shown in Figure 4.14. To report  $\bar{M}_{n,SEC}$  and  $\bar{M}_w/\bar{M}_n$  values would not provide significant information but an evaluation of the distributions is useful.

## Chapter Four: Homogeneous RAFT Polymerizations

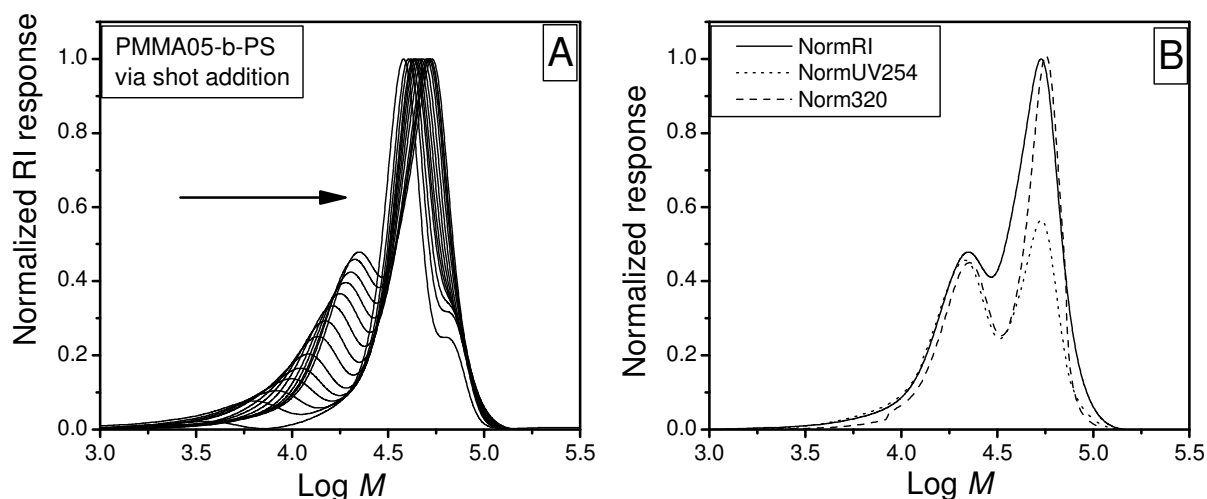


Figure 4.14 A: Size-exclusion chromatograms of the block formation of MMA05 mediated by CVADTB extended with PS via monomer shot addition. See Table 4.3 for experimental details. B: The UV-RI response overlays of the final sample in the block copolymerization reaction of the same polymer in A. The dotted line represents UV absorbance at 254nm, while the dashed line represents UV absorbance at 320nm.

The growth of a low molecular weight living peak, which is almost certainly homopolymer of PS in the system mediated via the RAFT process, is clearly illustrated in plot A. In addition, there is the initial living PMMA peak that is being chain extended as well as a higher molecular weight peak that becomes masked by the larger distribution as the polymerization proceeds. In plot B, the UV-RI response overlays of the final sample in the polymerization assisted in identifying these distributions. The presence of Sty homopolymer at the lower molecular weight end, as well as the fact that chain extension did occur, is confirmed. There is a strong 320nm UV absorbance in the second, higher molecular weight distribution, while the 254nm response is reduced. This indicates that the distribution comprises of PMMA chains that have Sty attached to them. The additional uncontrolled species at the furthest end is most likely terminated material, whether from the starting segment or the block material itself.

### (ii) CVATTB

For the chain extension of the PMMA mediated by a trithiocarbonate with Sty via a shot addition a similar behaviour to the dithiobenzoate was found. SEC results are not documented for the same argument mentioned in (i) previously.

## Chapter Four: Homogeneous RAFT Polymerizations

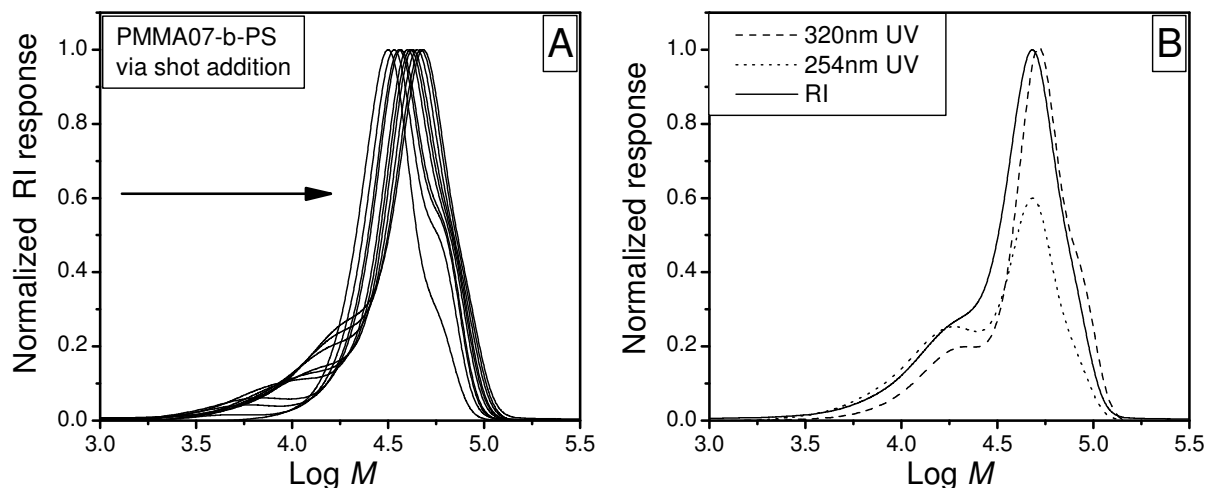


Figure 4.15 A: Size-exclusion chromatograms of the block formation of MMA07 mediated by CVATTB extended with PS via a monomer feed system. See Table 4.3 for experimental details. B: The UV-RI response overlays of the final sample in the block copolymerization reaction of the same polymer in A. The dotted line represents UV absorbance at 254nm; while the dashed line represents UV absorbance at 320nm.

The low molecular weight peak attributed to PS, the initial controlled polymer of PMMA, its chain extended derivative, and the higher molecular weight peak consistent with a termination by combination mechanism, are all present. In monomers that display high degrees of branching it has also been observed that a tripling of molecular weight occurs due to the formation of three arm stars. As neither of the monomers used here display excessive branching it is unlikely that this is the explanation for the behaviour observed. The difference in mediation behaviour seems to play a role in the amount of styrene homopolymer forming after its addition to the system. Upon investigating the 254nm UV response, it appears as if more styrene units were incorporated for chain extension. It also appears that some of the initial PMMA chains experienced a loss of RAFT agent functionality due to termination reactions.

### b) Feed addition

#### (i) CVADTB

The use of the feed addition system for the chain extension of MMA05 again led to the formation of a homopolymer contaminant. In comparison with the polymer presented in Figure 4.14, the distribution in Figure 4.16 shows a decreased amount of contaminant at the low molecular weight side. Again, this suggests that the Sty monomer fed into the system was much rather inclined to block formation than homopolymerization. This is indicative of the positive influence that monomer feed systems have in block copolymer purity.

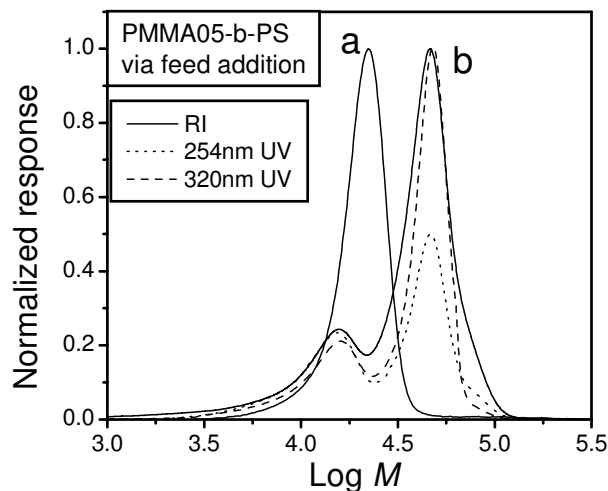
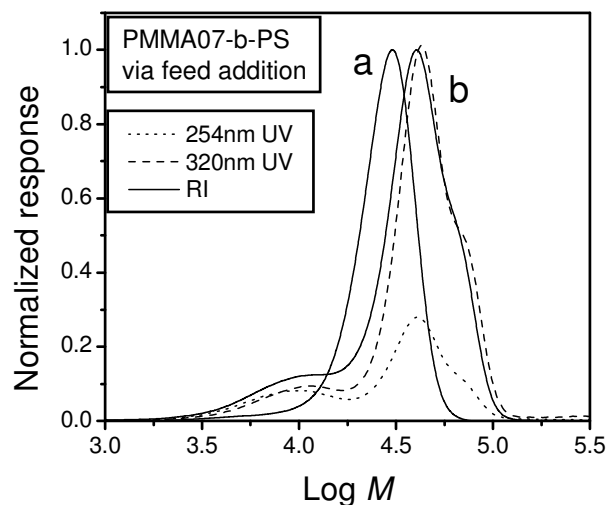


Figure 4.16 Size-exclusion chromatograms of the block formation of MMA05 mediated by CVADTB extended with PS via a monomer feed system (b). See Table 4.3 for experimental details. The UV-response overlays of the block copolymer are presented: the dotted line represents UV absorbance at 254nm; while the dashed line represents UV absorbance at 320nm. The RI response of the starting block material (a) is also included.

The presence of a higher molecular weight shoulder is still observed, the cause of which is probably similar to that explained in the case of Figure 4.14. Due to a lower final conversion compared to the shot addition reaction, its presence is not masked. To argue that termination occurred to a larger extent in the feed system would be over-simplifying.

**(ii) CVATTB**

The chain extension of MMA07 with Sty shows similar behaviour to that in the shot addition. The decrease in the lower molecular weight PS species is consistent with the other results found for the feed systems. The loss of UV signal in this instance suggests that much shorter PMMA chains were also formed in the process.

*Chapter Four: Homogeneous RAFT Polymerizations*

*Figure 4.17 Size-exclusion chromatograms of the block formation of MMA07 mediated by CVATTB extended with PS via a monomer feed system (b). See Table 4.3 for experimental details. The UV-response overlays of the block copolymer are presented; the dotted line represents UV absorbance at 254nm; while the dashed line represents UV absorbance at 320nm. The RI response of the starting block material (a) is also included.*

The initial PMMA polymer show evidence of block formation as a clear positive shift in molecular weight can be seen from the normalized signals. The chain extended derivative has a fair amount of Sty segments incorporated, yet the increased presence of the high molecular weight shoulder indicating an increase in termination reactions within the system is noticeable.

## 4.4 Conclusions

### (i) Styrene and methyl methacrylate polymers

The synthesis of polystyrene and polymethyl methacrylate polymers mediated by 4-cyano-4-((thiobenzoyl) sulfonyl) pentanoic acid (cyanovaleric acid dithiobenzoate) (CVADTB) and S-4-cyanopentanoic acid-S'-benzyltrithiocarbonate (CVATTB) were successfully carried out in solution polymerization. The reactions conditions were such that it was difficult to draw strong conclusions concerning the difference in rates due to mediation behaviour of the two applied RAFT agents. Results did show that all the polymers synthesized were equipped to perform further block copolymerization reactions.

- The differences between the rates of polymerization were not significant enough to be able to conclude that the RAFT agents provided different polymerization behaviour. Results showed a minimal difference in terms of rate effects in the Sty polymerization runs while in the MMA runs, the trithiocarbonate showed signs of controlled polymerization occurring, yet the dithiobenzoate mediated runs were subjected to artifacts in the system. In contrast as to what was expected, it appeared unlikely that the rate of polymerization in the reaction mediated by the trithiocarbonate were much higher than that of the dithiobenzoate under the conditions used.
- For both model monomers, CVATTB mediated polymerizations provided the better control. The polydispersity values obtained were similar verging lower than those of the dithiobenzoate mediated runs and  $\bar{M}_{n,SEC}$  values fitted the theoretical values excellently. CVADTB still provided sufficient control as indicated from the UV-RI overlays.

### (ii) Block copolymers

Block copolymer formation in both sequence PS-b-PMMA and PMMA-b-PS was successfully carried out in solution polymerization using PS and PMMA mediated by CVADTB and CVATTB as RAFT agents.

#### a) PS-b-PMMA

- Despite this polymerization sequence traditionally being the unfavorable one, block formation did occur in all instances.
- The behaviour of the RAFT agents lending their polymers to chain extensions is similar within each addition method. The trithiocarbonate showed a more pronounced shift on the log M scale in the shot addition method compared to the

## Chapter Four: Homogeneous RAFT Polymerizations

---

dithiobenzoate, suggesting a larger amount of block formation occurring vs that of dithiobenzoate.

- Although conversions obtained for the feed systems were much lower than that of the shot additions, it appears as if the quality of blocks were much improved. The CVATTB feed system, showed little evidence of either low or high molecular weight impurities present and represented the best result in the data set of this polymerization sequence.

### b) PMMA-b-PS

- The preferred sequence of block formation proved to be more complex. The block copolymer distributions obtained via SEC analysis indicated that several different species were present. Their composition varied from homopolymer formed from the newly added monomer to the desired block copolymer as well as terminated material. The extent to which the above mentioned was present depended on the particular RAFT agent being addressed as well as the method of addition.
- With regards to the shot addition, the mediation behaviour of the CVATTB end-capped polymer was similar to that of the dithiobenzoate. Less PS homopolymer was present and it appears that the block copolymer component of the distribution obtained was of higher quality as less terminated material seemed to be present.
- The feed addition method gave the best result, as much less homopolymer contaminant was formed in the process and although the presence of the high molecular weight shoulder is still observable it is much less prevalent.

Analysis showed that block copolymer synthesis can successfully be achieved in both polymerization sequences. The mediation behavior of CVATTB to allow block formation has proven to be superior or at least similar compared to that of CVADTB, depending on the addition strategy and the polymerization sequence. Size-exclusion chromatography was useful in determining whether block formation occurred but more in depth investigations are required before any definite conclusions can be made with regards to block copolymer purities. This study however confirms that optimal results can be obtained via the use of the feed addition strategy.

---

*Chapter Four: Homogeneous RAFT Polymerizations*

---

**4.5 References**

- (1) Albertin, L.; Stenzel, M. H.; Barner-Kowollik, C.; Foster, L. J. R.; Davis, T. P. *Macromolecules* **2005**, *38*, 9075-9084.
- (2) Jahanzad, F.; Karatas, E.; Saha, B.; Brooks, B. W. *Colloids Surf., A: Physicochem Eng Asp* **2007**, *302*, 424-429.
- (3) Rizzardo, E.; Chiefari, J.; Chong, B. Y. K.; Ercole, F.; Krstina, J.; Jeffery, J.; Le, T. P. T.; Mayadunne, R. T. A.; Meijs, G. F.; Moad, C.; Moad, G.; Thang, S. H. *Macromol Symp* **1999**, *143*, 291-307.
- (4) Thomas, D. B.; Convertine, A. J.; Myrick, L. J.; Scales, C. W.; Smith, A. E.; Lowe, A. B.; Vasilieva, Y. A.; Ayres, N.; McCormick, C. L. *Macromolecules* **2004**, *37*, 8941-8950.
- (5) Chiefari, J.; Chong, Y. K. B.; Ercole, F.; Krstina, J.; Jeffery, J.; Le, T. P. T.; Mayadunne, R. T. A.; Meijs, G. F.; Moad, C. L.; Moad, G.; Rizzardo, E.; Thang, S. H. *Macromolecules* **1998**, *31*, 5559-5562.
- (6) Monteiro, M. J.; de Brouwer, H. *Macromolecules* **2001**, *34*, 349-352.
- (7) Moad, G.; Chiefari, J.; Chong, B. Y.; Krstina, J.; Mayadunne, R. T.; Postma, A.; Rizzardo, E.; Thang, S. H. *Polym Int* **2000**, *49*, 993-1001.
- (8) Goto, A.; Sato, K.; Tsujii, Y.; Fukuda, T.; Moad, G.; Rizzardo, E.; Thang, S. H. *Macromolecules* **2001**, *34*, 402-408.
- (9) Barner-Kowollik, C.; Buback, M.; Charleux, B.; Coote, M. L.; Drache, M.; Fukuda, T.; Goto, A.; Klumperman, B.; Lowe, A. B.; McLeary, J. B.; Moad, G.; Monteiro, M. J.; Sanderson, R. D.; Tonge, M. P.; Vana, P. *J Polym Sci Part A: Polym Chem* **2006**, *44*, 5809-5831.
- (10) Barner-Kowollik, C.; Quinn, J. F.; Nguyen, T. L. U.; Heuts, J. P. A.; Davis, T. P. *Macromolecules* **2001**, *34*, 7849-7857.
- (11) Vana, P.; Davis, T. P.; Barner-Kowollik, C. *Macromol Theory Simul* **2002**, *11*, 823-835.
- (12) Weber, W. G.; McLeary, J. B.; Sanderson, R. D. *Tetrahedron Lett* **2006**, *47*, 4771-4774.
- (13) Benaglia, M.; Rizzardo, E.; Alberti, A.; Guerra, M. *Macromolecules* **2005**, *38*, 3129-3140.
- (14) Chong, Y. K. B.; Krstina, J.; Le, T. P. T.; Moad, G.; Postma, A.; Rizzardo, E.; Thang, S. H. *Macromolecules* **2003**, *36*, 2256-2272.
- (15) Peklak, A. D.; Butte, A.; Storti, G.; Morbidelli, M. *J Polym Sci Part A: Polym Chem* **2006**, *44*, 1071-1085.
- (16) Matyjaszewski, K.; Davis, T. P. *Handbook of Radical Polymerization*; John Wiley and Sons, Inc: Hoboken, **2002**; pp 846-847.
- (17) Buback, M.; Gilbert, R. G.; Hutchinson, R. A.; Klumperman, B.; Kuchta, F.-D.; Manders, B. G.; O'Driscoll, K. F.; Russell, G. T.; Schweer, J. *Macromol Chem Phys* **1995**, *196*, 3267-3280.
- (18) Quinn, J. F.; Rizzardo, E.; Davis, T. P. *Chem Comm* **2001**, 1044-1045.
- (19) Arita, T.; Buback, M.; Vana, P. *Macromolecules* **2005**, *38*, 7935-7943.
- (20) Rizzardo, E.; Chen, M.; Chong, B. Y. K.; Moad, G.; Skidmore, M.; Thang, S. H. *Macromol Symp* **2007**, *2*, 104-116.
- (21) Le, T. P.; Moad, G.; Rizzardo, E.; Thang, S. H.; In PCT. Int. Appl.; wo98/01478; **1998**
- (22) Moad, G.; Solomon, D. H. *The Chemistry of Free Radical Polymerization*, 2nd Ed.; Elsevier Science Ltd: Oxford, **2006**.
- (23) Matyjaszewski, K.; Davis, T. P. *Handbook of Radical Polymerization*; John Wiley and Sons, Inc: Hoboken, **2002**.
- (24) Chong, B. Y. K.; Le, T. P. T.; Moad, G.; Rizzardo, E.; Thang, S. H. *Macromolecules* **1999**, *32*, 2071-2074.

## ***Chapter 5: RAFT Mediated Miniemulsion Polymerizations***

### **Abstract**

The methodologies was first, to polymerize styrene and methyl methacrylate respectively with either RAFT agent CVADTB or CVATTB by miniemulsion polymerization and then through a second stage, polymerize the second monomer to prepare block copolymers either under shot, pre-swelling or feed conditions. The polymers were characterized by double detection [i.e. ultraviolet (UV) and differential refractive detector (DRI)] size exclusion chromatography. Latex properties were investigated via TEM and particle size analysis.

*Excerpts from the following two chapters were the main focus of the poster “Analysis of RAFT mediated miniemulsion block copolymers” which was one of the eight selected student oral presentations at the International Symposium on Radical Polymerization: Kinetics and Mechanism (SML) Conference 2006 meeting, Il Ciocco, Tuscany – Italy.*

## 5.1 Introduction

With the introduction of living/controlled radical polymerization to prepare novel polymers with designer architectures invoking the interest of academia and industry<sup>1</sup>, the challenge soon arose to prepare these architectures in an environmentally friendly media such as water.<sup>2-5</sup> The polymerization kinetics are however complicated by the partitioning of the activating species between different phases, their transportation rate as well as that of larger dormant compounds to the reaction loci, surfactant choices and the control over particle size distributions. During the early years of implementing living radical polymerization in dispersed media, these systems had however become notorious for having problems associated with loss of living character and colloidal stability. These effects have been thoroughly investigated by Prescott *et al.*<sup>6-8</sup> Living radical polymerization techniques based on degenerative transfer have proven to be more successful, as the number of active radical species is not affected in the system. A large number of studies relate to RAFT polymerization in heterogeneous media and the latest reviews were published by McLeary and Klumperman<sup>9</sup> and Save *et al.*<sup>10</sup> Early work showed that RAFT mediated batch emulsion polymerization yielded less satisfactory results<sup>11,12</sup> and it was suggested that the poor performance was probably related to the diffusion and/or localization issues of the transfer agent, which can be overcome by avoiding its transport through the aqueous phase. Miniemulsion polymerization eliminates this problem as the reagents are present within the polymerization loci at the onset of polymerization and will ideally be homogeneously distributed between the particles. The use of the RAFT process in miniemulsion polymerization initially yielded low conversions<sup>13,14</sup> (not higher than 40%) and several difficulties had to be overcome. Ionic surfactants failed to give stable latexes in studies done by de Brouwer<sup>15</sup> and Tsavalas<sup>16</sup> when using dithiobenzoates as RAFT agents, but more success was obtained in substituting them with nonionic surfactants. Theoretical analyses were conducted by Luo *et al.*<sup>17,18</sup> to provide an explanation for the lack of efficiency. Further investigations carried out by several groups<sup>19-22</sup> resulted in successful polymerization of ionically stabilized latexes. Despite the fact that the application of RAFT in dispersed media is not without its difficulties the advantages of compartmentalization can still be exploited.

The work presented in this chapter involves the RAFT mediated miniemulsion polymerization of styrene and methyl methacrylate and the use of the obtained stable latexes as seeds for block copolymerization. The investigation can be divided into two sections. Part one discusses the

## *Chapter Five: Miniemulsion Polymerizations*

---

syntheses of RAFT-mediated homopolymers exhibiting “living/controlled” characteristics with established miniemulsion procedures and recipes, implementing an oil-soluble initiator, ionic surfactant, hexadecane as ultra-hydrophobe, and two different RAFT agents. Investigations were carried out to determine the degree of control of molecular weight, the behaviour of the reaction rates for polymerizations with each of the RAFT agents, and the typical sizes of the particles obtained in the latexes. Part two provides experimental evidence on how compartmentalization in dispersed systems can be manipulated with the use of a living technique, such as the RAFT process, to infer living character and provide improved block copolymer purity by varying the method by which the second monomer is added to the system. It illustrates the block copolymer synthesis by using the homopolymer latexes as seeds; thereby investigating the ability of the respective RAFT agents to yield block polymers of controlled architecture in aqueous media. Two different block sequences were attempted and three different monomer addition methods were used. Analyses of the block copolymers were carried out using SEC, particle size analysis and transmission electron microscopy (TEM) analysis.

## **5.2 Experimental**

### **5.2.1 Materials/Reagents**

Cetyl trimethylammonium bromide (CTAB) [57-09-0] 99% (Acros Organics); hexadecane [544-76-3] 99% (Aldrich) and azobis (isobutyronitrile) (AIBN) (Riedel de Haen) were used as received. Styrene (99.5%, Protea chemicals) and MMA (99.9%, ICI Chemicals and Polymers) were washed with a 0.3 M KOH solution to remove inhibitors and then distilled under reduced pressure. The water used in all reactions was distilled de-ionized (DDI) water, obtained from a Millipore Milli-Q purification system.

### **5.2.2 General**

The syntheses of the two RAFT agents used, 4-cyano-4-((thiobenzoyl) sulfonyl) pentanoic acid (cyanovaleric acid dithiobenzoate) (1) and S-4-cyanopentanoic acid-S'-benzyltrithiocarbonate (2) were described in Chapter 3 (Section 3.2). The presentation of the structures is repeated here to assist the reader in the discussions in this chapter.

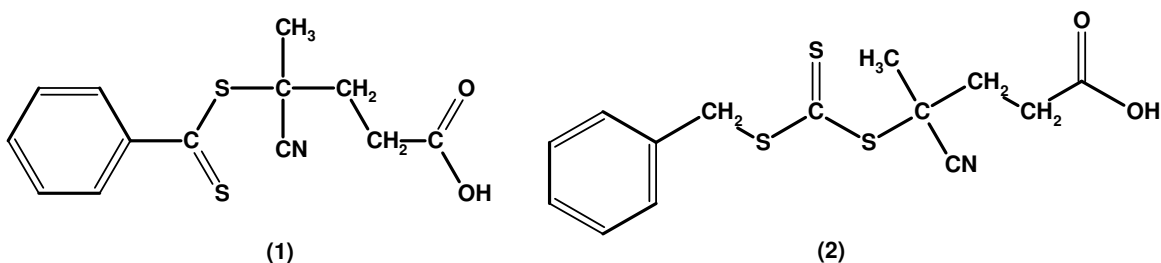
*Chapter Five: Miniemulsion Polymerizations*

Figure 5.1 Chemical structures of RAFT agents 4-cyano-4-((thiobenzoyl) sulfonyl) pentanoic acid (cyanovaleic acid dithiobenzoate) (CVADTB) (1) and S-4-cyanopentanoic acid-S'-benzyltrithiocarbonate (CVATTB) (2).

### 5.2.3 Miniemulsion preparation procedure

In the preparation of the pre-emulsion mixtures, the components of the oil and water phase were dissolved separately. CTAB (2g) was dissolved in DDI water (80g), while AIBN (0.1g), RAFT agent 1 or 2 (0.25g) and hexadecane (0.8748g) were dissolved in monomer (20g). The two phases were mixed and then subjected to a high stir rate for approximately 60 min. The pre-emulsion was sonicated at 80% amplitude (energy) for 15 min at 50°C in a temperature-controlled vessel to minimize heating of the pre-emulsion, using a Sonics and Material Vibra cell Autotune series high intensity ultrasonic processor 750 VCX, with no pulse.

### 5.2.4 Polymerizations

#### 5.2.4.1 RAFT mediated miniemulsion homopolymerization of styrene and methyl methacrylate

The miniemulsion polymerization of styrene and methyl methacrylate was carried out under a nitrogen atmosphere at 75°C and 80°C, respectively. The sonicated pre-emulsion mixture was transferred to a three neck round bottom flask and degassed under continuous stirring. The reaction was allowed to commence immediately to avoid (or minimize) the chance of the latex destabilizing. For this purpose the oilbath was preheated to the desired temperature. After completion of the reaction, the final latex was cooled and stored. Reaction details for the polymerization reactions of the starting block polymers are tabulated in Table 5.1.

*Chapter Five: Miniemulsion Polymerizations*

*Table 5.1 Quantities of reagents and temperatures used for the RAFT-mediated polymerizations of styrene and methyl methacrylate in miniemulsion. The Sty polymerizations were carried out at 75 °C, while the MMA polymerizations were done at 80 °C.*

Reaction number	Monomer (mol)	RAFT agent	RAFT (mol x 10 <sup>-4</sup> )	AIBN (mol x 10 <sup>-4</sup> )	Hexadecane (mol x 10 <sup>-3</sup> )	CTAB (mol x 10 <sup>-3</sup> )	DDI water (g)	Reaction time (h)
mSty08	0.1921	CVADTB	9.149	6.364	3.865	5.531	81.53	26
mSty09	0.1928	CVADTB	9.016	6.151	3.856	5.652	80.03	22
mSty12	0.1958	CVATTB	8.618	6.565	3.877	5.488	80.03	22
mSty14	0.1921	CVATTB	9.168	6.126	3.878	5.488	80.87	7
mMMA01	0.1999	CVADTB	8.988	6.181	3.809	5.508	80.05	4
mMMA03	0.1998	CVADTB	8.969	6.346	3.869	5.499	80.09	2
mMMA06	0.2010	CVATTB	9.118	6.400	3.891	5.501	80.02	4
mMMA07	0.2002	CVATTB	9.128	6.406	3.892	5.570	81.69	2

**5.2.4.2 Chain extension of starting block polymers**

A calculated mass of the starting block polymer latex was placed in a reactor under continuous nitrogen purging and stirring. The solids content was kept constant by the addition of DDI water. The reaction commenced immediately after the addition of fresh monomer and initiator via three different strategies: shot addition, which involved the addition of monomer and initiator in one shot, after which the reaction started immediately; “pre-swelling”, which involved stirring of the latex overnight at room temperature after the addition of monomer and initiator before polymerization took place and “feed addition”, which occurred via a feed pump system at a specified rate. The rate of addition in the last approach depended on the monomer concentration to be added and the reaction time anticipated for the polymerization to be completed. In this particular reaction the polymerization commenced at the beginning of the additions. Feed additions were performed with the use of a Metrohm 711 Liquino and 700 Dosino (Swiss Labs). After the completion of the reactions the latexes were left to cool, then stored. The experimental details of the block copolymerization reactants from the seeded latexes are described in Section 5.3.2.

## *Chapter Five: Miniemulsion Polymerizations*

---

### **5.2.5 Kinetic analysis**

Samples of the reaction mixtures were taken at time intervals throughout the polymerizations for gravimetric analysis to follow conversion of monomer to polymer. Samples were removed via a septum by needle, placed into sample pans and left to dry. All sample sets were further dried in a vacuum oven at appropriate temperatures.

### **5.2.6 SEC analysis**

Molecular weights of the kinetic samples were determined using SEC. The SEC instrument comprised of a Waters 1515 isocratic HPLC pump, a Waters 717 plus auto-sampler, Waters 600E system controller (run by Breeze Version 3.30 SPA) and a Waters 610 fluid unit. A Waters 2414 differential refractometer was used at 30°C in series with a Waters 2487 dual wavelength absorbance UV/Vis detector operating at variable wavelengths. Tetrahydrofuran (THF, HPLC grade, stabilized with 0.125% BHT), sparged with IR-grade helium, was used as eluent at flow rates of 1 ml min<sup>-1</sup>. The column oven was kept at 30°C and the injection volume was 100  $\mu$ l. Two PLgel (Polymer Laboratories) 5  $\mu$ m Mixed-C (300x7.5 mm) columns and a pre-column (PLgel 5  $\mu$ m Guard, 50x7.5 mm) were used. Calibration was done using narrow polystyrene standards ranging from 800 to 2x10<sup>6</sup> g mol<sup>-1</sup> (Polymer Labs). All molecular weights were reported as polystyrene equivalents.

### **5.2.7 Particle size analysis**

Particle sizes were determined by dynamic light scattering using a Malvern Instruments Zetasizer 100 HA<sub>S</sub> with a fixed scattering angle of 90° at 25°C, assuming monomodal distribution. The software for data processing was Malvern Instruments, PCS v1.61 @Malvern Instruments Ltd. 2002. 10mmol NaCl nanostandards were used to reference the instrument and for light scattering determinations. The latexes were diluted with 10mmol NaCl solution.

### **5.2.8 Transmission electron microscopy**

TEM images were obtained from the JEOL 200 CX instrument at the University of Cape Town's electron microscopy unit. Aliquots of samples were diluted with distilled water. Solutions were homogenized by shaking and then transferred to a copper TEM grid by pipette. The grid was left to dry at ambient temperature before analyses were performed.

## 5.3 Results and Discussion

### 5.3.1 Styrene and methyl methacrylate polymers

Established miniemulsion recipes were used to synthesize RAFT-end capped PS and PMMA polymers.<sup>21,23</sup> For both monomers, CVADTB and CVATTB were utilized, and reactions were repeated at least twice for repeatability and optimization of the reaction time for each reaction system. In all cases, stable miniemulsion latexes were obtained after completion of the polymerizations. The following results were recorded for systems containing hexadecane, AIBN, CTAB and water. Table 5.2 tabulates the results obtained in the RAFT-mediated miniemulsion polymerizations.

Table 5.2: Final polymers produced by the RAFT-mediated miniemulsion polymerizations of styrene and methyl methacrylate. The data is representative of the reactions run as shown in Table 5.1.  $f = 0$

Polymer	RAFT agent	Conversion (%)	$\bar{M}_n$ , theoretical	$\bar{M}_n$ , SEC	$\bar{M}_w/\bar{M}_n$
mPS08	CVADTB	80.43	17857	23410	1.29
mPS09	CVADTB	89.72	20260	26500	1.27
mPS12	CVATTB	97.33	23513	20351	1.29
mPS14	CVATTB	96.86	21466	22200	1.21
mPMMA01	CVADTB	94.82	21087	21550	1.11
mPMMA03	CVADTB	90.32	20422	21456	1.15
mPMMA06	CVATTB	95.42	21274	22094	1.13
mPMMA07	CVATTB	97.05	21631	21337	1.15

The polydispersities and number average molar mass values were obtained from the SEC analysis and the conversions were calculated via gravimetric analysis. In all the reactions, conversions of over 80% were obtained and polydispersities stayed well below 2. This corresponds well with the results of miniemulsion polymerization studies of Sty<sup>14,18,21,23-26</sup> and MMA<sup>21,23,27</sup> carried out by other authors using ionic surfactants. Although several studies used sodium dodecyl sulfate (SDS) as ionic surfactant, Landfester *et al* showed that CTAB could stabilize miniemulsions with an efficiency similar to SDS.<sup>28</sup>

*Chapter Five: Miniemulsion Polymerizations*

The theoretical number average molar mass values were obtained using the following equation:

$$\bar{M}_n = M_{\text{RAFT}} + \frac{x[M]_0 M_{\text{monomer}}}{[\text{RAFT}]_0 + Cf [I]_0 (1 - e^{-kdt})} \quad (5.1)$$

Where  $\bar{M}_n$  is the number average molar mass,  $M_{\text{monomer}}$  is the monomer molar mass,  $M_{\text{RAFT}}$  is the molar mass of the RAFT agent,  $[M]_0$  and  $[\text{RAFT}]_0$  are the initial concentrations of the monomer and RAFT agent respectively, and  $x$  is the fractional conversion. The efficiency factor  $f$  is the measure of the fraction of radicals that will form polymer chains and contains contributions from both the initiator efficiency and the efficiency for water phase radicals to enter polymer particles. The use of oil-soluble AIBN as initiator has several advantages,<sup>29-31</sup> which include minimizing the chance of polymerization in the aqueous phase and canceling out the presence of undesired initiator derived ionic groups.

The locus of initiation with oil-soluble initiators in (macro) emulsions is more complex than with its water-soluble counterparts. Initiator molecules can partition between the aqueous phase and the oil-phase. A long standing debate exists about the actual origin of the effective free radicals, ensuring the initiation of polymerization, as their polymerization kinetics are similar to those using water-soluble initiators. One hypothesis postulates that once the oil-soluble initiator decomposes in a micelle or particle (both small in size) the two newly generated radicals will terminate with each other before monomer propagation or radical exit can occur. Nomura *et al* believes that the effective radicals actually originate in the aqueous phase, from the small fraction of total initiator that is dissolved in the aqueous phase.<sup>32-34</sup> The other assumption supported by several authors, is that one of the newly formed radicals in a micelle or particle can desorb from the micelle or particle before mutual termination occurs. The remaining radical is then free to propagate.<sup>35-37</sup> In miniemulsion polymerization, the focus is on the nucleation of polymer particles due to radicals generated in the monomer droplets.

The use of oil-soluble initiators in miniemulsions has successfully been carried out by several authors.<sup>35,38</sup> Luo and Schork<sup>39</sup> carried out emulsion and miniemulsion polymerization using 2,2'-azobis[2-(2-imidazolin-2-yl) propane] dihydrochloride in the presence of an aqueous phase free radical scavenger. They concluded that for miniemulsion particles of up to 100nm in diameter, even with an oil-soluble initiator, radicals originating in the aqueous phase play an important role in

## *Chapter Five: Miniemulsion Polymerizations*

---

initiating polymerization. This supports the theory of the recombination of the two radicals generated from the decomposition of an initiator molecular within the particle. In studying the emulsion polymerization of Sty in seeded and unseeded systems using AIBN, Nomura *et al*<sup>32</sup> used the same theory to investigate the average number of radicals per particle, as determined by the fraction of AIBN initiator present in the aqueous phase, and the outcome of these radicals. They found that the partitioning of AIBN between water and styrene at 50°C was 1:115, indicating the low efficiency of AIBN in the systems. For the purpose of this study a simplified equation of Equation 5.1 was used to calculate the theoretical molecular weights. In order to eliminate the role of the initiator concentration in determining the theoretical molecular weights, the efficiency factor  $f$  was set at zero.

### **5.3.1.1 Rate of reactions**

The semilogarithmic plots of monomer conversion versus reaction time for the RAFT mediated miniemulsion polymerization of Sty and MMA carried out using the conditions given in Table 5.1 are presented in Figure 5.2. Plot A represents the polymerizations of mSty08 and mSty14. A significant difference can be seen between the mediation behaviour of the two RAFT agents in terms of rate effects.

## Chapter Five: Miniemulsion Polymerizations

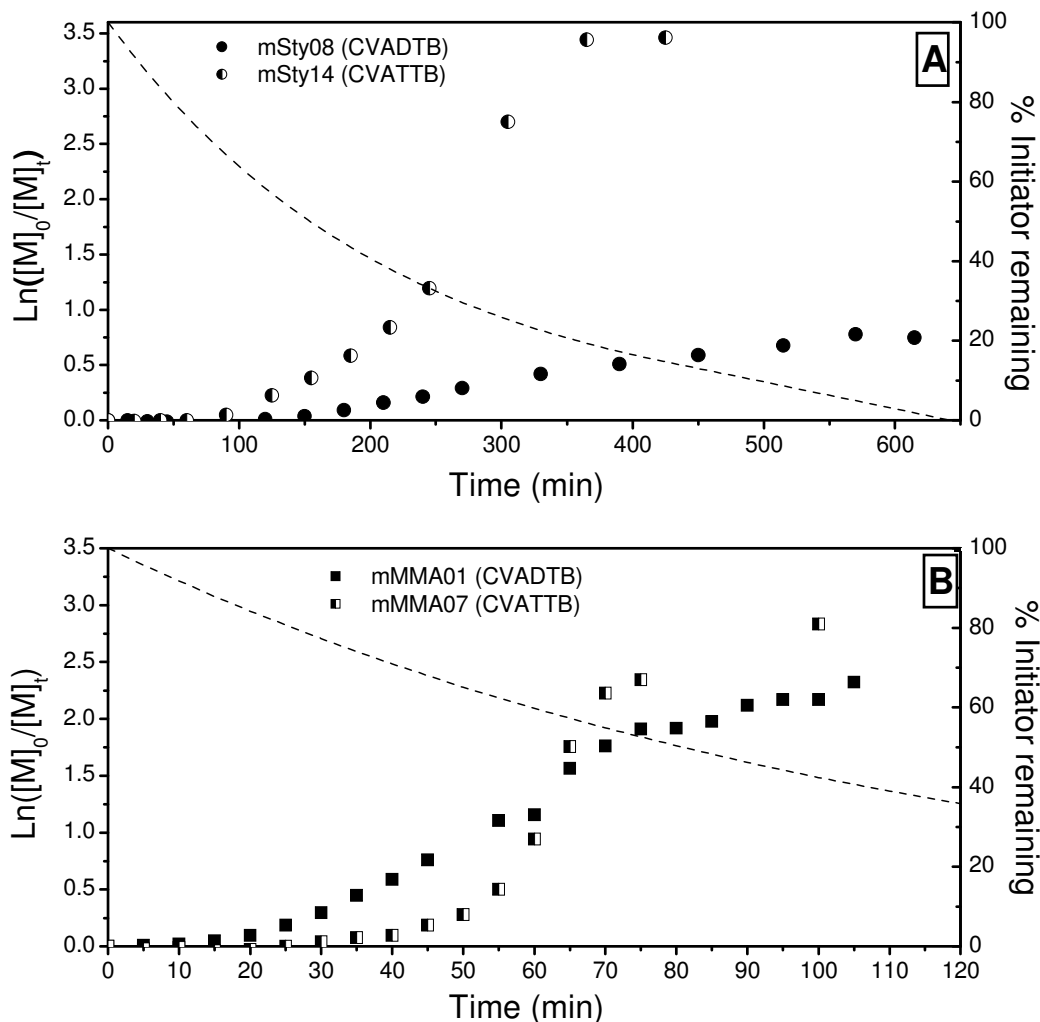


Figure 5.2 Semilogarithmic plots of monomer conversion versus reaction time. A: The styrene miniemulsion polymerization reactions of mSty08 and mSty14 at 75 °C. B: The methyl methacrylate miniemulsion polymerizations reactions of mMMA01 and mMMA07 at 80 °C. All reaction conditions were kept constant, apart from the RAFT agent type for the purpose of comparison

The polymerizations of CVATTB reached much higher conversions (Table 5.2) and the time within which the reactions ran to completion decreased from 24 to 7 hours. At the beginning of the polymerizations both reactions have a similar induction period, after which the rate of the trithiocarbonate reaction increases much faster than that of the dithiobenzoate reaction. The inhibition/retardation effect has been well documented.<sup>40,41</sup> In the RAFT process it is possible that rapid transfer of the R radicals generated from the initial RAFT agent molecules leads to the generation of short leaving groups in the initial stages of the polymerization.<sup>19</sup> These small sized radicals may undergo termination in the aqueous phase or re-entry to particles to terminate growing chains. Gilbert and coworkers<sup>8</sup> found that these reactions could cause a RAFT-induced exit of

## *Chapter Five: Miniemulsion Polymerizations*

---

radicals from the particles, leading to retardation of polymerization rate. The fairly water-soluble R group forming after fragmentation is exactly the same for both RAFT agents, hence the similar induction periods is due to similar migration behaviour to the aqueous phase of these radicals in the system.<sup>20</sup> The influence of RAFT reactions on the (mini) emulsion polymerization kinetics was also investigated using the modified Smith-Ewart theory.<sup>18</sup> It was found that the rate of retardation is an intrinsic kinetic property of RAFT (mini)emulsion polymerization, even in the case where the RAFT-induced exit is negligible.

Typically, the polymerization reactions of methyl methacrylate occurred within a much shorter reaction time as MMA has a higher propagation rate constant than Sty and the reaction temperature was slightly higher. Conversions of over 90% were obtained in less than 4 hours for both RAFT agents, and although the trithiocarbonate mediated polymerizations gave higher final conversion values the difference between the latter and the dithiobenzoate mediated polymerization is not as pronounced as in the styrene runs. Figure 5.2 B, shows that the inhibition period was longer for CVATTB and up to half way into the polymerization, the rate was lower than that of the CVADTB mediated run. The sharp increase later in the propagation rate can be explained in terms of the stability of the intermediate radical being formed in the RAFT process.

Since the AIBN concentration and reaction temperatures for the polymerizations were identical for each monomer set, the radical generation rate is the same and the calculated percentage of AIBN remaining in the reaction is shown as the dashed curve in the graphs. The intermediate radical of the thio-carbonyl moiety of the trithiocarbonate is less stable than that of the dithiobenzoate, therefore fragmentation, releasing the R-group for further polymerization before the propagating radicals are trapped again, proceeds faster. The total radical population is a ratio between intermediate and propagating radicals, therefore increasing the one decrease the other. The concentration of propagating species is higher in the case of the trithiocarbonate, resulting in a faster rate of polymerization. CVATTB showed a much faster rate for both monomer polymerizations compared to CVADTB.

### **5.3.1.2 Molecular weight distribution in RAFT mediated miniemulsion polymerization**

Information on the evolution of molecular weight as a function of conversion was obtained by SEC analysis. The values of the molecular weight and polydispersities were obtained from the refractive index (RI) traces of the SEC analysis. Figure 5.3 A shows the evolution of molecular weight and polydispersity with conversion for the polymerization reactions of mSty08 and mSty14.

## Chapter Five: Miniemulsion Polymerizations

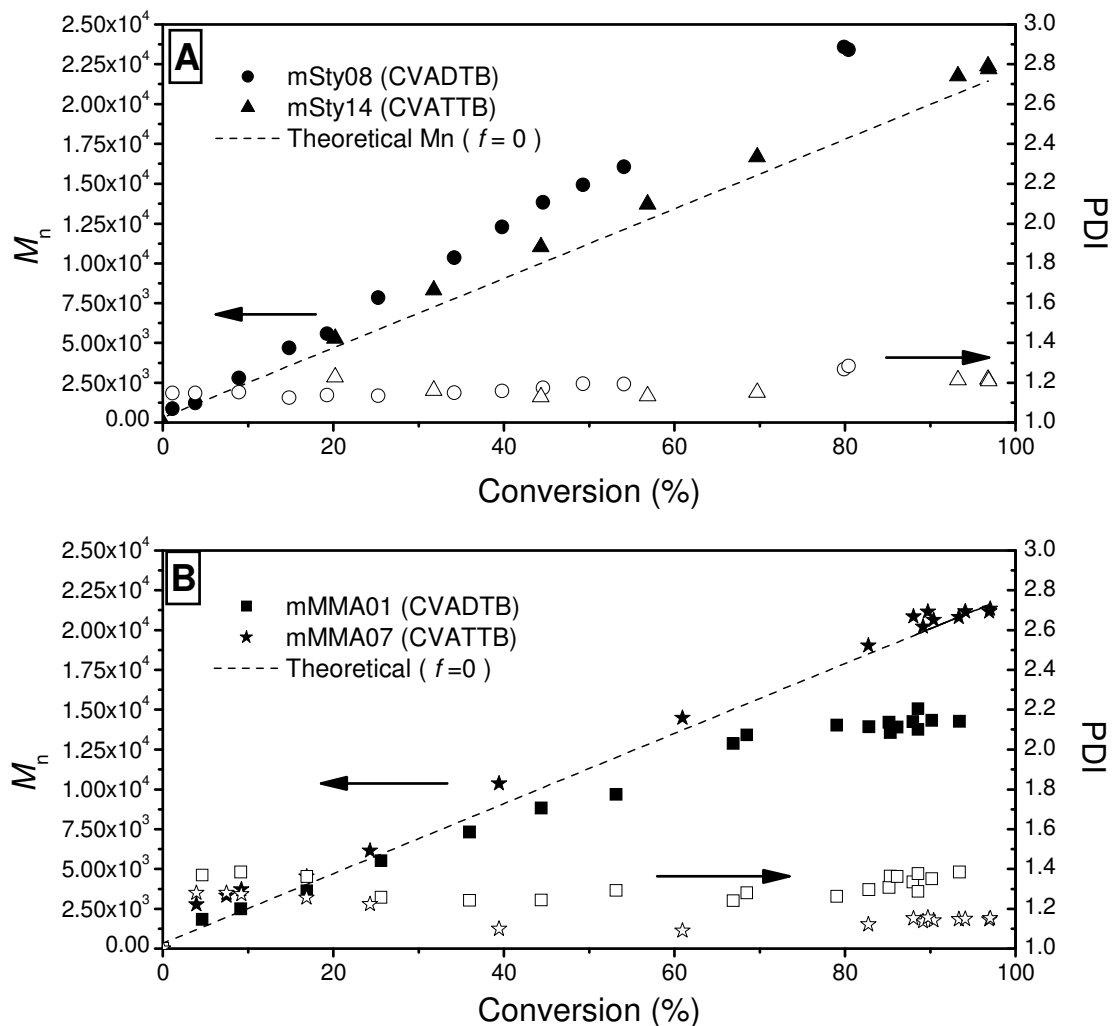


Figure 5.3 Evolution of  $\bar{M}_n$  and PDI with conversion. A: The miniemulsion polymerization of styrene at 75 °C in the presence of CVADTB (mSty08) and CVATTB (mSty14). B: The miniemulsion polymerization of methyl methacrylate at 80 °C in the presence of CVADTB (mMMA01) and CVATTB (mMMA07).

The reactions for both RAFT agents CVADTB and CVATTB showed a linear increase of molecular weight with increasing conversion. Up to 20% conversion the RAFT agents exhibited similar behaviour, after which the dithiobenzoate data started drifting from the theoretical value of  $\bar{M}_n$ .

The deviation can be explained by the appearance of a secondary distribution on the high molecular weight end of the scale. This is illustrated in the chromatogram in Figure 5.4, where it is clear that there is a fair amount of high molecular weight polymer present which contributes to the experimental  $\bar{M}_n$  values. The trend is supported by the polydispersity values which start off at 1.15,

*Chapter Five: Miniemulsion Polymerizations*

decrease during the polymerization to 1.13 and then start to increase slowly to give an end value of 1.29.

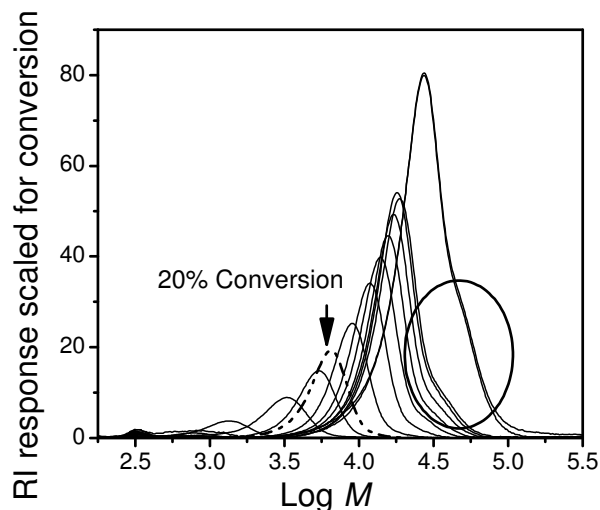


*Figure 5.4 Size-exclusion chromatograms of the molecular weight distribution of polystyrene synthesized in the presence of CVADTB (mPS08). The high molecular weight secondary distribution creating the increase in polydispersity values in Figure 5.3 A is encircled.*

The results obtained from mSty14 indicated that the  $\bar{M}_n$  values of the styrene polymer from CVATTB had an improved fit over that of CVADTB to the theoretically calculated  $\bar{M}_n$  and the final polydispersity values were lower. Although slight tailing occurred at the higher molecular weight end (Figure 5.5), much less termination occurred as the reaction time was shorter and the effect was less than in the case of CVADTB. Overall, CVATTB provided much better control compared to CVADTB for the Sty polymerizations.

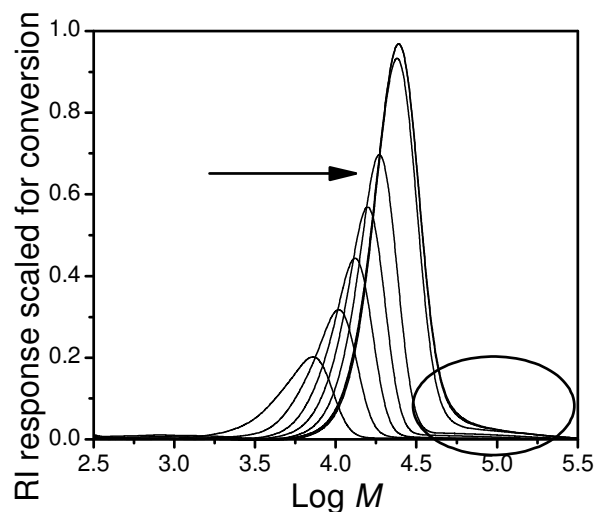


Figure 5.5 Size-exclusion chromatograms of the molecular weight distribution of polystyrene synthesized in the presence of CVATTB (mPS14).

The evolution of molecular weight and polydispersity with conversion for the MMA reactions of mMMA01 and mMMA07 are shown by Figure 5.2 B. For CVATTB there was a linear increase in molecular weight with conversion throughout the reaction and polydispersities decreased from 1.28 at the onset of the reaction to 1.15. The lowest experimental value for polydispersity was found to be 1.09, after which it increased at higher conversion. Initially, at low conversion (<10%), the experimental  $\bar{M}_n$  was higher than that of the theoretical value which could be due to the fact that not all the RAFT agent has been consumed at this stage. The molecular weight is significantly higher than that expected based on the complete consumption of RAFT agent during this period.<sup>42</sup> This slow consumption of RAFT agent correlates to the longer induction period found in the CVATTB mediated MMA polymerization (mMMA07, Fig 5.2 B). Besides the radical exit phenomenon, the consumption of CVATTB was less efficient than CVADTB. Figure 5.6 shows the chromatograms of the PMMA distributions of mPMMA07. The molecular weight distribution at low conversion shows bimodality, suggesting oligomeric material is present that can either be consumed or as the concentration of higher molecular weight material increases, simply becomes invisible.

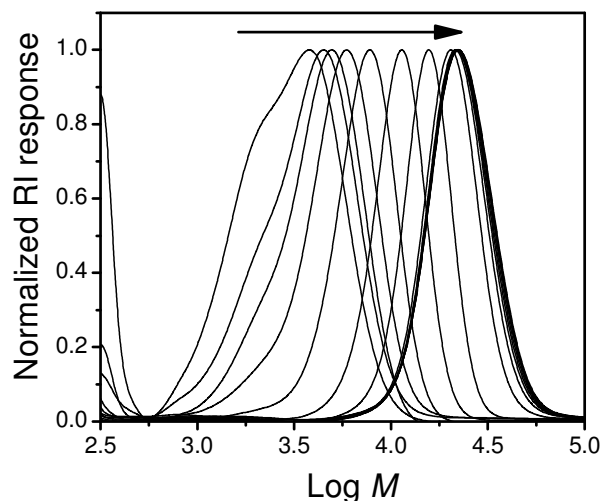


Figure 5.6 Size-exclusion chromatograms of the molecular weight distribution of poly(methyl methacrylate) synthesized in the presence of CVATTB (mPMMA07).

Barner-Kowollik *et al*<sup>43</sup> discussed a hybrid behaviour of “conventional” chain transfer and living free radical polymerization in a RAFT mediated MMA based system. The RAFT agent was depleted at a slower rate, allowing a “conventional” chain transfer distribution to emerge and the onset of the reversible addition fragmentation equilibrium was delayed. Once the conversion increased above 25%, the bimodality character of the distribution disappeared and the polydispersities started to decrease.

In the present study, after 16% conversion the data set correlated very well with the theoretical values and a marked decrease in polydispersity values can be observed.

The deviation of the  $\bar{M}_n$  values from theory in the case of the PMMA with CVADTB is very typical (Fig 5.3 B). At very high conversions the measured number average molecular weight decreases due to the formation of shorter chains. The polydispersities are higher than that obtained from the trithiocarbonate RAFT agent polymers, yet it still shows controlled polymerization character with a final value of 1.3. The broadening in values can be explained by the tailing as seen in the molecular weight distribution chromatograms of this reaction (Fig 5.7). It is likely that there is material present early in the reaction that does not grow. The UV-RI overlays will shed more light on this matter.

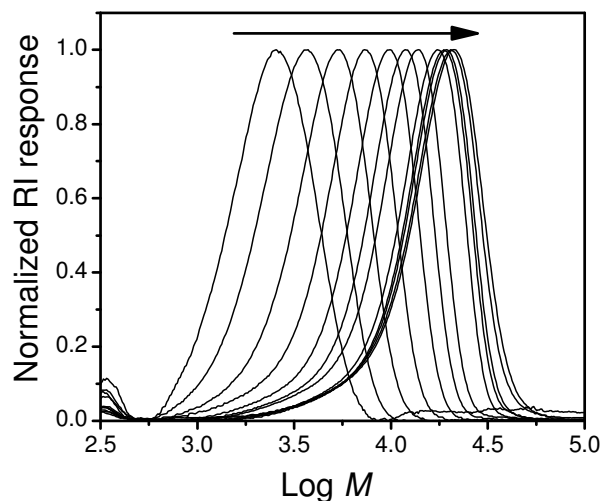


Figure 5.7 Size-exclusion chromatograms of the molecular weight distribution of poly(methyl methacrylate) synthesized in the presence of CVADTB (mPMMA01).

### 5.3.1.3 UV-RI analysis

In the following section the UV-RI overlays are investigated for the miniemulsion polymers of PS and PMMA synthesized and discussed in preceding sections. The nature of each polymer in Table 5.2 at different stages of its polymerization was studied by how well the UV response corresponded with that of the RI. As discussed in Chapter 4 (Section 4.3.1.3) the presence of the RAFT moiety was clarified using UV analysis through the dual detection available during SEC analysis. Keeping in mind that the RAFT moiety is known to absorb in a wavelength range of 280-350nm and that it has been established (Chapter 3) that the thiocarbonyl thio moiety of both of the RAFT agents absorbs strongly at 320nm, the UV detector was set to this wavelength along with the 254nm corresponding to styrene. Mathematical manipulation of the data as discussed earlier (Section 4.3.2) would not add to the interpretation of the UV-overlay figures presented in this chapter and was therefore not carried out.

#### (i) Styrene polymers

In Figure 5.8 the UV-RI overlay signals of the styrene polymers mPS08 and mPS14 are shown. Referring back to Section 5.3.2.1, molecular weight values obtained from SEC analysis of the dithiobenzoate mediated reaction started showing a drift from the predicted values after 20% conversion. A high molecular weight shoulder was identified, which caused the broadening in the distribution values. Investigating the response of the UV-RI overlays at increasing conversions of the polymerization confirmed that the second high molecular weight distribution consisted of terminated species that have lost their living character (RAFT-moiety).

## Chapter Five: Miniemulsion Polymerizations

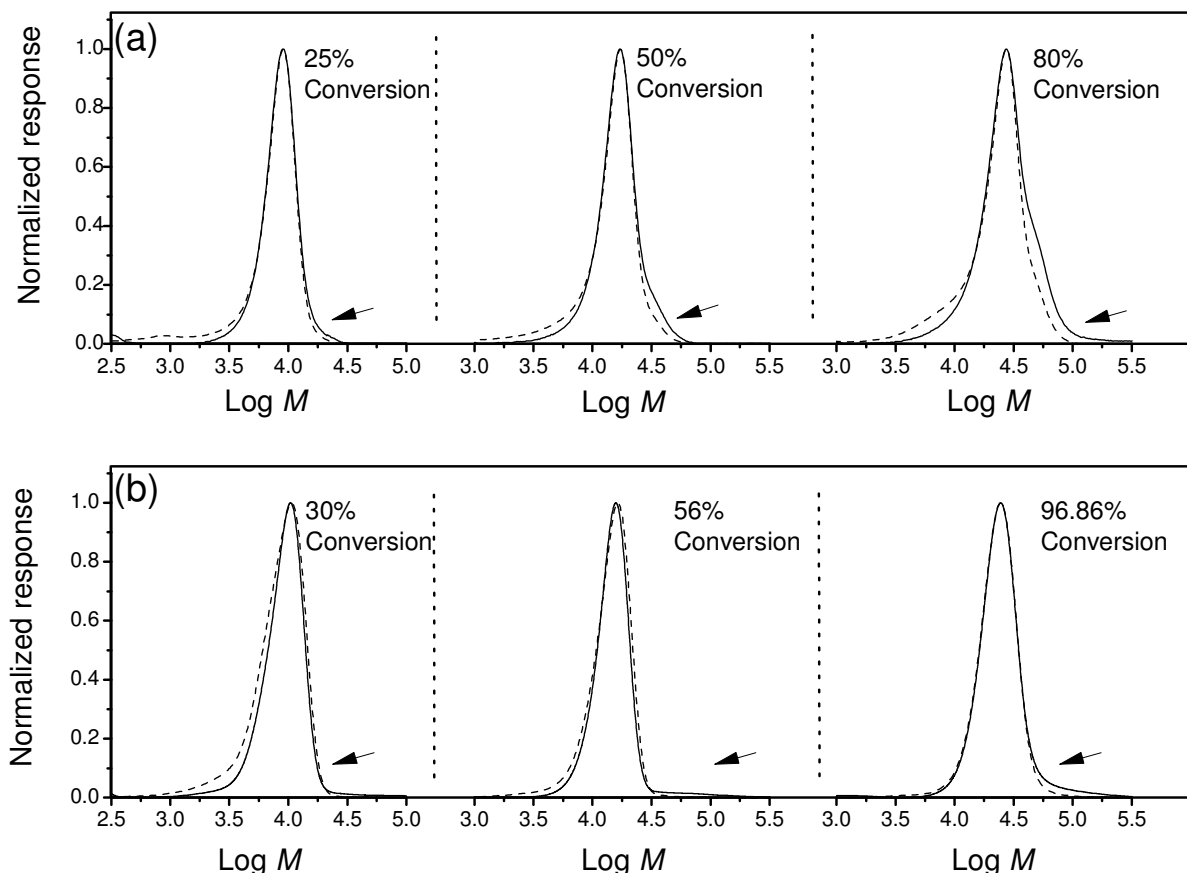


Figure 5.8 UV-RI overlays of the styrene miniemulsion polymers. Illustration of the deviation of UV signals from the RI with increasing conversion. (- - -) UV signal at 320nm. (—) RI signal. (a) Results from mPS08 (CVADTB). (b) Results from mPS14 (CVATTB).

The increasing loss of UV signal from 25% through to 80% conversion at the high molecular weight end is clear in Figure 5.8 (a). At approximately parallel conversions, the trithiocarbonate mediated Sty polymers showed an improved living character. A loss of UV response at the high molecular weight end is only evident at 96% conversion. The strong UV signals at the lower molecular weight end for all the distributions is a result of the high concentration of RAFT agent per mass of chain as chain lengths are much shorter.

(ii) Methyl methacrylate polymers

The distributions of the methyl methacrylate polymers, mPMMA01 and mPMMA07 exhibited a lower molecular weight tailing for both RAFT agents. The reaction mediated by CVADTB, showed that at 35% conversion (Figure 5.9 (a)), the UV response already started losing intensity. This occurred all the way to the end of the polymerization.

## Chapter Five: Miniemulsion Polymerizations

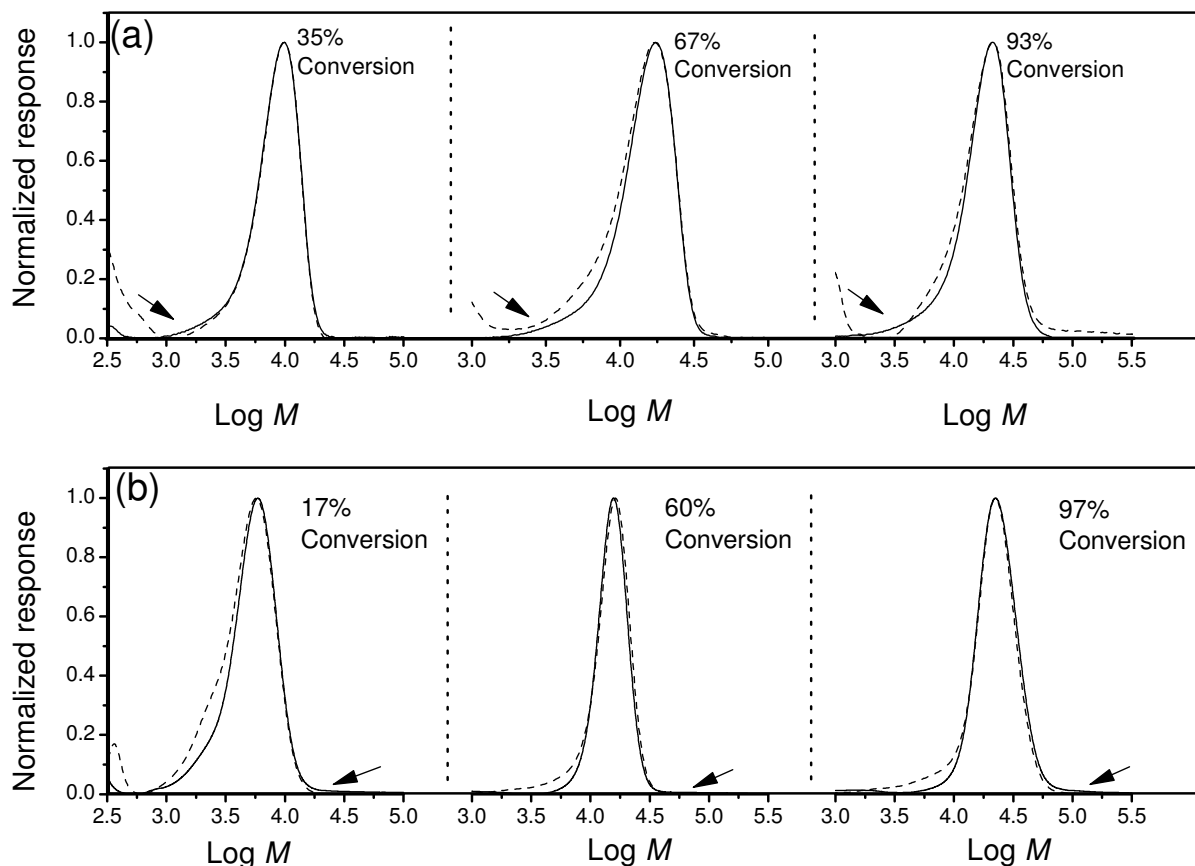


Figure 5.9 UV-RI overlays of the methyl methacrylate miniemulsion polymers. Illustration of the deviation of UV signals from the RI with increasing conversion. (---) UV signal at 320nm. (—) RI signal. (a) Results from mPMMA01 (CVADTB). (b) Results from mPMMA14 (CVATTB).

MMA is more hydrophilic than Sty, thus the chance of homogenous polymerization is higher. The likelihood that this occurred in this system is not very high as the latexes obtained were stable and no coagulation was present. The consistent tailing is rather due to the formation of lower molecular weight material that ceased growing, their presence contributing to the increase in polydispersity (Figure 5.3 B).

In the case of the reaction mediated by CVATTB, the formation of short chains leading to tailing was only seen at lower conversions (Figure 5.9 (b)). The UV-RI overlays at 60% conversion showed that the tailing disappeared as the reaction proceeded due to the RAFT agent being totally consumed. The initial oligomeric material experienced further growth and polydispersity values decreased with increasing conversion (Figure 5.3 B). This correlates very well to the hybrid theory mentioned earlier (section 5.3.1.2). At 97% conversion, only a slight loss of UV response was found, supporting the fact that much less termination occurred in the CVATTB system.

## Chapter Five: Miniemulsion Polymerizations

---

In conclusion, the UV-RI overlays shed light and added to the understanding and discussion of the results obtained from SEC analysis. It assisted in investigating the difference in mediation behaviour of the RAFT agents employed and confirmed the presence of the RAFT-moiety at the chain ends of the Sty and MMA polymers.

### 5.3.2 Chain extension of the starting block polymers

The use of RAFT under emulsion polymerization conditions to successfully form block copolymers and narrow polydispersity homopolymers has been reported as early as the advent of the process itself.<sup>13,44</sup> In 2000 Moad *et al*<sup>14</sup> synthesized poly(methyl methacrylate)-block-polystyrene copolymers by ‘one pot’ procedures involving the sequential addition of the monomers. They attempted, and were successful in both polymerization sequences even though in earlier experiments the polystyrene-block-poly(methyl methacrylate) (PS-b-PMMA) sequence failed.<sup>45</sup> They claimed that their success was based on the fact that the MMA monomer was added via a feed addition method, in which the instantaneous concentration of monomer in the system was maintained at a low level. Soon after, Monteiro and his team were successful in synthesizing a variety of block copolymers by implementing the RAFT process in miniemulsion stabilized by nonionic surfactants.<sup>15</sup> They suggested that, due to compartmentalization, the system allowed for improved block copolymer purity compared to that of homogeneous systems.

Butté *et al*<sup>20</sup> combined experimental studies with mathematical modeling in their study of RAFT miniemulsion polymerization and block copolymers of poly(methyl methacrylate)-block-polystyrene (PMMA-b-PS) and polystyrene-block-butyl acrylate (PS-b-BA) were prepared. They noted the importance of the partitioning properties of the RAFT leaving group in influencing the polymerization rate. It was found that a greater tendency to diffuse into the aqueous phase reduces the radical concentration within the particles and therefore leads to rate retardation.

Within the scope of sequential addition of monomer, different results can be obtained when the addition is done by different methods. Monomer can be added in one shot or fed into the system at different rates and different concentrations. Semi-continuous addition (feed) of monomer should lead to an improved living character or control of the reaction, as the ratio of the exchange reaction, which is independent of monomer concentration, to the propagation reaction is enhanced. If the monomer is charged in a single shot, the polymer particles become saturated with monomer and the propagation reaction, which is dependent on monomer concentration, will be increasingly favoured.

## *Chapter Five: Miniemulsion Polymerizations*

---

A third method is a variation on the shot addition, in which the monomer is charged in one shot under stirring and the onset of polymerization is delayed to allow optimized diffusion of the fresh monomer to the already existing particles. This approach is specific to heterogeneous systems. The choice of method for introducing monomer to the reaction vessel can have significant effects on the final latex properties. The key feature of any semi-batch process is the controlled introduction of monomer to the reaction vessel, thereby facilitating control over the course of the polymerization, the rate of heat generation, and the properties and morphology of the polymer particles formed. This plays a large role, especially in controlling the composition of copolymer latexes.

The rate at which monomer is introduced to the existing latex is crucial because it controls the availability of monomer for polymerization and hence the concentration of monomer in the particles. Monomer-starved conditions generally give optimized results. If the reaction mixture is analyzed at any time during the polymerization the instantaneous conversion is generally very high. This is because the molecules of the monomer in each small increment of monomer added are polymerized completely almost immediately upon entering the reaction vessel, due to their low concentration relative to the propagation rates. In this study the homopolymer latexes of styrene and methyl methacrylate, prepared in Section 5.3.1, were used as seeds for block copolymerization. The experimental details are set out in Table 5.3.

In all instances the solids content was kept constant and fresh monomer and initiator were added simultaneously. In all the feed addition reactions, polymerization was ceased one hour after the total monomer/initiator aliquots were added. Both polymerization sequences were attempted and the mediation behaviour of CVADTB and CVATTB towards block copolymer formation was investigated. The effect of varying the method of monomer addition on the block copolymer purity was also studied. Analyses of the synthesized block copolymers were carried out using SEC, particle size analysis and TEM.

*Chapter Five: Miniemulsion Polymerizations*

Table 5.3: Experimental details of the block copolymerization of the RAFT end-capped styrene and methyl methacrylate polymers from the seeded latexes. The PS-*b*-PMMA polymerizations were carried out at 80°C, while the PMMA-*b*-PS polymerizations were carried out at 75°C.

Starting polymer	Polymer-RAFT (mol x 10 <sup>-5</sup> )	$\bar{M}_{n,SEC}$	$\bar{M}_w/\bar{M}_n$	Monomer added	Monomer (mol x 10 <sup>-3</sup> )	Addition reaction	AIBN (mol x 10 <sup>-5</sup> )	Feeding rate (ml/min)	Time (h)
mPS08	9.8415	23410	1.29	MMA	24.91	Shot	7.7339	-	3
					24.90	Pre-swelling	7.1249	-	2
					24.89	Feed	6.0897	0.02	3
mPS14	12.4612	22200	1.21		29.99	Shot	10.7179	-	2
					29.99	Pre-swelling	8.2211	-	2
					29.97	Feed	6.0897	0.05	2
mPMMA01	8.5258	21550	1.31	Sty	20.97	Shot	6.6987	-	12
					20.78	Pre-swelling	8.3429	-	12
					20.47	Feed	6.0897	0.01	4
mPMMA07	13.009	21337	1.15		28.92	Shot	7.7949	-	7
					28.95	Preswelling	9.0128	-	7
					28.80	Feed	6.0897	0.01	7

The final polymers of mPS08, mPS14, mPMMA01 and mPMMA07 were used in the chain extension polymerizations. The preservation of the end functionality of the starting blocks was confirmed via UV-RI analysis (refer to Section 5.3.1.3 for results). The selected polymers each consisted of the thiocarbonyl thio moiety at the majority of the chain ends, therefore were potentially active for chain extension.

### 5.3.2.1 PS-*b*-PMMA copolymers

The following section presents the results obtained for the chain extension of RAFT-mediated miniemulsion polystyrene latexes with MMA monomer. The additions of monomer using the different methods are presented as cases (i), (ii) and (iii), which refer to shot, pre-swelling and feed addition, respectively. Results of the latexes mediated by RAFT agent CVADTB are presented first.

*Chapter Five: Miniemulsion Polymerizations**(a) CVADTB-mediated polymerizations*

The original latex sample (mPS08, Table 5.3) displayed a high molecular weight shoulder, most probably due to termination and the chains in this shoulder were not expected to grow. The UV signals (Section 5.3.1.3) established that the chains in the shoulder lack the RAFT-moiety supporting the terminated nature. Figure 5.10 clearly shows the occurrence of block copolymer formation from the remainder of the starting polystyrene latex mediated by CVADTB. The normalized signal traces exhibited different behaviour for each monomer addition method and it is expected that different purities of block copolymers resulted.

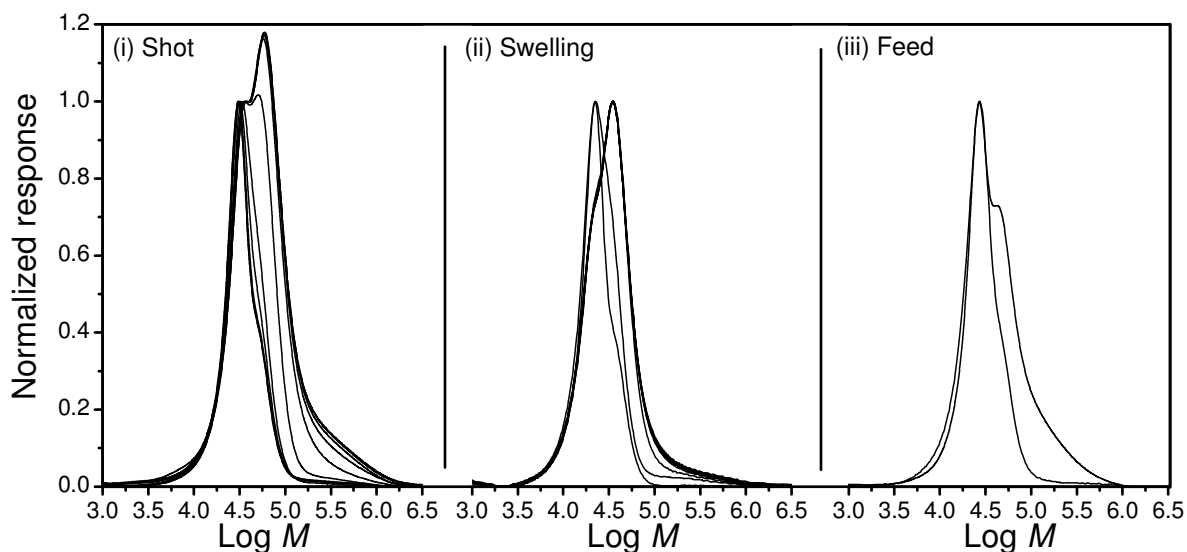


Figure 5.10 Normalized SEC chromatograms of the block formation from mPS08 mediated by CVADTB via the three different addition methods of MMA monomer. See Table 5.3 for experimental details.

In all three cases, the development of true chain extension of the primary living peak can be seen. A narrow peak is evident, which shifts to a log  $M$  of around 5. Case (i), in which the monomer was added in one shot, differs from the other two, as a large secondary distribution at the high molecular weight end was formed. The pre-swelling and feed addition methods showed similar behaviour in chain extension, yet the concentration of the second distribution progressively decreased. The UV-RI overlays in Figure 5.11 assisted in providing more information with regards to the block copolymer purity and nature of the newly formed species.

## Chapter Five: Miniemulsion Polymerizations

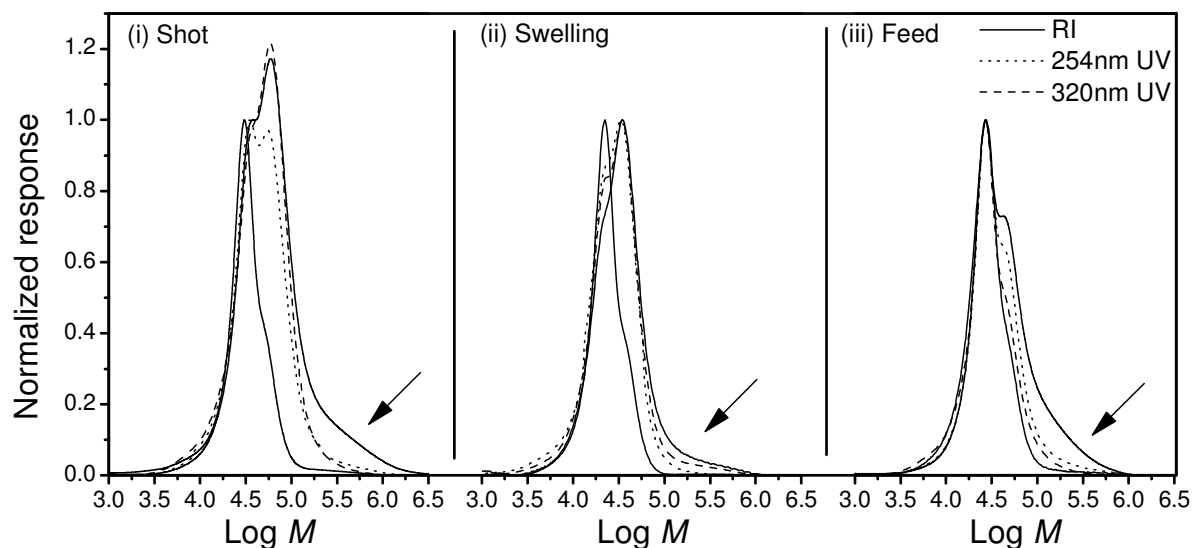


Figure 5.11 The UV-RI response overlay chromatograms of the block formation from *mPS08* mediated by CVADTB via the three different addition methods of MMA monomer. The starting block as well as the final sample in the block copolymerization reaction is shown. The dotted line represents UV absorbance at 254nm, while the dashed line represents the UV absorbance at 320nm. The arrows indicate the presence of terminated high molecular weight chains.

Case (i) showed that although the original styrene chains were activated, the formation of high molar mass polymer in the region of  $\log M$  6 -6.5 dominated. The lack of UV signal at 320nm in the high molar mass region is strongly indicative of uncontrolled polymer. Examining the results of the feed system (iii), the SEC chromatogram displays similar characteristics to that of the shot addition presented in case (i). It is clear that some block formation is occurring, some initial polymer is not reactivated (due to termination, or lack of radicals in the particles) and that there is a high molecular weight peak forming that is consistent with an uncontrolled polymerization.

The pre-swelling result showed substantial improvement; the monomer has had time to swell the particles and secondary particle nucleation in the aqueous phase was avoided. The monomer had the opportunity to enter the particles and was therefore at the polymerization locus to start polymerization in the existing particles. Reinitiation of the chains and a strong block component are evident. The fact that some initial material did not experience significant further growth can be due to two possibilities. The end group stability may be poor or the termination of the initial material was high after addition of the new batch of initiator.<sup>46</sup> The amount of exposure of the RAFT end-groups to water is probably fairly insignificant but studies done by Thomas *et al*<sup>46</sup> indicated that hydrolysis of dithioesters chain transfer agents is possible.

*Chapter Five: Miniemulsion Polymerizations**(b) CVATTB-mediated polymerizations*

The attempt to block the styrene polymer mediated by CVATTB provided very interesting results. From Figure 5.12 it appears as if the initial polymer did not chain extended at all and that the only significant change was the growth of a second distribution at the high molecular weight end, irrespective of the addition method used.

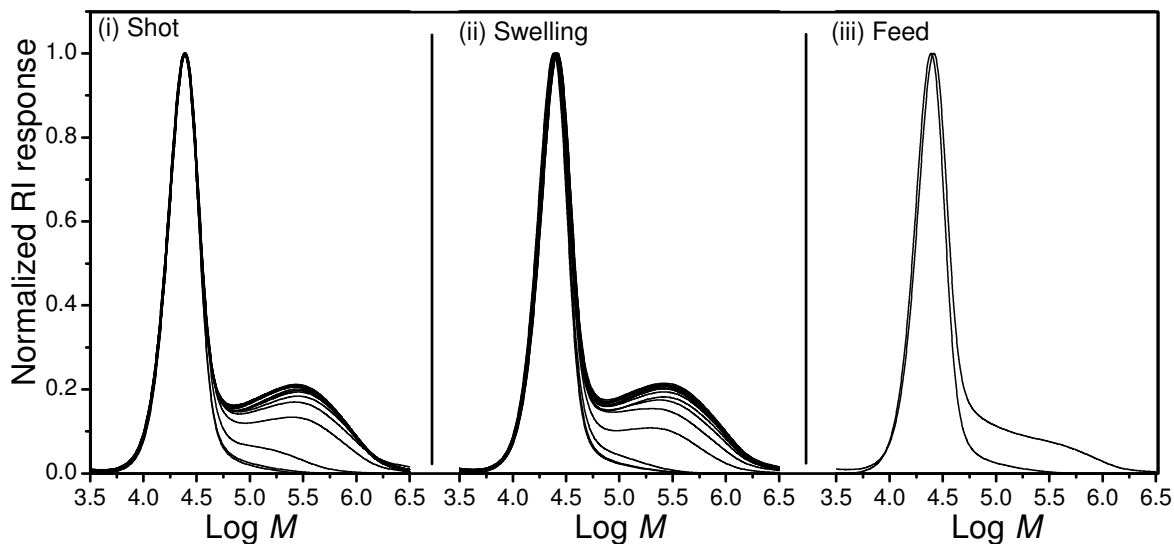


Figure 5.12 Normalized SEC chromatograms of the block formation from mPS14 mediated by CVATTB via the three different addition methods of MMA monomer. See Table 5.3 for experimental details.

A closer look at the UV-RI overlays showed that the initial material preserved the RAFT-moiety as the 320nm UV signal is maintained. Figure 5.13 also confirmed that the higher molecular weight distribution was uncontrolled and had no UV response.

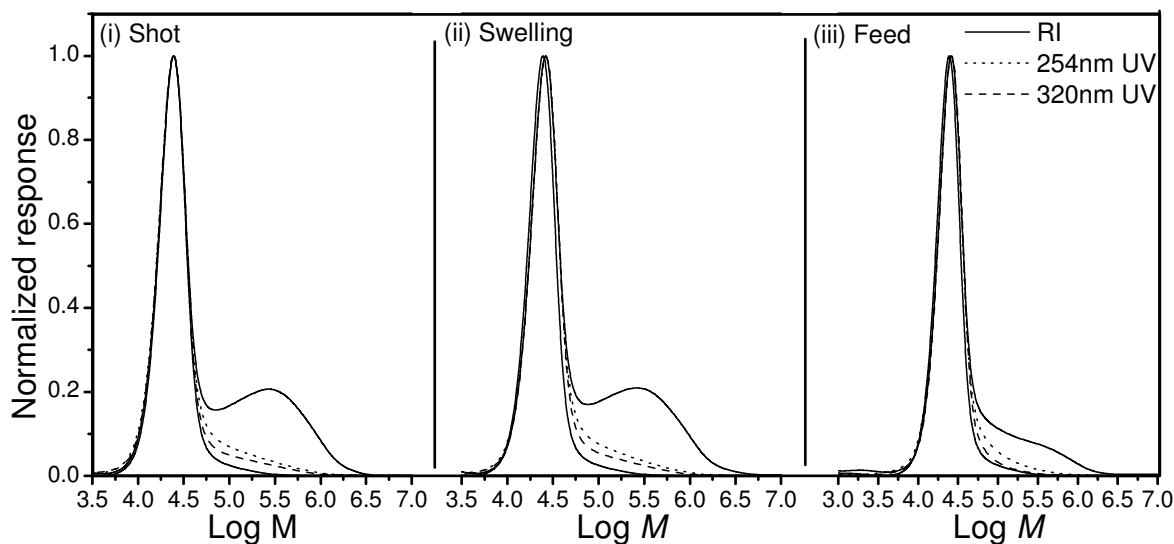


Figure 5.13 The UV-RI response overlay chromatograms of the block formation from mPS14 by CVATTB via the three different addition methods of MMA monomer. The starting block as well as the final sample in the block copolymerization reaction is shown. The dotted line represents UV absorbance at 254nm, while the dashed line represents UV absorbance at 320nm.

The difference in results from the previous scenario where CVADTB was used, is related to the function of the RAFT agents, in specific their ability to reactivate the chains when the second monomer is a methacrylate. The fact that the only experimental difference is that the initial polymer does not show slight bimodality and that it has less terminated material, plays a lesser role. This suggests that in the case of the dithiobenzoate it is possible to get some reactivation of the RAFT end group chains; however there is a loss of activation potential in the case of the trithiocarbonate. There is a much stronger selectivity for the MMA radical to fragment, with the result that no reactivation occurs. Unlike the improvement that was found in the case of the dithiobenzoate, no difference in behaviour occurred when utilizing the pre-swelling or feed addition methods. This is strong evidence in support of the difference in reactivation potential of the two RAFT agents with this specific monomer combination. The results of the trithiocarbonate chain extension runs are completely consistent with the hypothesis that it is very difficult to reactivate this particular Z-group with a methacrylate when styrene is the initial monomer chosen.

### 5.3.2.2 PMMA-b-PS copolymers

The following section discusses the results found for the chain extension of RAFT-mediated miniemulsion poly(methyl methacrylate) latexes with styrene monomer. To simplify the discussion, results for the block copolymerization from the starting latexes mediated by the different RAFT agents are presented in two sub-sections. As done previously, the addition of monomer in the

## Chapter Five: Miniemulsion Polymerizations

different methods are presented as cases (i), (ii) and (iii), which refer to shot, pre-swelling and feed addition, respectively. Results of the latex mediated by RAFT agent CVADTB are presented first.

### (a) CVADTB-mediated polymerizations

When switching to the preferred monomer sequence, the expected improvements in results were obtained. The PMMA dithiobenzoate latex was easily chain extended under all monomer addition conditions as can be seen in Figure 5.14. In this polymerization sequence the methacrylate radical has a higher affinity to be reactivated by fragmentation from the thio-carbonyl thio moiety with styrene monomer being added to the system, creating styrenic radicals to allow the RAFT process to occur. Once the radicals are activated in the particles a monomer gradient is created that will draw monomer from the aqueous phase into the particles, leading to efficient chain extension. The normalized SEC distributions suggest that the pre-swelling or feed systems will not necessarily provide improved results.

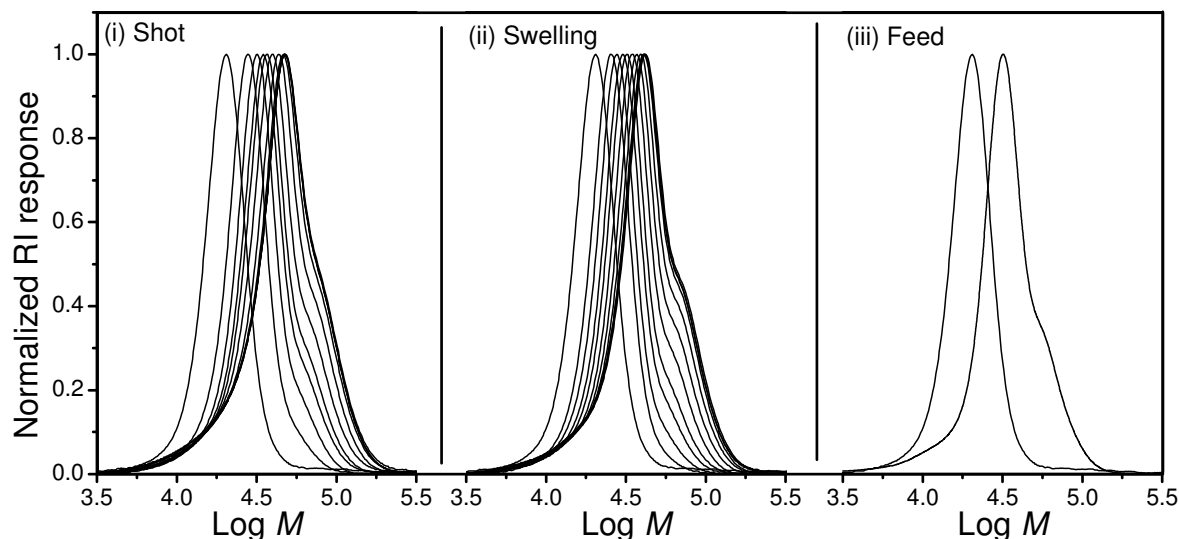


Figure 5.14 Normalized SEC chromatograms of the block formation from mPMMA01 mediated by CVADTB via the three different addition methods of styrene monomer. See Table 5.3 for experimental details.

The UV-RI response overlay chromatograms in Figure 5.14 illustrate the control that was achieved in the shot addition of monomer. This behaviour was repeated in the case of the pre-swelling and feed systems. Very little secondary particle nucleation was observed. The strong high molecular weight shoulder coming through is evident, but upon carefully examining the SEC curves it seems that the reactivation of the polymer was still very efficient.

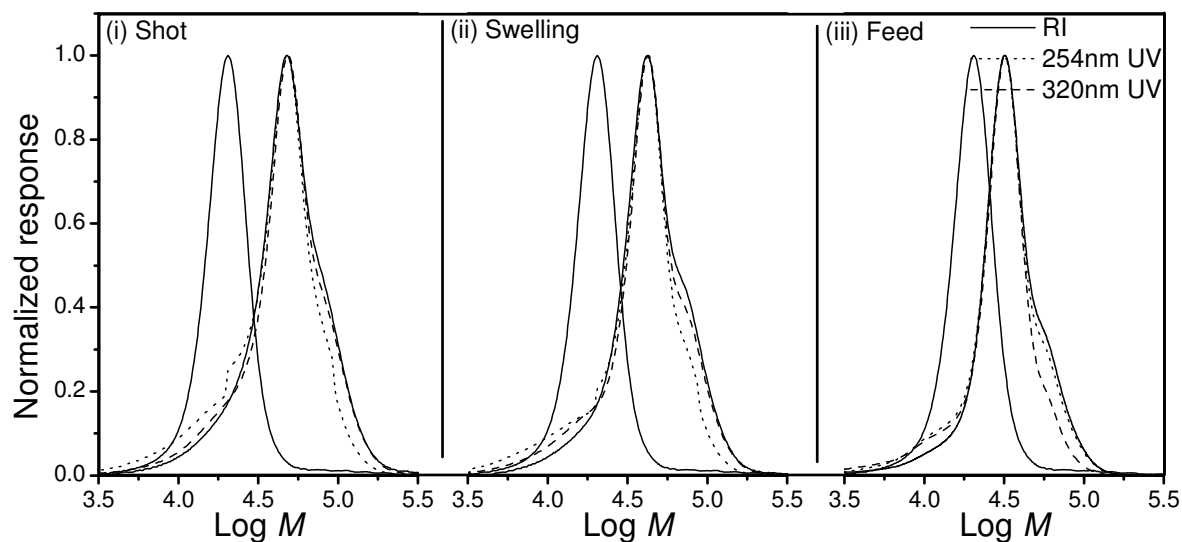
*Chapter Five: Miniemulsion Polymerizations*

Figure 5.15 The UV-RI response overlay chromatograms of the block formation from mPMMA01 mediated by CVADTB via the three different addition methods of styrene monomer. The starting block as well as the final sample in the block copolymerization reaction is shown. The dotted line represents UV absorbance at 254nm, while the dashed line represents UV absorbance at 320nm.

The loss of the UV response only becomes apparent in the pre-swelling and feed systems, and involves the high molecular weight shoulder distribution. The feed system was more prone to termination as the amount of chains that underwent reactivation was reduced. As the system was starved from monomer, instead of undergoing further growth the chains were more likely to terminate each other. This explains the larger loss in UV response compared to the other addition methods.

The feed addition was not expected to provide a significantly increased understanding of the systems. It is clear however that for the dithiobenzoate mediated system at least, there is consistency in terms of the expected result. The initial polymer was mostly consumed and some indication of a homopolymer contaminant is present. It is however difficult to differentiate between homopolymer contaminant and initial polymer that was not reactivated through the use of SEC. More detailed information could only be obtained by using hyphenated techniques such as those presented later in this thesis (Chapter 6).

**(b) CVATTB-mediated polymerizations**

The trithiocarbonate results indicate the formation of a new distribution of polymer at the low molecular weight end and that the high molecular weight shoulder that was a characteristic feature of the dithiobenzoate-mediated runs in the previous section (a) is now absent. In this polymerization sequence the trithiocarbonate result is consistent with that of the dithiobenzoate polymerization with

*Chapter Five: Miniemulsion Polymerizations*

regards to the limited benefit that is derived from introducing the monomer in a more controlled fashion into the polymerization system. The block copolymerization behaviour seems fairly similar from cases (i) through to (iii) (Figure 5.16).

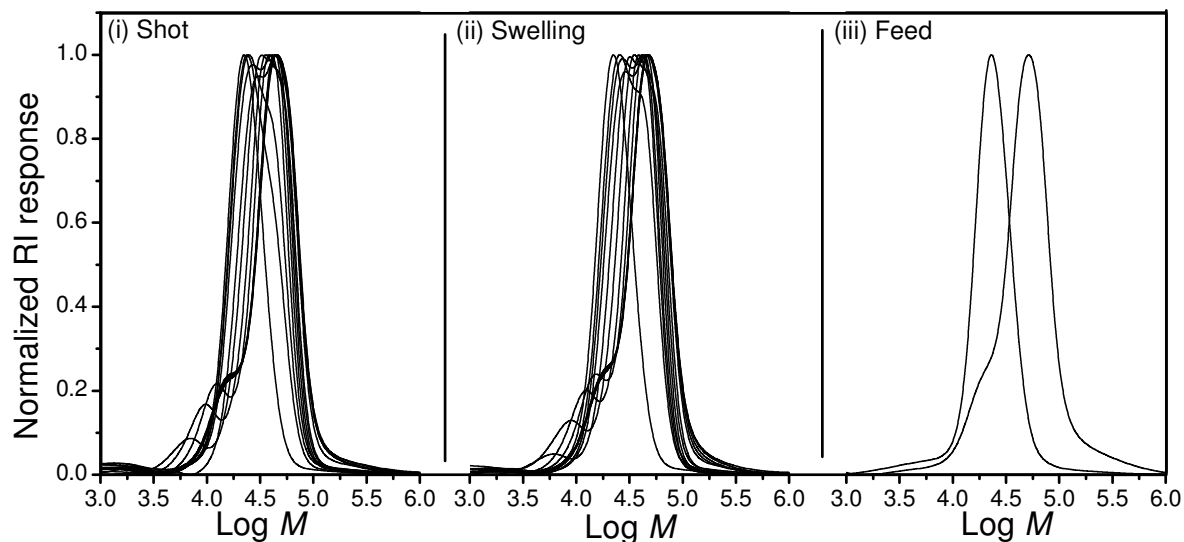


Figure 5.16 Normalized SEC chromatograms of the block formation from *mPMMA07* chains mediated by CVATTB) via the three different addition methods of styrene monomer. See Table 5.3 for experimental details.

Another consistent factor is the difference in activation of the original polymer from that of the dithiobenzoate RAFT agent mediated runs, as discussed previously in Section 5.3.2.1. Again the initial block polymer is not reactivated in a uniform manner. The reasons for this behaviour are probably related to the speed at which specific particles obtain propagating radicals and reactivate chains. Block copolymer formation is still efficient however, as can be seen from the shift of the original distribution to higher molecular weight in all cases.

UV-RI overlays in Figure 5.17 identify the newly formed distribution of polymer at the low molecular weight end as controlled styrene homopolymer. It appears as if a significant number of chains were initiator-derived rather than derived from the initial block polymer present in the system. In dithiobenzoate polymerizations it is expected that the propagating radical concentration is significantly reduced as the dithiobenzoates capture large amounts of radicals. This provides the efficient control of the block reactivation. Another characteristic feature of the dithiobenzoate system is the presence of a high molecular weight shoulder, which is clearly absent in the trithiocarbonate mediated runs. This shoulder is often suggested as being due to termination of propagating chains. However, if this was the explanation, then the effect is expected to be

*Chapter Five: Miniemulsion Polymerizations*

pronounced in the case of the trithiocarbonate as the concentration of propagating radicals is known to be higher due to faster fragmentation. Other options that have been suggested include intermediate termination and branching, both being unlikely for this system. It is more likely that the probability for termination to take place in a dithiobenzoate reaction due to longer reaction times is increased. The limiting factor in the case of the dithiobenzoate polymerization is clearly the dithiobenzoate fragmentation rate.

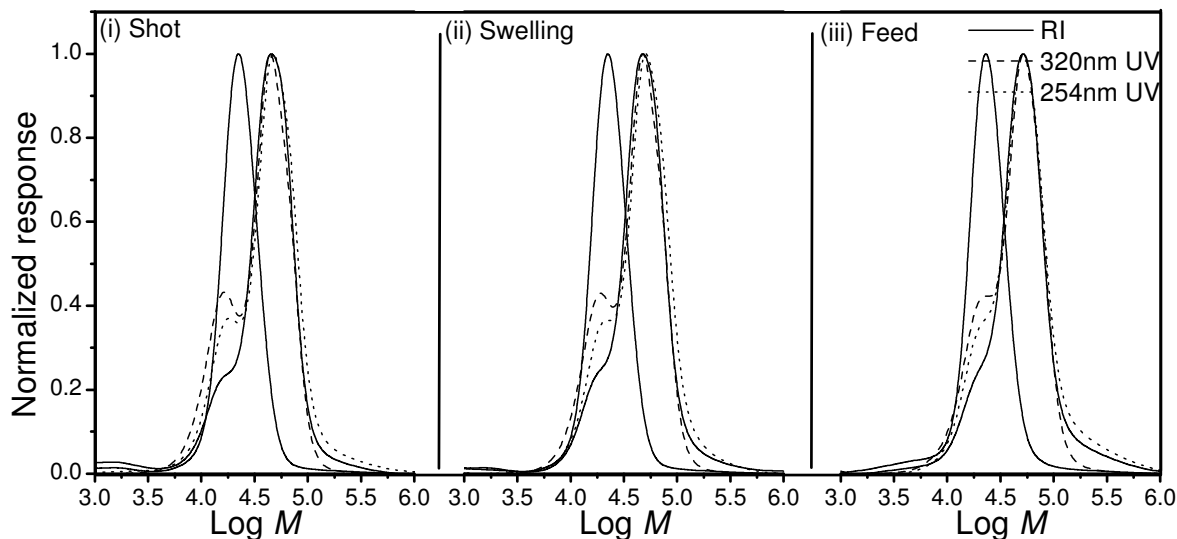


Figure 5.17 UV-RI response overlay chromatograms of the block formation from mPMMA07 chains mediated by CVATTB) via the three different addition methods of styrene monomer. The starting block as well as the final sample in the block copolymerization reaction is shown. The dotted line represents UV absorbance at 254nm, while the dashed line represents UV absorbance at 320nm.

Conversely, in the trithiocarbonate polymerizations, the higher number of propagating radicals leads to many more initiator derived chains, which are also capable of undergoing a RAFT process. The higher number of these propagating radicals in the system is most likely responsible for the generation of the styrene homopolymers.

In the case of the trithiocarbonate, the limiting step may well be the radical capture by the particles. Compared to the other addition methods, case (iii) showed a larger loss of the 320nm UV signal, indicating that the system was yet again prone to termination of the chains rather than chain growth, probably due to a larger radical flux relative to monomer concentration in these particles. The result is that the dithiobenzoate polymer, although suffering from the high molecular weight shoulder, may actually produce narrower polymer due to the lack of the homopolymer contaminant and the improved reactivation of the initial block copolymer.

**5.3.3. Latex investigations: A closer look at the prepared latexes with dynamic light scattering (DLS) and transmission electron microscopy (TEM)**

One of the key factors in distinguishing a miniemulsion latex from its conventional emulsion counterpart is the production of very small monomer droplets (50-500nm) through a high shear process to enforce droplet nucleation. Ideally a narrow distribution of droplets are to be formed, yet the concept of miniemulsion aiming to produce a latex which is a 1:1 copy of the original droplets to achieve direct control over the number of particles and avoid complex nucleation steps, has proved to be a challenge.<sup>47</sup> A surfactant/co-stabilizer system in combination with the shearing is critical to retard coalescence caused by Brownian motion, settling or Stokes-law creaming or settling. Although droplets much smaller than those of a conventional emulsion system are formed, a broad distribution of droplet sizes are still found. Conflicting results have been reported for particle size distributions, supporting different theories. Some authors<sup>48</sup> support the 1:1 copy of droplet to particles theory, whereas others propose that only a fraction of the monomer droplets become nucleated.<sup>38</sup> What is without question though is that the characteristics of the miniemulsion charged into the reaction depend on the formulation, homogenization procedure and storage time of the latex. The processes involved by which latex particles form and grow are all important. These include the evolution of particle size (or number) and size distribution, the development of molar mass and molar mass distribution and the polymerization rate profile during the course of polymerization. In turn, these properties are influenced by the basic polymerization parameters such as the monomer, surfactant and initiator type and concentration, temperature, mode and rate of monomer addition.

In effect, differences based on formulation and homogenization are cancelled out by the fact that in this study, the miniemulsion recipes and sonication times were identical for both monomers and RAFT agents under investigation. The results obtained are therefore limited to being related only to monomer and RAFT agent behaviour and efficiency. From dynamic light scattering analysis (DLS) particle sizes were determined for polystyrene and PMMA homopolymer latexes mediated by CVADTB and CVATTB as well as for the subsequent block copolymers synthesized (Section 5.3.2, Table 5.3). The size of particles in an emulsion affects the rate of polymerization due to compartmentalization effects;<sup>49</sup> the smaller the particle size, the faster the rate. Table 5.4 shows that the particle sizes for the dithiobenzoate mediated polymers were smaller than their trithiocarbonate counterparts in the case of both monomers. Conversely, the polymerization rates of the styrene and

*Chapter Five: Miniemulsion Polymerizations*

methacrylate runs mediated by CVATTB were found to be higher than those of CVADTB (Section 5.3.1.1). This suggests that the mediation behaviour of the RAFT agent had a dominating effect on the rates.

*Table 5.4 Particle size analysis of the seed latexes of styrene mediated by the two different RAFT agents and the subsequent block copolymers via each addition method.  $Z_{average}$  (nm) is the mean diameter based upon the intensity of scattered light. (All entries refer to the polymers synthesized and discussed in Section 5.3.1, Table 5.2.)*

<b>Monomer</b>	<b>RAFT agent</b>	<b>Latex</b>	<b><math>Z_{average}</math> (nm)</b>
<i>Sty</i>	CVADTB	mSty08	67.2
	CVATTB	mSty14	80.0
<i>MMA</i>	CVADTB	mMMA01	84.3
	CVATTB	mMMA07	88.4

The PMMA latexes had larger particles than the styrene latexes, irrespective of the type of RAFT agent used. This could be due to the fact MMA is more water soluble than styrene and is more susceptible to particle degradation via Oswald ripening.<sup>50</sup> As a result, the initial monomer droplets are larger and hence relatively larger particles are formed. The TEM analysis images of the homopolymers, all labeled A in Figures 5.18-5.21 support the results from the light scattering by showing that, in the case of styrene, smaller particles were formed but with a larger particle size distribution. In addition, the polymerizations mediated by the trithiocarbonate showed a more pronounced presence of finer particles.

### **5.3.3.1 PS-b-PMMA sequence**

Particle size analysis results for the latexes from the polymerization sequence PS-b-PMMA are summarized in Table 5.5. For the respective RAFT agents, the different monomer addition methods showed an increase in particle size.

*Chapter Five: Miniemulsion Polymerizations*

Table 5.5 Particle size analysis of the seed latexes of styrene mediated by the two different RAFT agents and the subsequent block copolymers via each addition method.  $Z_{average}$  (nm) is the mean diameter based upon the intensity of scattered light.

<b>PS-b-PMMA sequence</b>	<b>POLYMER</b>	<b><math>Z_{average}</math> (nm)</b>
<b>CVADTB</b>	<b>mPS08</b>	<b>67.2</b>
	mPS08-b-PMMA Case (i)	77.3
	mPS08-b-PMMA Case (ii)	74.3
	mPS08-b-PMMA Case (iii)	73.2
<b>CVATTB</b>	<b>mPS14</b>	<b>80.0</b>
	mPS14-b-PMMA Case (i)	89.0
	mPS14-b-PMMA Case (ii)	90.8
	mPS14-b-PMMA Case (iii)	85.3

*(i) CVADTB latexes*

A closer look at the TEM images of the polystyrene-b-poly(methyl methacrylate) block copolymer latexes synthesized from styrene chains end-capped with CVADTB (Figure 5.18) revealed the following. The block copolymer latexes labeled B and D showed similar distributions of particles sizes. Besides the finer particles visible in the background, particle sizes for B ranged from about 84nm to 108nm, while the particles for D varied from 53nm to 112nm. These two addition methods (shot and feed) already yielded similar results, as discussed earlier for the SEC analysis (Section 5.3.2.1a). It is clear from the images that, due to block copolymer formation, some particles underwent further growth, but the existence of new particles from the MMA monomer cannot be ignored. The pre-swelling latex supported the earlier theory of showing improvement over the other two addition methods as the particle size range decreased to sizes from approximately 78nm to 89nm.

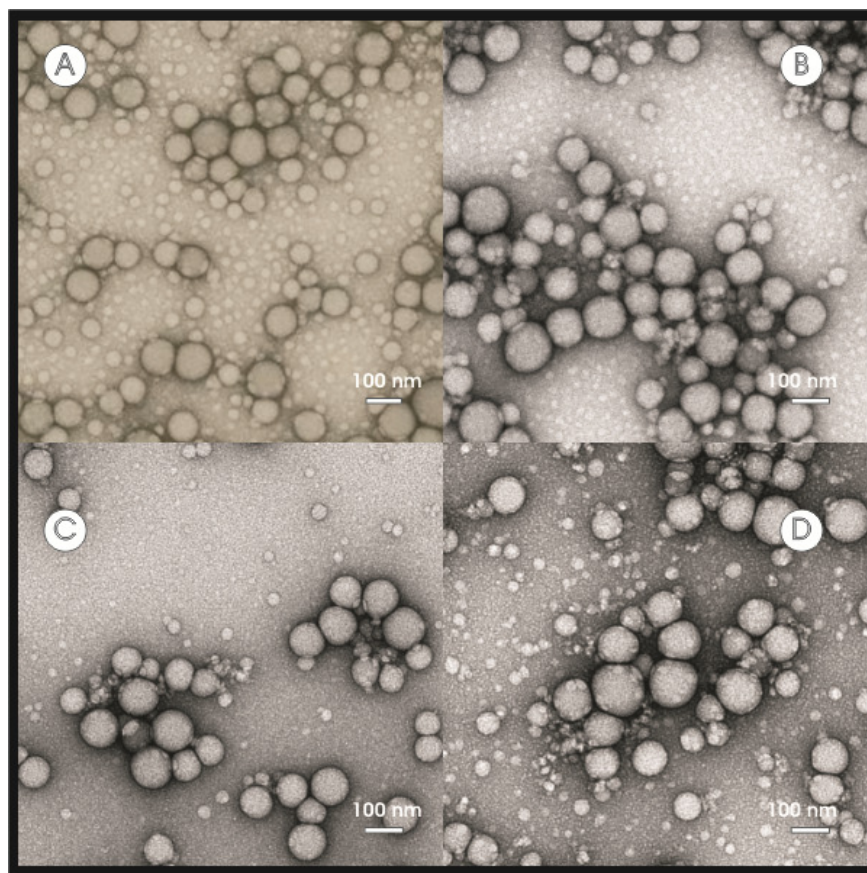


Figure 5.18 TEM images of the PS-*b*-PMMA block copolymer latexes obtained from the chain extension of mPS08, mediated by CVADTB, indicated by A. The three addition methods are identified as B=shot addition, C=pre-swelling and D=feed addition. (Refer to Table 5.3 for latex compositions.)

**(ii) CVATTB latexes**

In Figure 5.19, the TEM images of the PS-*b*-PMMA block copolymer latexes synthesized from styrene chains end-capped with CVATTB showed that the formation and growth of new MMA particles dominate. All three monomer addition methods showed that very few particles showed traces of particle growth, supporting the SEC results. It appears as if no real improvement or difference occurs in switching from shot addition to the feed or pre-swelling method.

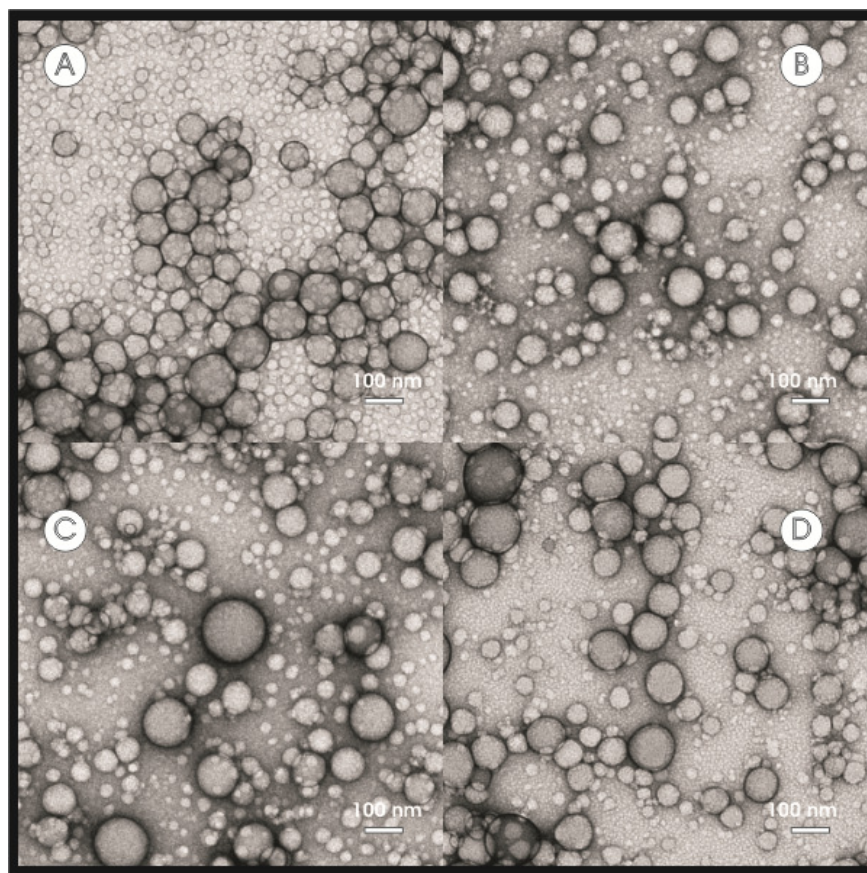


Figure 5.19 TEM images for the PS-*b*-PMMA block copolymer latexes obtained from the chain extension of mPS14, mediated by CVATTB, indicated by A. The three addition methods are identified as B=shot addition, C=pre-swelling and D=feed addition. (Refer to Table 5.3 for latex compositions)

Images B, C and D illustrate that most of the particles in the block copolymer latex have an average size of 88nm. As this corresponds to the particle size measured for the original starting latex (Table 5.5), these particles can be identified as styrene that did not undergo further growth. Very few particles actually show an increase in size to support block formation and the smaller sized ones are clearly due to secondary nucleation in the aqueous phase.

### 5.3.3.2 PMMA-*b*-PS sequence

The particle size analysis results for the latexes from the polymerization sequence PMMA-*b*-PS are summarized in Table 5.6. Results obtained from latexes involving CVADTB were very different from those involving CVATTB.

*Chapter Five: Miniemulsion Polymerizations*

Table 5.6 Particle size analysis of the seed latexes of PMMA mediated by the two different RAFT agents and the subsequent block copolymers via each addition method.  $Z_{average}$  (nm) is the mean diameter based upon the intensity of scattered light.

<b>PMMA-b-PS sequence</b>	<b>POLYMER</b>	<b><math>Z_{average}</math> (nm)</b>	<b>PDI</b>
<b>CVADTB</b>	<b>mPMMA01</b>	<b>84.3</b>	<b>0.14</b>
	mPMMA01-b-PS Case (i)	100.0	0.22
	mPMMA01-b-PS Case (ii)	90.3	0.09
	mPMMA01-b-PS Case (iii)	89.8	0.08
<b>CVATTB</b>	<b>mPMMA07</b>	<b>88.4</b>	<b>0.21</b>
	mPMMA07-b-PS Case (i)	86.7	0.09
	mPMMA07-b-PS Case (ii)	87.0	0.09
	mPMMA07-b-PS Case (iii)	92.2	0.14

The particles of the latex mediated by CVADTB experienced much more growth in size than those of the latexes mediated by CVATTB

*(i) CVADTB latexes*

The TEM images of the PMMA-b-PS block copolymer latexes obtained from the latex mediated by the dithiobenzoate are visual evidence of the success achieved with block copolymer formation in this polymerization sequence. In Figure 5.20 all three addition methods show that most of the existing particles increased in size. It is only with regards to the feed addition method that the finer particles present in the background come into play again.

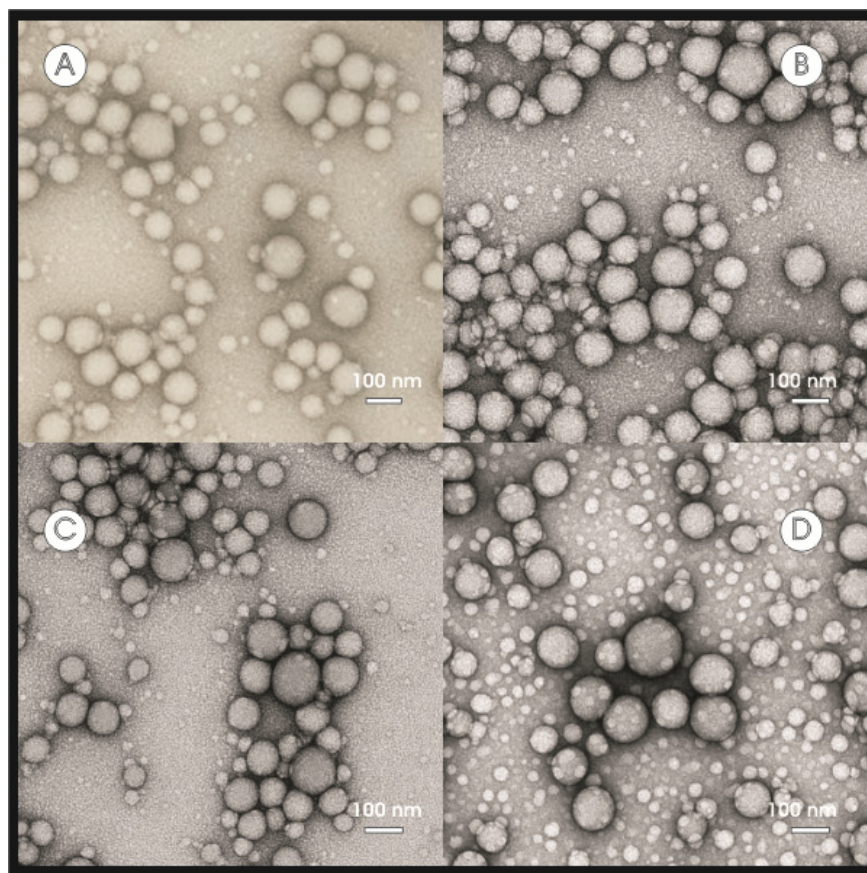
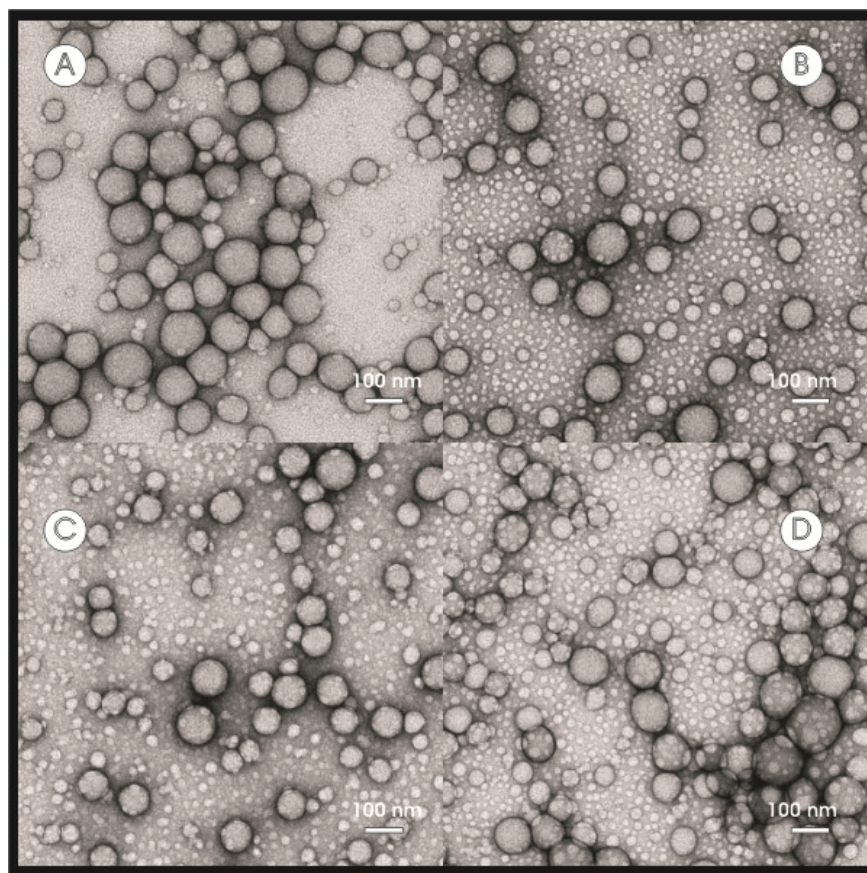


Figure 5.20 TEM images for the PMMA-*b*-PS block copolymer latexes obtained from the chain extension of mPMMA01, indicated by A. The three addition methods are identified as B=shot addition, C=pre-swelling and D=feed addition. (Refer to Table 5.3 for latex compositions)

**(ii) CVATTB latexes**

As the SEC results discussed earlier indicated that CVATTB showed a lesser tendency, compared to CVADTB, to be reactivated for block copolymerization, it was to be expected that the fresh styrene monomer added would in turn be responsible for the formation of new particles. These particles would originate from the monomer droplets forming in the system and they would therefore have a very broad distribution. This explains the finer particles present in the latexes of all three monomer addition methods. Figure 5.21 shows that their presence is more pronounced in the shot and feed methods.



*Figure 5.21 TEM images for the PMMA-*b*-PS block copolymer latexes obtained from the chain extension of mPMMA07, indicated by A. The three addition methods are identified as B=shot addition, C=pre-swelling and D=feed addition. (Refer to Table 5.3 for latex compositions)*

In the case of the pre-swelling method, some of the monomer had the opportunity to diffuse to the already existing particles and increased the chance for the PMMA chains to undergo further growth. The average particle sizes obtained from TEM analysis corresponded well with the light scattering data. The  $Z_{\text{average}}$  (nm) values for the block copolymers are less than the value of the starting block due to the large number of smaller sized particles present in the system involving the trithiocarbonate as transfer agent.

## 5.4 Conclusion

### (I) Styrene and methyl methacrylate miniemulsion polymers

The syntheses of PS and PMMA polymers mediated by 4-cyano-4-((thiobenzoyl) sulfonyl) pentanoic acid (cyanovaleric acid dithiobenzoate) (CVADTB) and by S-4-cyanopentanoic acid S'-benzyltrithiocarbonate (CVATTB) were successfully carried out in miniemulsion polymerizations.

- A significant difference was found between the mediation behaviour of the two different RAFT agents in terms of rate effects. CVATTB showed a much faster rate for both monomer polymerizations compared to CVADTB. The similar migration behaviour of the fragmented group of the transfer agent to the aqueous phase accounted for the induction period found at the onset of all reactions. The faster propagation rate increase in the case of CVATTB is explained in terms of the stability of the intermediate radical. The intermediate radical of the thio-carbonyl thio moiety of the trithiocarbonate is less stable than that of the dithiobenzoate and fragmentation proceeds faster.
- Overall, CVATTB provided much better control compared to CVADTB for the Sty and MMA polymerizations. In the case of the former, the  $\bar{M}_n$  values had an improved fit to the theoretically calculated  $\bar{M}_n$  and the polydispersities were lower. In the Sty runs mediated by CVATTB, the polymerization time played a significant role as shorter reaction times led to less termination and loss of RAFT-functionality compared to CVADTB. The MMA runs mediated by CVATTB had  $\bar{M}_n$  values higher than the theoretically calculated  $\bar{M}_n$  values and broad polydispersities in the beginning stages of the polymerization which was explained by incomplete consumption of RAFT agent. The molecular weight distribution showed bimodality at low conversion, suggesting the presence of oligomeric material that eventually grows as reaction continues. The UV-RI overlays for the Sty and MMA polymers indicated that CVADTB still provided sufficient control and that the polymers qualified for further block copolymerizations.

## *Chapter Five: Miniemulsion Polymerizations*

---

### (II) Block copolymers synthesized from the seed latexes of styrene and methyl methacrylate

Block copolymer formation in both sequence PS-*b*-PMMA and PMMA-*b*-PS was successfully carried out in seeded emulsion polymerization using PS and PMMA latexes mediated by CVADTB and CVATTB.

- In both polymerization sequences, CVATTB proved to be less efficient in reactivation for block formation than CVADTB. In the PS-*b*-PMMA sequence the results of all the trithiocarbonate runs were consistent with the hypothesis that the Z-group in question does not lend itself very easily to reactivation with a methacrylate when the initial monomer is styrene. With regards to the PMMA-*b*-PS sequence, the limiting factor causing the inefficiency of the trithiocarbonate to allow block copolymerization was the inability to capture radicals in the particles. As expected, generally more success was achieved with the PMMA-*b*-PS sequence in terms of block copolymer formation.
- In the PMMA-*b*-PS sequence very little benefit was derived from introducing monomer in a more controlled fashion into the system and the block copolymerization behaviour was fairly similar for each addition method within the scope of each respective RAFT agent. For copolymerizations involving CVADTB, the initial polymer was mostly consumed and a slight indication of homopolymer contaminant was present. The reactions mediated by CVATTB showed the appearance of a low molecular weight styrene homopolymer originating from initiator derived chains. The PS-*b*-PMMA sequence illustrated that different behaviours in copolymerizations occurred for each monomer addition method with each respective RAFT agent. The pre-swelling method gave the best result for reactions involving CVADTB, due to limiting secondary nucleation in the aqueous phase. Reactions mediated by CVATTB showed that although very little chain extension occurred, the feed addition and pre-swelling methods showed improvement over the shot addition. In the case of the pre-swelling a larger fraction of the initial material underwent further growth but the feed addition resulted in a lower concentration of high molecular weight methyl methacrylate polymer.

## *Chapter Five: Miniemulsion Polymerizations*

---

### (III) Latex investigations

Particle size analyses showed a consistency for all Sty and MMA miniemulsion latexes under similar sonication conditions and polymerization recipes. The values obtained for the particle sizes all fell within the distribution range traditionally associated with miniemulsion polymerization particles. Irrespective of the RAFT agent involved, smaller particles were obtained for Sty latexes compared to MMA latexes. TEM analyses corresponded well with the results of the light scattering analysis for the seed and block copolymer latexes. In the case where the RAFT agent was not as active towards chain extension, the system was more susceptible to secondary nucleation in the aqueous phase and the presence of a large distribution of finer particles was evident in the TEM images.

It is evident that in the syntheses of block copolymers in emulsion/miniemulsion systems that nucleation of new particles (not containing the initial block) during the polymerization of the second block can be particularly detrimental to the purity of the block copolymer. The ideal is that further chain growth should occur from existing particles and that secondary nucleation in the aqueous phase in these systems should be carefully avoided.

In the following chapter a detailed chromatographic examination of the polymers using hyphenated techniques will be presented to provide further insight to the purity of the block copolymers synthesized in this study.

---

*Chapter Five: Miniemulsion Polymerizations*

---

**5.5 References**

- (1) Matyjaszewski, K.; Qiu, J.; Shipp, D. A.; Gaynor, S. G. *Macromol Symp* **2000**, *155*, 15-29.
- (2) Wang, X.-S.; Lascelles, S. F.; Jackson, R. A.; Armes, S. P. *Chem Comm* **1997**, 1817-1818.
- (3) Qiu, J.; Charleux, B.; Matyjaszewski, K. *Prog Polym Sci* **2001**, *26*, 2083-2134.
- (4) Braunecker, W. A.; Matyjaszewski, K. *Prog Polym Sci* **2007**.
- (5) Lowe, A. B.; McCormick, C. L. *Prog Polym Sci* **2007**, *32*, 283-351.
- (6) Prescott, S. W. *Macromolecules* **2003**, *36*, 9608-9621.
- (7) Prescott, S. W.; Ballard, M. J.; Gilbert, R. G. *J Polym Sci Part A: Polym Chem* **2005**, *43*, 1076-1089.
- (8) Prescott, S. W.; Ballard, M. J.; Rizzardo, E.; Gilbert, R. G. *Macromolecules* **2005**, *38*, 4901-4912.
- (9) McLeary, J. B.; Klumperman, B. *Soft Matter* **2006**, *2*, 45-53.
- (10) Save, M.; Guillaneuf, Y.; Gilbert, R. G. *Aust J Chem* **2006**, *59*, 693-711.
- (11) Monteiro, M. J.; de Barbeyrac, J. *Macromolecules* **2001**, *34*, 4416-4423.
- (12) Uzulina, I.; Kanagasabapathy, S.; Claverie, J. *Macromol Symp* **2000**, *150*, 33-38.
- (13) Le, T. P.; Moad, G.; Rizzardo, E.; Thang, S. H.; In PCT. Int. Appl.; wo98/01478; **1998**
- (14) Moad, G.; Chiefari, J.; Chong, B. Y.; Krstina, J.; Mayadunne, R. T.; Postma, A.; Rizzardo, E.; Thang, S. H. *Polym Int* **2000**, *49*, 993-1001.
- (15) de Brouwer, H.; Tsavalas, J. G.; Schork, F. J.; Monteiro, M. J. *Macromolecules* **2000**, *33*, 9239-9246.
- (16) Tsavalas, J. G.; Schork, F. J.; de Brouwer, H.; Monteiro, M. J. *Macromolecules* **2001**, *34*, 3938-3946.
- (17) Luo, Y.; Tsavalas, J. G.; Schork, F. J. *Macromolecules* **2001**, *34*, 5501-5507.
- (18) Luo, Y.; Wang, R.; Yang, L.; Yu, B.; Li, B.; Zhu, S. *Macromolecules* **2006**, *39*, 1328-1337.
- (19) Lansalot, M.; Davis, T. P.; Heuts, J. P. A. *Macromolecules* **2002**, *35*, 7582-7591.
- (20) Buttè, A.; Storti, G.; Morbidelli, M. *Macromolecules* **2001**, *34*, 5885-5896.
- (21) McLeary, J. B.; Tonge, M. P.; De Wet-Roos, D.; Sanderson, R. D.; Klumperman, B. *J Polym Sci Part A: Polym Chem* **2004**, *42*, 960-974.
- (22) Luo, Y.; Liu, X. *J Polym Sci Part A: Polym Chem* **2004**, *42*, 6248-6258.
- (23) Matahwa, H.; McLeary, J. B.; Sanderson, R. D. *J Polym Sci Part A: Polym Chem* **2006**, *44*, 427-442.
- (24) Yang, L.; Luo, Y.; Li, B. *J Polym Sci Part A: Polym Chem* **2006**, *44*, 2293-2306.
- (25) Yang, L.; Luo, Y.; Li, B. *Polymer* **2005**, *47*, 751-762.
- (26) Uzulina, I.; Gaillard, N.; Guyot, A.; Claverie, J. *C R Chimie* **2003**, *6*, 1375-1384.
- (27) Shim, S. E.; Lee, H.; Choe, S. *Macromolecules* **2004**, *37*, 5565-5571.
- (28) Landfester, K.; Bechthold, N.; Tiarks, F.; Antonietti, M. *Macromolecules* **1999**, *32*, 2679-2683.
- (29) Alduncin, J. A.; Forcada, J.; Asua, J. M. *Macromolecules* **1994**, *27*, 2256-2261.
- (30) Reimers, J. L.; Schork, F. J. *Ind Eng Chem Res* **1997**, *36*, 1085-1087.
- (31) Chern, C.-S.; Liou, Y.-C. *J Polym Sci Part A: Polym Chem* **1999**, *37*, 2537-2550.
- (32) Nomura, M.; Ikoma, J.; Fujita, K. *J Polym Sci Part A: Polym Chem* **1993**, *31*, 2103-2113.
- (33) Nomura, M.; Tobita, H.; Suzuki, K. *Adv Polym Sci* **2005**, *175*, 1-128.
- (34) Suzuki, K.; Nomura, M. *Macromol Symp* **2002**, *179*, 1-12.
- (35) Blythe, P. J.; Klein, A.; Phillips, J. A.; Sudol, E. D.; El-Aasser, M. S. *J Polym Sci Part A: Polym Chem* **1999**, *37*, 4449-4457.
- (36) Asua, J. M.; Sudol, E. D.; El-Aasser, M. S. *J Polym Sci Part A: Polym Chem* **1989**, *27*, 3903-3913.

*Chapter Five: Miniemulsion Polymerizations*

---

- (37) Alduncin, J. A.; Forcada, J.; Baranddaran, M. J.; Asua, J. M. *J Polym Sci Part A: Polym Chem* **1991**, *29*, 1265-1270.
- (38) Choi, Y. T.; El-Aasser, M. S.; Sudol, E. D.; Vanderhoff, J. W. *J Polym Sci Polym Chem Ed* **1985**, *23*, 2973-2987.
- (39) Luo, Y.; Schork, F. J. *J Polym Sci Part A: Polym Chem* **2002**, *40*, 3200-3211.
- (40) Monteiro, M. J.; Hodgson, M.; de Brouwer, H. *J Polym Sci Part A: Polym Chem* **2000**, *38*, 3864-3874.
- (41) Prescott, S. W.; Ballard, M. J.; Rizzardo, E.; Gilbert, R. G. *Macromolecules* **2002**, *35*, 5417-5425.
- (42) Moad, G.; John, C.; YK, C.; Krstina, J.; Mayadunne, R. T. A.; Postma, A.; Rizzardo, E.; Thang, S. H. *Polym Int* **2000**, *49*, 993-1001.
- (43) Barner-Kowollik, C.; Quinn, J. F.; Nguyen, T. L. U.; Heuts, J. P. A.; Davis, T. P. *Macromolecules* **2001**, *34*, 7849-7857.
- (44) Chiefari, J.; Chong, Y. K. B.; Ercole, F.; Krstina, J.; Jeffery, J.; Le, T. P. T.; Mayadunne, R. T. A.; Meijs, G. F.; Moad, C. L.; Moad, G.; Rizzardo, E.; Thang, S. H. *Macromolecules* **1998**, *31*, 5559-5562.
- (45) Chong, B. Y. K.; Le, T. P. T.; Moad, G.; Rizzardo, E.; Thang, S. H. *Macromolecules* **1999**, *32*, 2071-2074.
- (46) Thomas, D. B.; Convertine, A. J.; Hester, R. D.; Lowe, A. B.; McCormick, C. L. *Macromolecules* **2004**, *37*, 1735-1741.
- (47) Asua, J. *Prog Polym Sci* **2002**, *27*, 1283-1346.
- (48) Landfester, K.; Bechthold, N.; Forster, S.; Antonietti, M. *Macromol Rapid Comm* **1999**, *20*, 81-84.
- (49) Ghielmi, A.; Storti, G.; Morbidelli, M.; Ray, W. H. *Macromolecules* **1998**, *31*, 7172-7186.
- (50) Antonietti, M.; Landfester, K. *Prog Polym Sci* **2002**, *27*, 689-757.

# ***Chapter 6: Chromatographic Investigation of Block Copolymers via Hyphenated Techniques***

## **Abstract**

This chapter presents the results found during the chromatographic analysis of the block copolymers synthesized in preceding chapters. The extent to which differences in heterogeneity occurred due to the varying reaction conditions was studied. By the use of different modes of liquid chromatography and combining them, two-dimensional information on the different aspects of the molecular heterogeneity of the polymers was obtained.

## **6.1 Introduction**

Complex polymers refer to all macromolecular systems having more than one distributive property and comprise polymer blends, various copolymer types, as well as most stereo-regular, branched and functionalized polymers.<sup>1,2</sup> These polymeric materials exhibit complicated chemical and physical structures featuring differences in size, chemical nature and architecture. For block copolymers, specifically, several synthesis routes are available and numerous combinations of chemically different chains are inevitably prepared in the respective processes.<sup>3-5</sup> Depending on the composition of the monomer feed and the polymerization procedure involved, different types of heterogeneities may become important. As molecular characteristics are linked to the end-properties, a better understanding of these polymers and their molecular characteristics are vital. Powerful analytical methods to provide information on the different distributions are therefore required.<sup>6-10</sup>

The work presented in Chapters 4 and 5 indicated the need for a more detailed study of the synthesized copolymers other than by the single separation method of SEC. This chapter describes an investigation that was aimed at determining to what extent differences in heterogeneity are found due to the varying reaction conditions. Using different modes of liquid chromatography and combining them, two-dimensional information on the different aspects of the molecular heterogeneity of the Sty/MMA block copolymers was obtained.

## 6.2 Experimental

### 6.2.1 Synthesis of block copolymers

A detailed description of the syntheses of the block copolymers under investigation were presented in Chapters 4 and 5 of this study. The polymerization of Sty/PMMA block copolymers in homogeneous media mediated by 4-cyano-4-((thiobenzoyl)sulfonyl) pentanoic acid (cyanovaleric acid dithiobenzoate) are presented in Chapter 4 (Section 4.2.3.). The details of Sty/PMMA copolymers polymerized in heterogeneous media implementing both 4-cyano-4-((thiobenzoyl)sulfonyl) pentanoic acid (cyanovaleric acid dithiobenzoate) and S-4-cyanopentanoic acid-S'-benzyltrithiocarbonate (**2**) as RAFT agents are presented in Chapter 5 (Section 5.2.4.2).

### 6.2.2 Analysis of block copolymers

#### 6.2.2.1 Liquid chromatography under critical conditions: The first separation step

##### 6.2.2.1(i) Analytical equipment

###### Instrument

Waters 2690 separation module (Alliance)

###### Columns

- (i) Critical conditions for PMMA: Supelco Si 300 Å, 5µm average particle size, 250x4.6mm (ID); Nucleosil Si 100 Å, 5µm average particle size, 250x4.6mm (ID)
- (ii) Critical conditions for PS: C18 guard; Waters Symmetry C18 300 Å, 5µm average particle size, 4.6x250mm (ID); Supelco Nucleosil Si C18 100 Å, 5µm average particle size, 250x4.6mm (ID)

###### Detectors

Evaporative light scattering detector, ELSD-PL 1000 (Polymer Laboratories)

Ultra-violet (UV) detector, Agilent 1100 Series (Agilent)

##### 6.2.2.1(ii) Sample preparation and analysis conditions

Standards and samples were made up to a concentration of 5mg/ml and 10µl of the respective solutions was injected. The flow rate used was 0.5 ml/min and the setup temperature was 30°C. Critical conditions were determined with the use of linear mono-dispersed standards (Polymer Laboratories) of polystyrene and poly(methyl methacrylate) for both sets of critical conditions,

## *Chapter Six: Chromatographic Investigation*

---

respectively. The critical solvent composition for each homopolymer was determined as explained by Pasch and Trathnigg.<sup>11</sup> The mobile phases for LC-CC analysis under critical conditions are methylethylketone-cyclohexane for PMMA and tetrahydrofurane-acetonitrile for PS. The exact solvent compositions that were determined are presented in Section 6.3.1. Due to the different solvent combinations used, the settings of the ELSD varied.

- (i) Critical conditions for PMMA: Gas flow speed: 1 SLM; Nebulizer temp: 75°C; Evaporator temp: 110 °C
- (ii) Critical conditions for PS: Gas flow speed: 1 SLM; Nebulizer temp: 40°C; Evaporator temp: 90°C

### **6.2.2.2 Size-exclusion chromatography (SEC): The second separation step**

#### **6.2.2.2(i) Analytical equipment**

##### **Instrument**

Waters 515 HPLC pump (MICROSEP)

##### **Columns**

PSS SDV linearM, 5mm average particle size, 50x20 (ID) mm (PSS, Polymer Standards Service GmbH, Mainz, Germany)

##### **Detectors**

Evaporative light scattering detector, ELSD-PL 1000 (Polymer Laboratories)

#### **6.2.2.2(ii) Sample preparation and analysis conditions**

Polymer samples were dissolved in THF (HPLC grade, Sigma-Aldrich) and directly injected into a storage loop through a syringe fitted to an eight-port injection valve that was connected to the separation column. The mobile phase (THF, HPLC grade) was set at a flow rate of 4ml/min. The calibration was based on linear monodisperse polystyrene standards.

### **6.2.2.3 On-line two-dimensional chromatography**

By coupling Liquid Adsorption Chromatography (LAC) and SEC the separation of the polymers in two dimensions, to provide further insight into the chemical composition distribution, was done.

#### **6.2.2.3(i) Analytical equipment**

A modular chromatographic system comprising the two chromatographs connected via one electronically driven eight-port injection valve (Valco) and two storage loops was used. Each

## *Chapter Six: Chromatographic Investigation*

---

storage loop was 100 $\mu$ l in size. Chromatograph 1 represents the liquid adsorption chromatographic separation and Chromatograph 2 the size-exclusion chromatography separation. The columns used were identical to those used for each separation system individually and detection was carried out by the ELS detector.

### **6.2.2.3(ii) Analysis conditions and sample preparations**

The mobile phases used depended on the specific critical conditions investigated- in Chromatograph 1: (a) critical conditions for PMMA: MEK-cyclohexane 70.7:29.3; (b) critical conditions for PS: THF-ACN 50.8:49.2 and Chromatograph 2: THF. Samples were made up to 20mg/mL and 100 $\mu$ L aliquots were injected. Flow in the second dimension remained at 4mL/min, while the flow in the first dimension varied; as explained in Section 2.7.2.1. Similarly, the timing of the fraction collector, controlling the switching mechanism of the eight port injection valve, had to be calculated based on the same principle and subsequently varied. For all online 2D analyses the ELS detector settings were as follows: gas flow speed: 1.5 SLM; nebulizer temp: 75°C; evaporator temp: 110 °C.

### **6.2.2.4 Analytical software programs**

Data collection in both separation techniques as well as the operation of the coupled injection valves were controlled by the software “PSS Win GPC7”. Processing of the two-dimensional data was performed by “Win GPC 2D”. The software was obtained from Polymer Standards Service, Mainz, Germany.

## 6.3 Results and Discussion

### 6.3.1 Critical conditions of polystyrene and poly(methyl methacrylate)

Determining the critical point for any polymer is the most time consuming and labour intensive process. Although several groups have investigated and established conditions for several copolymer compositions in critical chromatography, in most cases their results serve only as a starting point.<sup>9,12-20</sup> The sensitivity of the technique requires that critical conditions should be investigated and set for each chromatographic system before attempting the analysis of polymer samples. A drift in the critical conditions can be brought about by a slight change of temperature, small differences in solvent composition concentrations and especially by the replacement of columns or column sets. In the present study, the critical points for PS and PMMA were determined by separating a series of standards of different molecular weights under a range of isocratic modes of solvent/non-solvent mixtures. The styrene and methacrylate standards were dissolved in the same isocratic solvent mixtures respectively and the data obtained are shown in Figure 6.1 and Figure 6.2. The curves in Figure 6.1 represent the separations of polystyrene standards under different isocratic conditions and show that at a concentration of 50.4/49.6 (v/v %) THF/ACN the standards eluted in SEC mode. The critical point for styrene was reached at a concentration of 50.3/49.7% (v/v %) THF/ACN and is characterized by the elution of all standards at the same retention time of 3.16min (6.32mL). For solvent concentrations of 50.2/49.8 (v/v %) THF/ACN and higher, elution occurred in the adsorption mode.

## Chapter Six: Chromatographic Investigation

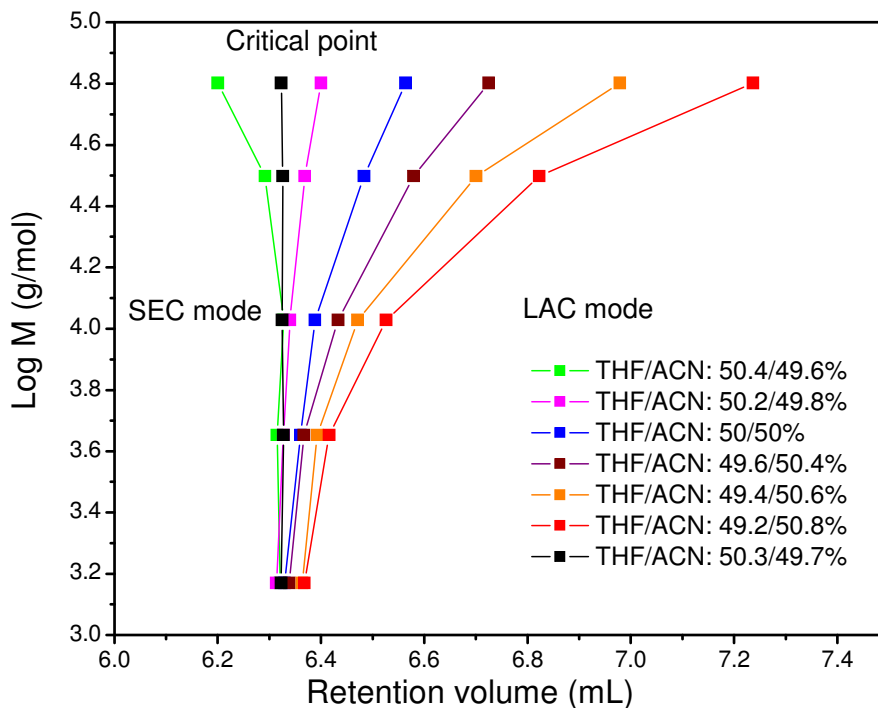


Figure 6.1 Critical conditions diagram of molar mass vs retention time for PS standards under solvent/non-solvent conditions. Stationary phase: C18 guard; Waters Symmetry C18 300 Å, 5µm average particle size, 4.6x250mm (ID); Supelco Nucleosil Si C18 100 Å, 5µm average particle size, 250x4.6mm (ID); mobile phase: THF and ACN; separation temperature: 30°C. Critical conditions were found at 50.3THF/49.7 ACN. Standards ranged between 1480 to 63350 g/mol.

Similarly, the critical point of PMMA was also obtained. Figure 6.2 shows the critical conditions chromatograms of the PMMA standards at the separation temperature of 30°C in the mobile phase of MEK/Cyclohexane. In principal, elution should occur independent of molar mass, yet it is clear that at higher molar mass the PMMA distributions started deviating from the critical point.

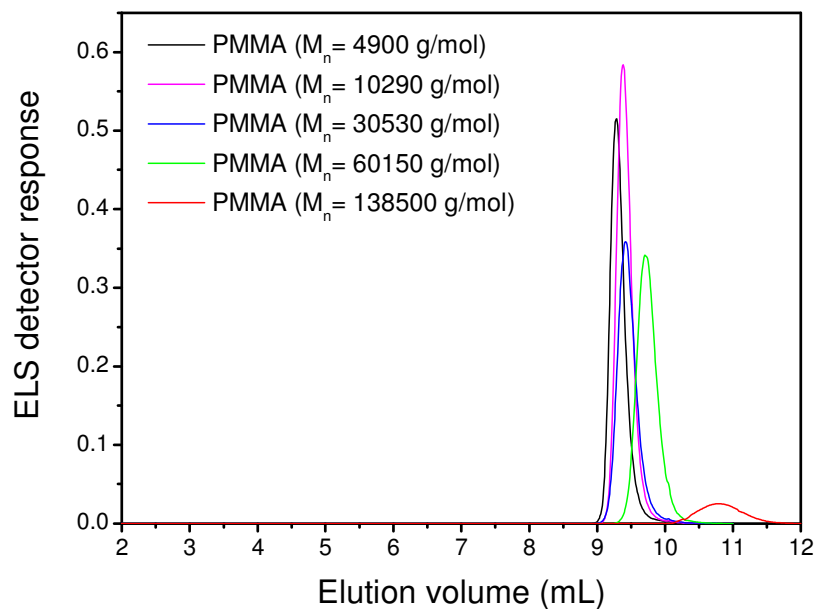
*Chapter Six: Chromatographic Investigation*

Figure 6.2 Critical conditions chromatograms for a range of PMMA standards at the critical point of PMMA. Stationary phase: Supelco Si 300 Å, 5µm average particle size, 250x4.6mm (ID); Supelco Nucleosil Si C18 100 Å, 5µm average particle size, 250x4.6mm (ID); mobile phase: MEK-cyclohexane 70.7:29.3(v/v%); separation temperature: 30 °C.

The block copolymers prepared in this study however, were characterized as described earlier (Chapters 4 and 5) by SEC and they were in the range of 10290 to 60150 g/mol. The likelihood however, of the copolymers under investigation to be of a molar mass higher than 60150 g/mol and elute in LAC mode is fairly small. The inclusion of a standard of 4900g/mol in finding the critical conditions was to allow for lower molar mass present in the copolymer composition, whether it be homopolymer from the second monomer added to the system or starting block material that did not undergo further growth. The retention time of PMMA under critical conditions was determined to be around 4.75min, with a mobile phase composition of 70.7/29.3 (v/v %) MEK/cyclohexane.

## *Chapter Six: Chromatographic Investigation*

---

### **6.3.2 Chromatographic analysis of RAFT mediated block copolymers prepared in homogeneous media.**

The block copolymers of styrene and methyl methacrylate prepared in homogenous media via the RAFT process, using CVADTB as RAFT agent (Chapter 4), were characterized. The analyses of these copolymers were based on separating the individual homopolymers from the other species at the respective critical points, thereby investigating the heterogeneity and the extent of copolymer content in the polymer. The critical conditions were achieved as discussed in Section 6.3.1. Only after the determination of the critical solvent composition for either of the two components in the system (namely Sty and MMA) and the determination whether the component (not eluted under critical conditions) elutes in the size exclusion or adsorption mode, can compositions of unknown samples be determined. The LC-CC results will be presented (the separation with regards to chemical composition), followed by the 2-dimensional chromatography plots where each of the identified species are separated with regard to molar mass. The purpose of using the 2-D technique is to shed more light on the characterization of the block copolymers due to the restrictions found with normal SEC.

#### **6.3.2.1 LC- CC**

##### ***6.3.2.1(a) Evaluation of the PS-*b*-PMMA block copolymers at the critical point of PS***

In Chapter 4 (Section 4.3.2.1) it was established that, although it was the less popular polymerization sequence, block formation did occur in the instance where fresh MMA monomer and initiator (AIBN) was added to the RAFT end-capped polystyrene chains. From the SEC results it was shown that several factors played a role in the extent to which the starting block material underwent further growth. The RAFT agent type was crucial, and it appeared as if the method of monomer addition played a lesser role in the block copolymer formation within each polymerization sequence, although the feed systems suggested an improved copolymer quality. It became clear however that a more in depth investigation was required before any definite conclusions could be made. Assisting the analysis, UV detection at 254nm was carried out in an effort to trace the styrene component present in the total composition. Figure 6.3 show the LC-CC elugrams of the PS-*b*-PMMA block copolymers synthesized by the shot (A) and feed (B) addition methods at the critical conditions for polystyrene. For both methods, the polystyrene eluted at the critical point. Considering the polymerization sequence, it is expected to be the unreacted starting block material. It is however quite apparent that the two polymers consist over different chemical

*Chapter Six: Chromatographic Investigation*

compositions as their block copolymer distributions vary substantially. In the shot addition method (plot A), a fair amount of styrene was detected, representing the initial block segment of copolymer.

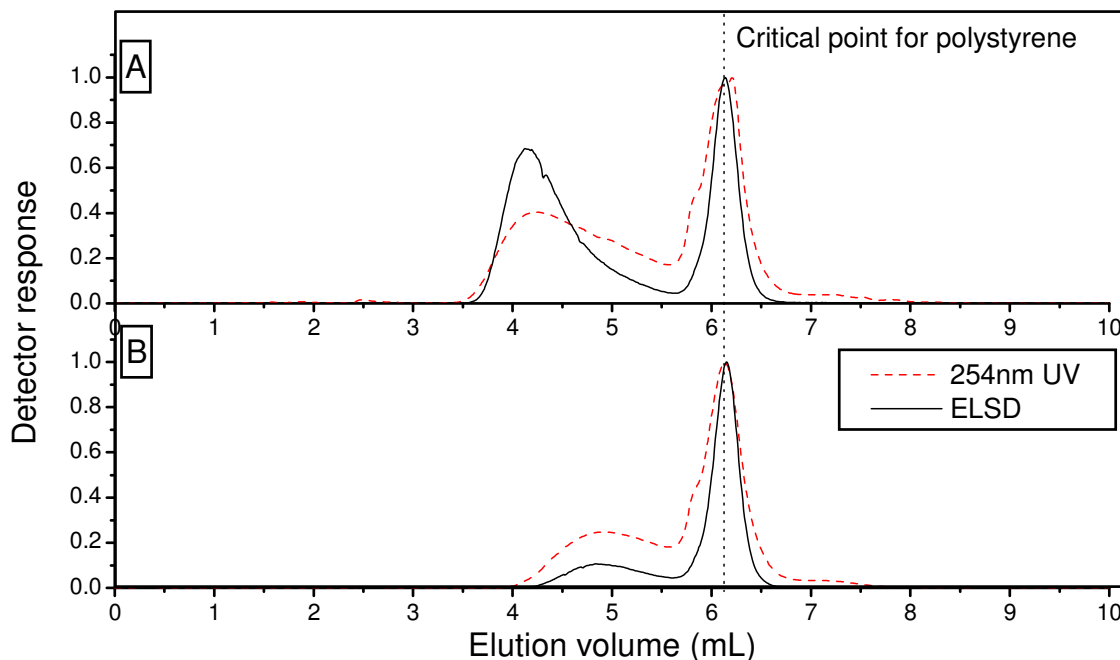


Figure 6.3 LC-CC elugrams of the PS-*b*-PMMA copolymers at the critical conditions for styrene. Stationary phase: C18 guard, Waters Symmetry C18 300 Å, Supelco Nucleosil Si C18 100 Å. Mobile phase: 50.3/49.7% (v/v %) THF/ACN. Analysis temp: 30 °C. (A) Shot addition, (B) Feed addition

In plot (B) the styrene appears to be present throughout the distribution. The signal intensity is not as strong compared to that of the ELSD in plot (A). It is possible that less block copolymer formed but, keeping in mind that much lower conversions were reached in the case of the feed additions, it does not mean that the copolymer is of lesser purity. The question arises as to what has become of the PMMA component of the polymer; i.e. whether all the methacrylate monomer that was added was incorporated into the already existing styrene chains or whether it formed PMMA homopolymer instead. The elugrams showed no evidence of a clearly separated PMMA peak. For a more complete picture the investigation of both critical points was therefore needed. The final result will be illustrated in following sections, with a discussion of the hyphenated techniques of online 2D chromatography.

### 6.3.2.1(b) Evaluation of the PMMA-*b*-PS copolymers at the critical point of PMMA

The LC-CC analysis of the PMMA-*b*-PS copolymers at the critical point of PMMA emphasized the difference in block copolymer formation when the polymerization sequence is reversed. If we

*Chapter Six: Chromatographic Investigation*

compare these results with those described in 6.3.2.1(a) it is evident from Figure 6.4 that very little starting material did not experience further growth and that copolymer formation was very successful. The concentration of PMMA might appear to be slightly higher in the feed addition method (B), but again this is related to the amount of conversion that was achieved in the block copolymer synthesis.

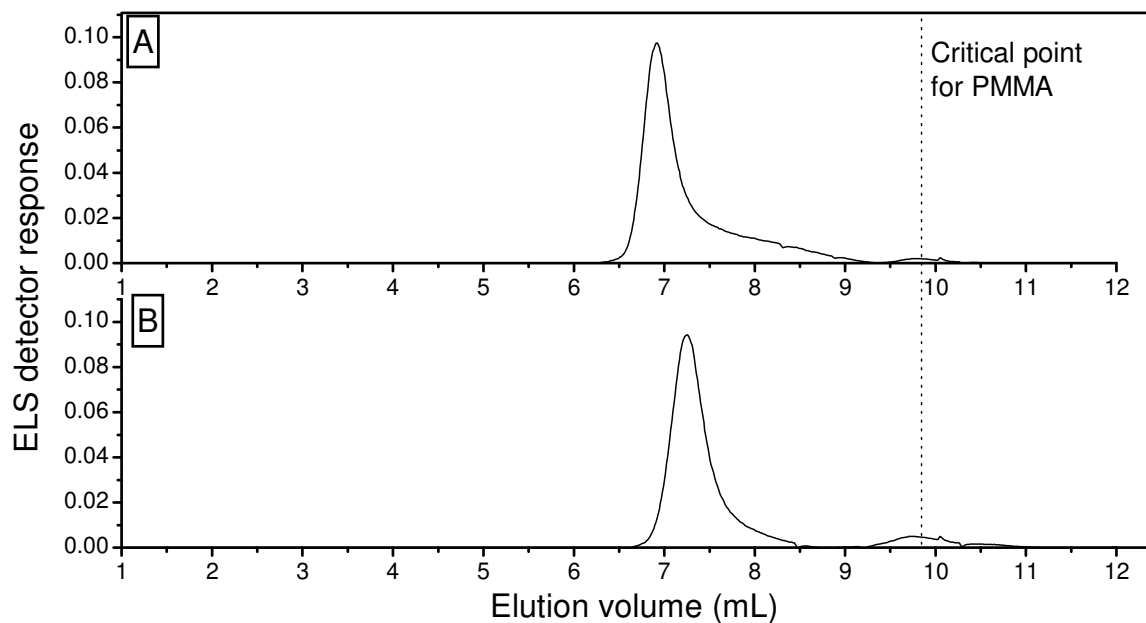


Figure 6.4 LC-CC elugrams of the PMMA-*b*-PS copolymers at the critical conditions for PMMA. Stationary phase: Supelco Si 300 Å, Nucleosil Si 100 Å. Mobile phase: 70.7/29.3 (v/v %) MEK/Cyclohexane. Analysis temp: 30 °C. (A) Shot addition, (B) Feed addition

UV detection was not possible in this chromatographic system as the MEK that was used as solvent absorbs at 254nm and interferes with the detection of the styrene chromophores.

### 6.3.2.2 Two-dimensional chromatography

The 2-D contour plots of the copolymers synthesized in both polymerization sequences and addition methods at both the critical points of Sty and MMA are presented. Each plot shows the separation based on chemical composition vs. the separation based on molar mass. The colour scale bar on the right hand side of each plot indicates the signal intensity, which is related to the concentration of chains present at a specific elution volume. The colour red corresponds to the maximum intensity and blue to the minimum intensity.

#### (a) PS-*b*-PMMA polymers

Figures 6.5 and 6.6 show the two-dimensional chromatography results corresponding to the PS-*b*-PMMA copolymers analyzed as described in Section 6.3.2.1. By using the data and information

*Chapter Six: Chromatographic Investigation*

collected from the individual LC-CC and SEC runs, the 2D-online system was optimized to obtain the following results. The contour plots of Figures 6.5(a) and 6.6(a) provide a visual picture of the poor block formation resulting when styrene is the starting material in sequential copolymerization with methyl methacrylate. The styrene polymer that did not chain extend eluted at the critical point and, in both addition cases, makes out the larger part of the composition. Analyzing the polymers at the critical conditions of polystyrene alone does not clarify the presence of homopolymer PMMA that possibly formed in the system.

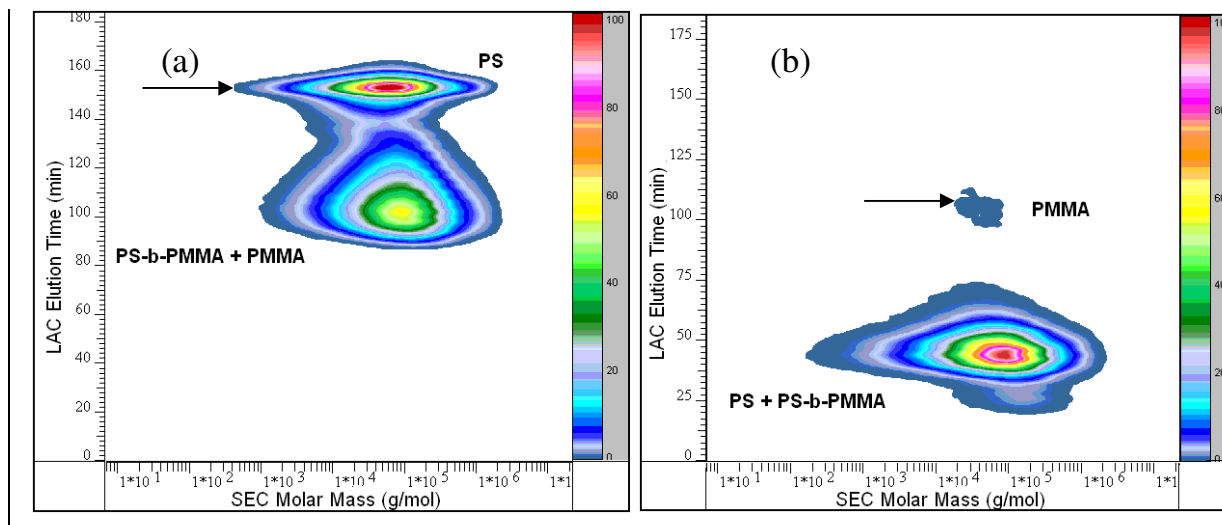


Figure 6.5 Two-dimensional LC-CC versus SEC contour plots of the CVADTB-mediated PS-b-PMMA block copolymer prepared via shot addition. (a) Critical conditions for Sty, (b) critical conditions for PMMA. (The arrows indicate the respective critical points.)

Figures 6.5 (b) and 6.6 (b) illustrate the analysis carried out at the critical point of PMMA for the same polymer samples. In Figure 6.5 (b) a small amount of PMMA was detected, whereas no PMMA homopolymer contaminant could be detected in the case of the feed addition method (Figure 6.6).

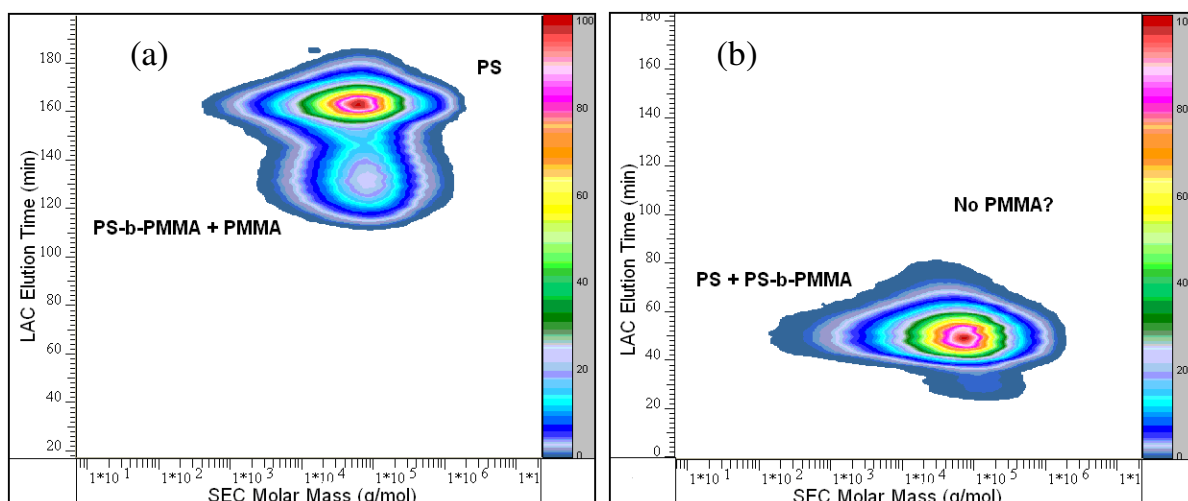
*Chapter Six: Chromatographic Investigation*

Figure 6.6 Two-dimensional LC-CC versus SEC contour plots of the CVADTB-mediated PS-b-PMMA block copolymer prepared via feed addition. (a) Critical conditions for Sty, (b) critical conditions for PMMA.

The contour plots support the initial conclusion, namely that there is clear evidence of living behaviour in the polymerization sequence of PS-b-PMMA, although a fair amount of styrene remains un-activated. Far less homopolymer is obtained in the case of the feed addition when compared to the shot addition.

**(b) PMMA-b-PS polymers**

Evidence of the improved nature of the feed system over that of the shot addition method was yet again found when looking at the contour plots for the PMMA-b-PS polymers. The amount of homopolymer PS contaminant was decreased, as can be seen in Figure 6.7(b) and Figure 6.8(b).

## Chapter Six: Chromatographic Investigation

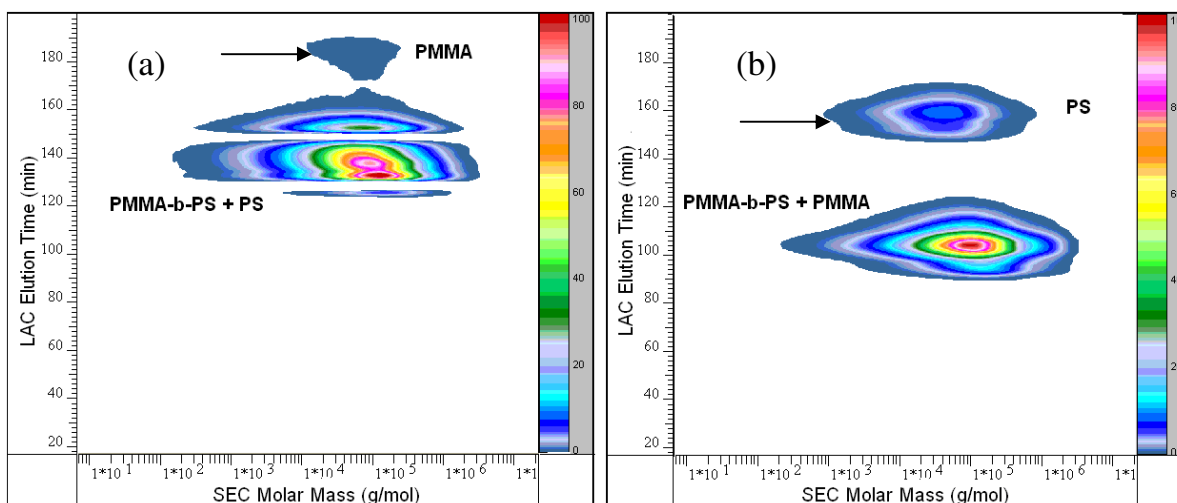


Figure 6.7 Two-dimensional LC-CC versus SEC contour plots of the CVADTB-mediated PMMA-*b*-PS block copolymer prepared via shot addition. (a) Critical conditions for PMMA, (b) critical conditions for Sty. (The arrows indicate the respective critical points.)

Figure 6.7 supports the conclusion that the styrene monomer fed into the system was much rather inclined to block formation than homopolymerization. This is indicative of the positive influence that monomer feed systems have in block copolymer purity. The success of block formation is also illustrated as the critical point of PMMA shows that very little PMMA starting material is present.

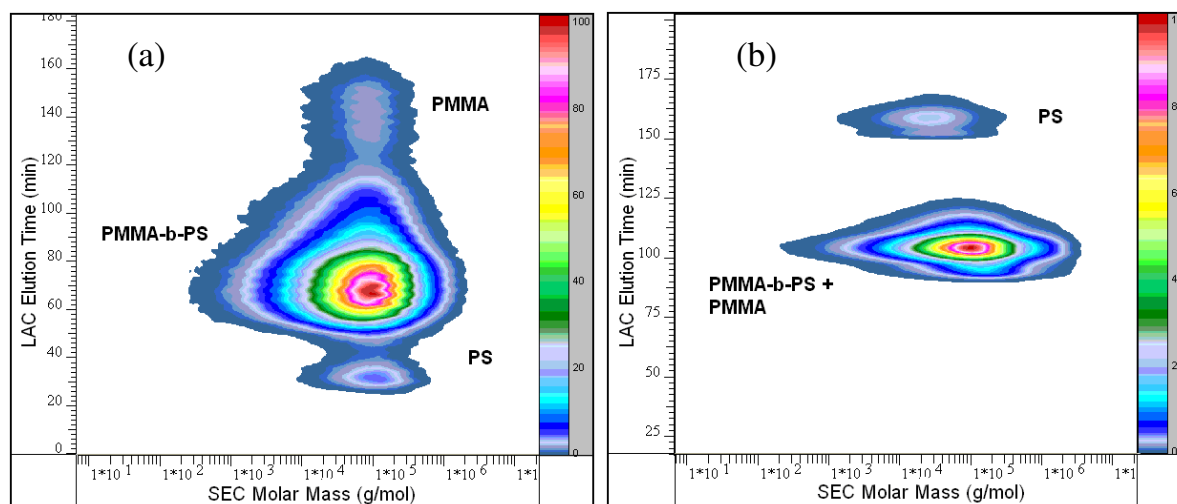


Figure 6.8 Two-dimensional LC-CC versus SEC contour plots of the CVADTB-mediated PMMA-*b*-PS block copolymer prepared via feed addition. (a) Critical condition for PMMA, (b) critical conditions for Sty.

The unusual distributions found in Figure 6.7 have their origin in artifacts occurring in the system when the fraction collector skips fractions. Figure 6.8 is a very good example of the separation that can be achieved in hyphenated chromatography analysis in the investigation of complex polymers.

## Chapter Six: Chromatographic Investigation

### 6.3.3 Online 2-D chromatography analysis of RAFT mediated block copolymers prepared in heterogeneous media

The block copolymers of styrene and methyl methacrylate prepared in heterogeneous media via the RAFT process, using CVADTB and CVATTB as RAFT agents (Chapter 5, Table 5.3), were investigated. Online 2-D chromatography analysis was conducted at both the critical points of PS and PMMA. The critical conditions were achieved as discussed in Section 6.3.1 and the 2-dimensional contour plots are presented. The polymerization sequence, the method of monomer addition as well as the RAFT agent type employed all played a role in influencing the resulting heterogeneity and copolymer purity in the block copolymer.

#### 6.3.3.1 PS-*b*-PMMA copolymers

From the SEC analysis presented in Chapter 5 (Section 5.3.2.1) it was concluded that in the PS-*b*-PMMA sequence different copolymerization behaviour resulted for each monomer addition method with each RAFT agent. The 2D-chromatography analysis of the copolymers involving CVADTB as RAFT agent supported this statement. Figures 6.9 to 6.11 illustrate the contour plots at both critical points for the block copolymer prepared via shot, pre-swelling and feed addition. Evaluation at the critical point of polystyrene (plots (a)) showed that although block formation occurred, the amount of PS homopolymer was still significant.

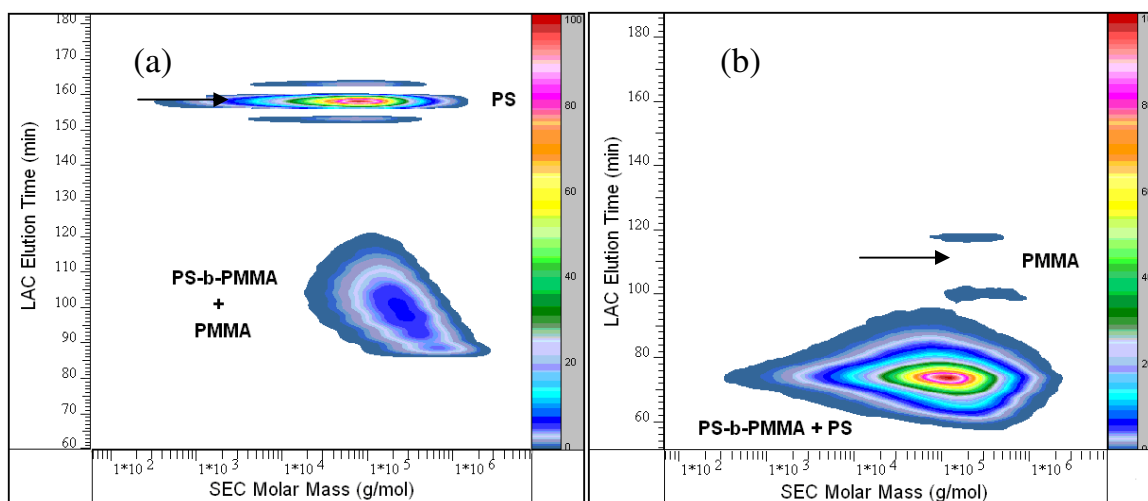


Figure 6.9 Two-dimensional LC-CC versus SEC contour plots of the CVADTB-mediated PS-*b*-PMMA miniemulsion block copolymer prepared via shot addition. (a) Critical conditions for PS, (b) critical conditions for PMMA. (The arrows indicate the respective critical points.)

*Chapter Six: Chromatographic Investigation*

Based on signal intensities, the pre-swelling method gave the most improved result, as a much larger distribution representing the block copolymer and PMMA homopolymer, was separated from the homopolymer which eluted at the critical point of styrene (Figure 6.10 (a)). In addition, the amount of PMMA homopolymer that formed was insignificant, as no signal could be detected by the ELS detector at the critical point of PMMA (Figure 6.10(b)).

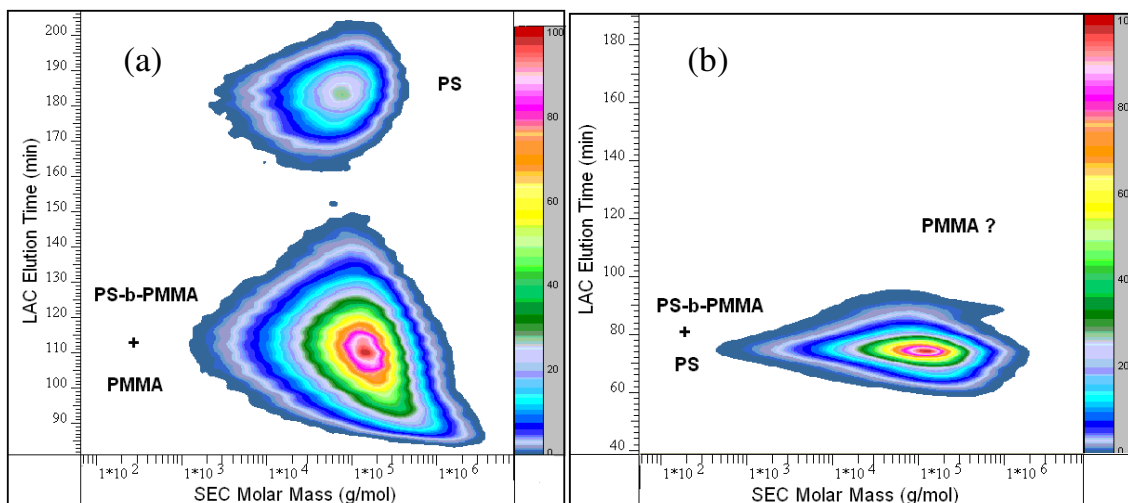


Figure 6.10 Two-dimensional LC-CC versus SEC contour plots of the CVADTB-mediated PS-*b*-PMMA miniemulsion block copolymer prepared via pre-swelling. (a) Critical conditions for PS, (b) critical conditions for PMMA.

The absence of a PMMA distribution was also found at the critical point of PMMA for the feed addition (Figure 6.11 (b)). This supported earlier statements (Section 5.3.2.1(a)), namely that the feed addition is an improvement over the shot addition method in that the amount of second homopolymer contaminant is decreased. Figure 6.9 (b) clearly shows the presence of PMMA in the system.

## Chapter Six: Chromatographic Investigation

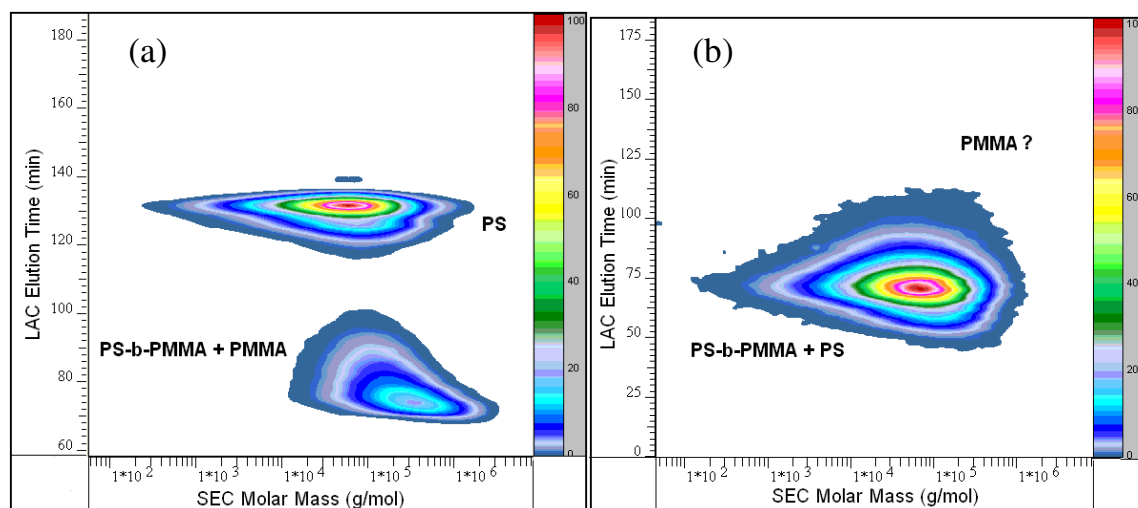


Figure 6.11 Two-dimensional LC-CC versus SEC contour plots of the CVADTB-mediated PS-*b*-PMMA miniemulsion block copolymer prepared via feed addition. (a) Critical conditions for PS, (b) critical conditions for PMMA.

For the copolymerizations mediated by CVATTB as RAFT agent, there was very little difference between the addition methods due to the lack of reactivation efficiency towards block copolymer formation, compared to when using the dithiobenzoate CVADTB as RAFT agent. The 2-D analysis of the block copolymer prepared via the feed addition is presented in Figure 6.12.

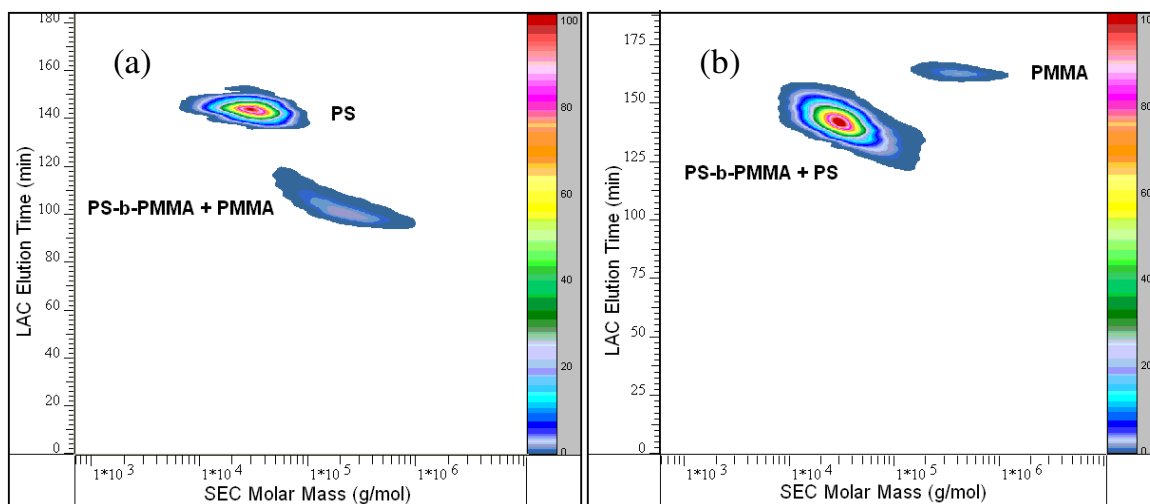


Figure 6.12 Two-dimensional LC-CC versus SEC contour plots of the CVATTB-mediated PS-*b*-PMMA miniemulsion block copolymer prepared via feed addition. (a) Critical conditions for PS, (b) critical conditions for PMMA.

The distribution eluting at the critical point of polystyrene had the highest intensity (plot (a)). The amount of chains related to the block copolymer (PS-*b*-PMMA) and homopolymer (PMMA) were reduced compared to that found in the CVADTB mediated copolymer analysis.

## Chapter Six: Chromatographic Investigation

Analysis at the critical conditions of PMMA showed that very little homopolymer PMMA eluted at the critical point. Feed addition proved to be consisted in being the superior method to minimize the second homopolymer contaminant.

### 6.3.3.2 PMMA-b-PS copolymers

All the contour plots in Figures 6.13 to 6.16 showed that at the critical point of PMMA, the concentration of chains representing the starting polymer material was minimal. The difference between the addition methods was not as pronounced as in the case of the PS-b-PMMA polymerization sequence when implementing the same RAFT agent. Figure 6.13 shows 2-D results of the copolymerization involving CVADTB as RAFT agent. The contour plots concerning the critical conditions for MMA are presented first. The current polymerization sequence involve the PMMA starting latex and the goal is determine to which extent the first block material underwent copolymerization. At the critical point of PMMA, the amount of starting material that did not undergo block formation could not be detected.

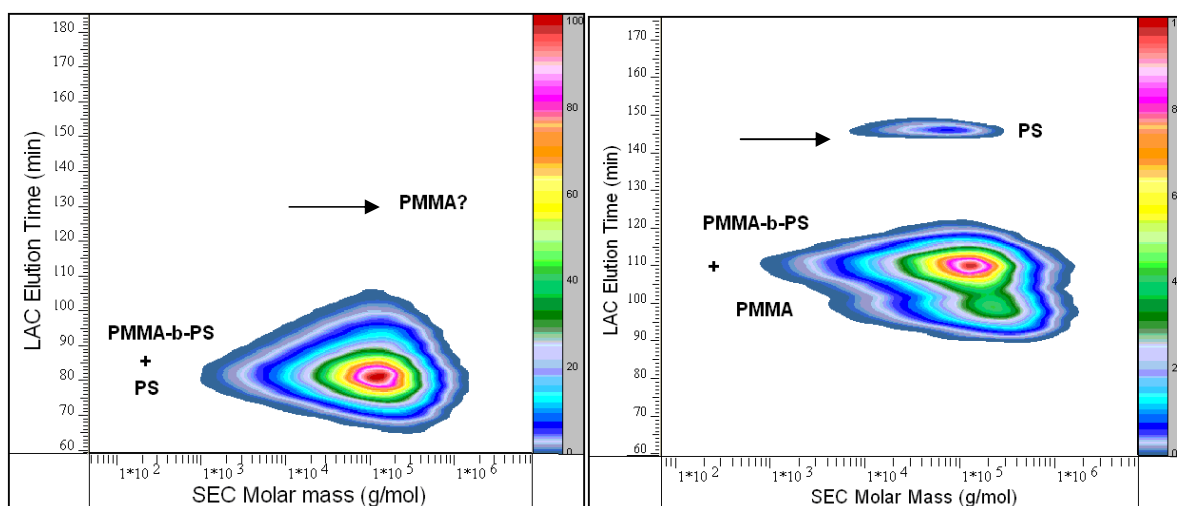


Figure 6.13 Two-dimensional LC-CC versus SEC contour plots of the CVADTB-mediated PMMA-*b*-PS miniemulsion block copolymer prepared via shot addition. (a) Critical conditions for PMMA, (b) critical conditions for PS. (The arrows indicate the respective critical points.)

The plots representing the pre-swelling (Figure 6.14 (a)) and feed additions (Figure 6.15 (a)) were too similar to draw any final conclusions in terms of their differences in chemical composition. Analysis at the critical point of polystyrene proved to be invaluable in determining the difference in copolymer purity. The amount of homopolymer polystyrene eluting at the critical point became

## Chapter Six: Chromatographic Investigation

increasingly less when going from the shot addition to the pre-swelling to the feed addition methods (Figures 6.13(b) to 6.15(b)).

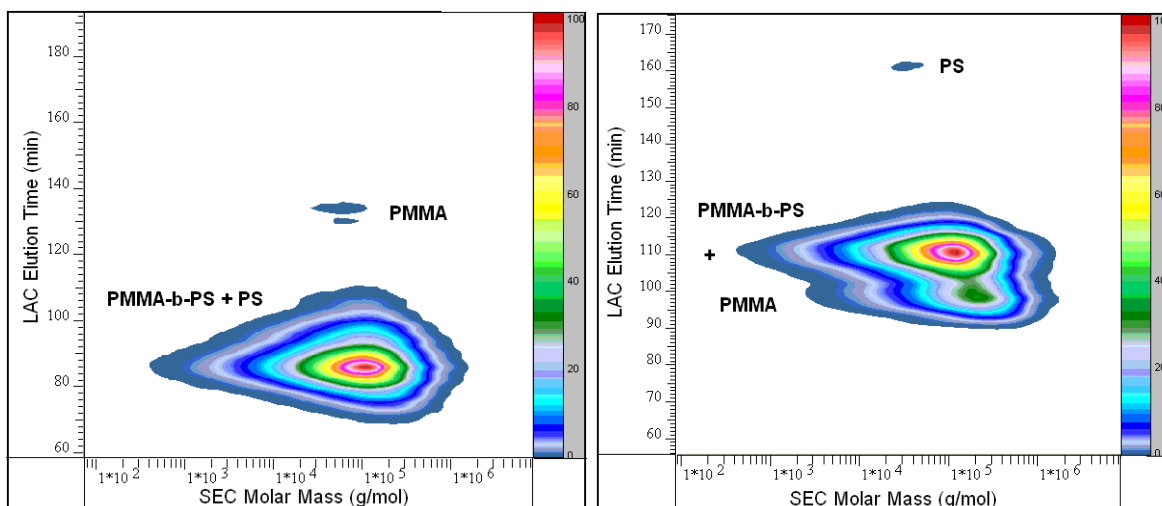


Figure 6.14 Two-dimensional LC-CC versus SEC contour plots of the CVADTB-mediated PMMA-*b*-PS miniemulsion block copolymer prepared via pre-swelling (a) Critical conditions for PMMA, (b) critical conditions for PS.

From investigating both critical points, it appears as if the feed addition method showed the most promising result in terms of copolymer purity as very little starting material was found, along with virtually no second homopolymer contaminant (Figure 6.15).

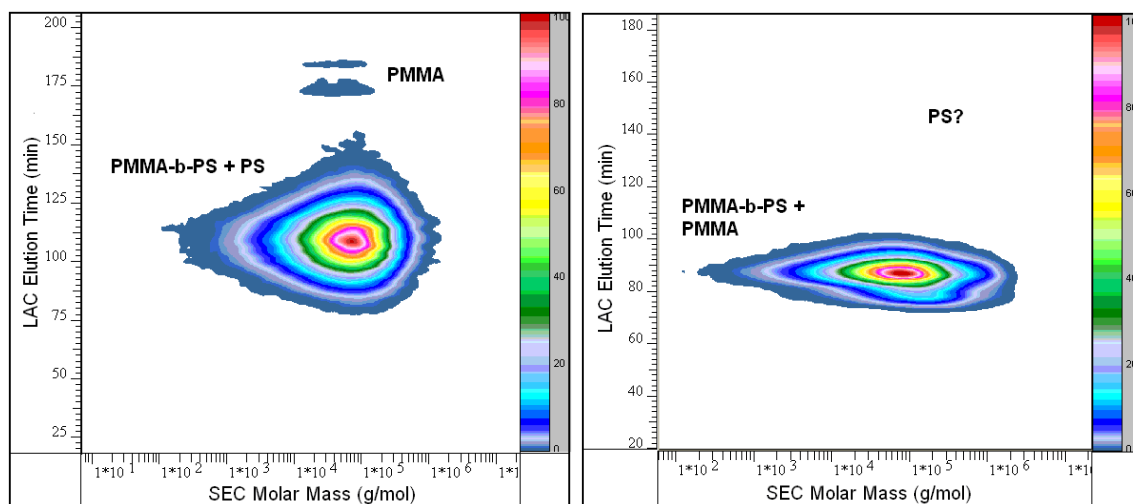


Figure 6.15 Two-dimensional LC-CC versus SEC contour plots of the CVADTB-mediated PMMA-*b*-PS miniemulsion block copolymer prepared via feed addition. (a) Critical conditions for PMMA, (b) critical conditions for PS.

Due to the consistency in behaviour of the trithiocarbonate CVATTB as RAFT agent in facilitating copolymerization, as well as no real differences obtained in addition methods, the 2D contour plot for the block copolymer prepared via the feed addition method is presented in Figure 6.16. From the

*Chapter Six: Chromatographic Investigation*

SEC analysis conducted as described in Section 5.3.2.2, it became apparent that the reactivation of the initial material for block formation was not so straightforward. It was therefore expected that through conducting chromatographic analysis on the copolymer, the chemical composition distribution would prove to be interesting.

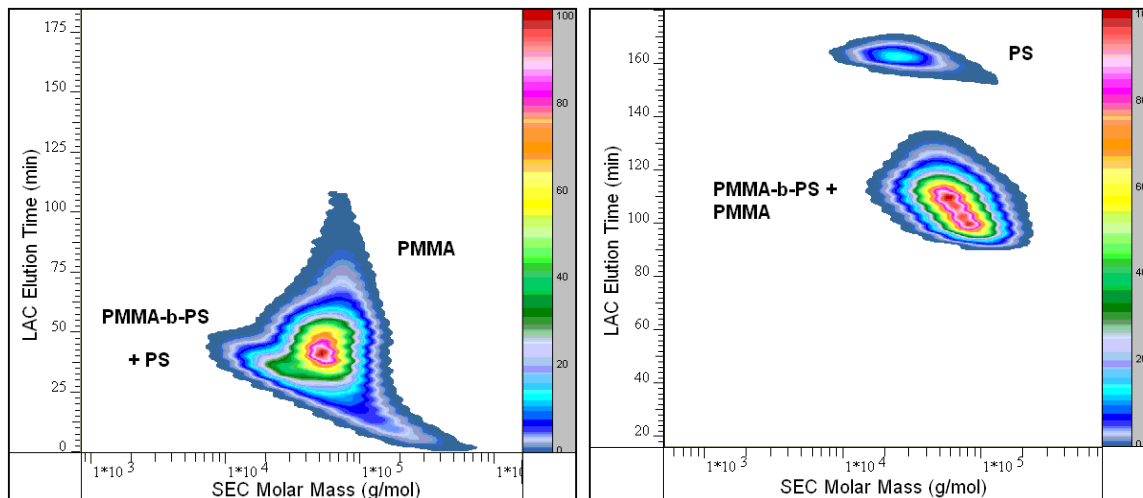


Figure 6.16 Two-dimensional LC-CC versus SEC contour plots of the CVATTB-mediated PMMA-*b*-PS miniemulsion block copolymer prepared via feed addition. (a) Critical conditions for PMMA, (b) Critical conditions for PS.

Figure 6.16(a) shows that there is no clear separation of the starting homopolymer at the critical point of PMMA, which made interpretation of the contour plot difficult. Evaluation of the critical point of PS shed more light on the different chemical species that made up the polymeric material. In plot (b), all the styrene homopolymer eluted at the critical point, while the retention of the other species was solely determined by the other, visible block. The intensity signals indicated that the second species (PMMA-*b*-PS and PMMA) made up most of the total distribution. The polystyrene chains corresponded to the theory, namely that the low molecular weight styrene homopolymer formed in the system originated from initiator-derived chains (Section 5.3.2.2). Overall, the increased success of block copolymerization in this polymerization sequence, in general, was evident.

## 6.4 Conclusions

Liquid chromatography analysis was successfully conducted on the Sty/PMMA block copolymers mediated by CVADTB and CVATTB as RAFT agents prepared in homogeneous and heterogeneous media. By the use of liquid chromatography at critical conditions (LC-CC) and SEC, and the online coupling of the two modes for two-dimensional (2D) chromatography, separation based on chemical composition and molecular weight was achieved.

### (I) Chromatographic analysis of RAFT mediated block copolymers prepared in homogeneous media.

The critical conditions for both Sty and methyl MMA were achieved and applied. The LC-CC analysis confirmed that the PMMA-b-PS polymerization sequence was more successful. Results of the online 2D chromatography showed that the feed addition method yielded block copolymers with the highest purity in both polymerization sequences.

### (II) Online 2-D chromatography analysis of RAFT mediated block copolymers prepared in heterogeneous media

The two-dimensional separation analysis of the block copolymers supported the results of SEC analysis obtained as described in previous chapters. The contour plots provided visual evidence why PMMA-b-PS is the sequence of choice in the block copolymerization of Sty/MMA systems, regardless of the polymerization media. It also showed the differences in the reactivation behaviour towards block copolymer formation when the starting materials consist of different RAFT end-groups. In the PS-b-PMMA sequence, the pre-swelling method resulted in the largest block copolymer distribution when CVADTB was employed as RAFT agent. The feed addition method proved to be the most efficient in minimizing homopolymerization of the second monomer, regardless of the sequence or RAFT agent type.

*Chapter Six: Chromatographic Investigation*

---

**6.5 References**

- (1) Pasch, H. *Macromol Symp* **2001**, *174*, 403-412.
- (2) Pasch, H. *Macromol Symp* **2002**, *178*, 25-37.
- (3) Braunecker, W. A.; Matyjaszewski, K. *Prog Polym Sci* **2007**.
- (4) Smid, J.; Van Beylen, M.; Hogen-Esch, T. E. *Prog Polym Sci* **2006**, *31*, 1041-1067.
- (5) Hadjichristidis, N.; Iatrou, H.; Pitsikalis, M.; Mays, J. *Prog Polym Sci* **2006**, *31*, 1068-1132.
- (6) Pasch, H. *Adv Polym Sci* **1997**, *128*, 1-45.
- (7) Heftmann, E. *Chromatography Part A: Fundamentals and Techniques*, 5th Ed.; Elsevier: Amsterdam, **1992**; Vol. 51A.
- (8) Heftmann, E. *Chromatography Part B: Applications*, 5th Ed.; Elsevier: Amsterdam, **1992**; Vol. 51B.
- (9) Berek, D. *Prog Polym Sci* **2000**, *25*, 873-908.
- (10) Van der Horst, A.; Schoenmakers, P. J. *J Chromatogr A* **2003**, *1000*, 693-709.
- (11) Pasch, H.; Trathnigg, B. *HPLC of Polymers*; Springer: Berlin, **1997**.
- (12) Pasch, H. *Polymer* **1993**, *34*, 4095-4099.
- (13) Pasch, H.; Rode, K.; Chaumien, N. *Polymer* **1996**, *37*, 4079-4083.
- (14) Berek, D.; Nguyen, S. H.; Hild, G. *Eur Polym J* **2000**, *36*, 1101-1111.
- (15) Lee, W.; Park, S.; Chang, T. *Anal Chem* **2001**, *73*, 3884-3889.
- (16) Gorbunov, A.; Trathnigg, B. *J Chromatogr A* **2002**, *955*, 9-17.
- (17) Jiang, X.; Van der Horst, A.; Lima, V.; Schoenmakers, P. J. *J Chromatogr A* **2005**, *1076*, 51-61.
- (18) Ikegami, T.; Hara, T.; Kimura, H.; Kobayashi, H.; Hosoya, K.; Cabrera, K.; Tanaka, N. *J Chromatogr A* **2006**, *1106*, 112-117.
- (19) Im, K.; Kim, Y.; Chang, T.; Lee, K.; Choi, N. *J Chromatogr A* **2006**, *1103*, 235-242.
- (20) Macko, T.; Hunkeler, D. *Adv Polym Sci* **2006**, *163*, 61-136.

## *Chapter 7: Conclusions and Recommendations*

### **Abstract**

A summary of the main conclusions in previous chapters and a short discussion on recommendations for future research is presented.

## 7.1 Conclusions to the study

1. The syntheses of the two RAFT agents, 4-cyano-4-((thiobenzoyl)sulfonyl) pentanoic acid (cyanovaleric acid dithiobenzoate) (CVADTB) and S-4-cyanopentanoic acid-S'-benzyltrithiocarbonate (CVATTB) were successfully carried out. The facile route for the preparation of the novel trithiocarbonate RAFT agent proved to be much faster and less complicated.
2. (i) The RAFT mediated polymerization of styrene and methyl methacrylate was successfully carried out in homogenous media with both monomers separately. The trithiocarbonate (CVATTB) mediated polymerizations were better controlled; polydispersity values were lower than those obtained for the dithiobenzoate mediated (CVADTB) runs and  $\bar{M}_{n,SEC}$  values fitted the theoretical values excellently. The dithiobenzoate (CVADTB) nonetheless still provided sufficient control. The polymers that were obtained were suitable for use in further block copolymerizations.

(ii) SEC analysis showed that block copolymer formation in both sequence PS-b-PMMA and PMMA-b-PS was successfully conducted. The mediation behavior of CVATTB to allow block formation was superior or at least similar, to that of CVADTB, depending on the monomer addition strategy (shot and feed) and the polymerization sequence.

In the PS-b-PMMA sequence the behaviour of the RAFT agents lending their polymers to chain extensions was similar within each addition method, while the quality of blocks was much improved with the feed systems. The CVATTB feed system, represented the best result in the data set of this polymerization sequence.

The PMMA-b-PS sequence yielded several different species, which varied from homopolymer formed from the newly added monomer to the desired block copolymer, as well as terminated material. The extent to which the abovementioned were present depended on the particular RAFT agent used as well as the method of addition. In the shot addition approach the two RAFT agents showed similar mediation behaviour, while the feed addition method was superior in providing much less homopolymer contaminant in the system. Results of this study confirmed that optimal results can be obtained via the use of the feed addition strategy.

*Chapter Seven: Conclusions and Recommendations*

---

3. (i) The synthesis of polystyrene and poly (methyl methacrylate) polymers mediated by CVADTB and CVATTB were successfully carried out in miniemulsion polymerization. Overall, RAFT agent CVATTB provided much better control compared to CVADTB for both monomer polymerizations as the  $\bar{M}_n$  values had an improved fit to the theoretically calculated  $\bar{M}_n$  and the polydispersities were lower. A significant difference was found between the mediation behaviour of the RAFT agents in terms of rate effects. CVATTB showed a much faster rate for both monomer polymerizations compared to CVADTB. The UV-RI overlays indicated that the polymers were adequately suitable for further block copolymerization.

(ii) Block copolymer formation in both sequence PS-b-PMMA and PMMA-b-PS was successfully carried out in seeded emulsion polymerization, using PS and PMMA latexes mediated by CVADTB and CVATTB.

In both polymerization sequences, CVATTB proved to be less efficient in reactivation for block formation than CVADTB.

As expected, generally more success was achieved with the PMMA-b- PS sequence in block copolymer formation, yet very little benefit was derived from introducing monomer in a more controlled fashion into the system. The block copolymerization behaviour was fairly similar for each addition method within the scope of each respective RAFT agent.

The PS-b-PMMA sequence illustrated different behaviour in copolymerization for each monomer addition method with each respective RAFT agent. The pre-swelling method showed the most improved result in terms of block formation with reactions involving CVADTB. Results for reactions mediated by CVATTB illustrated that, although very little chain extension occurred, the feed addition and pre-swelling methods showed improvement.

(iii) Results of particle size analysis showed a consistency for all styrene and methyl methacrylate miniemulsion latexes prepared using similar sonication conditions and polymerization recipes. Irrespective of the RAFT agent involved, smaller particles were obtained for styrene latexes compared to methyl methacrylate. Results of TEM analysis corresponded well with those of light scattering analysis for the seed and block copolymer latexes. In the case where the RAFT agent was not as active towards chain extension, the system was more susceptible to secondary nucleation in the aqueous phase and the presence of a large distribution of finer particles was evident in the TEM images.

*Chapter Seven: Conclusions and Recommendations*

---

4. Liquid chromatography analysis was successfully conducted on the Sty/PMMA block copolymers mediated by CVADTB and CVATTB as RAFT agents and prepared in homogeneous and heterogeneous media. The critical conditions for both styrene and methyl methacrylate were determined and successfully applied.

(i) LC-CC analysis conducted on the blocks synthesized in homogeneous media confirmed that the PMMA-b-PS polymerization sequence was more successful. Online 2D chromatography concluded that the feed addition method yielded block copolymers with the highest purity in both polymerization sequences.

(ii) Results of online 2-D chromatography analysis of the block copolymers prepared in heterogeneous media supported the results from the SEC analysis. The contour plots provided visual evidence why PMMA-b-PS is the sequence of choice in the block copolymerization of Sty/MMA systems. The chromatography results confirmed that the feed addition method proved to be the most efficient approach to synthesize block copolymers, regardless of the sequence or RAFT agent type.

## 7.2 Recommendations for future investigation

The following recommendations for future research are made:

1. As it is a novel RAFT agent, further investigation on the mediation behaviour of S-4-cyanopentanoic acid-S'-benzyltrithiocarbonate (CVATTB) should be conducted. The limitations of its efficiency should be determined, and it should be studied with regard to its implementation in different monomer systems, reaction conditions and polymerization media.
2. The commercial significance of waterborne products constantly generates the need to research and develop polymerization processes that are viable in terms of cost and efficiency. Two emulsion polymerization techniques that show promise are *ab initio* emulsion and *in situ* surfactant emulsion polymerization. Preliminary studies have indicated that much faster polymerization rates can be obtained with similar efficiency of control found in miniemulsion systems when implementing appropriate RAFT agents. Several aspects play a role in establishing stable monomer latexes; therefore the scope of exploration is broad.
3. A more in depth chromatography analysis of the block copolymers is recommended. Through additional calibration of both the first and second dimension of separation, the individual block length of the block copolymers can be determined. A calibration in the second dimension based on poly(methyl methacrylate) standards would also make for interesting results. In turn, quantitative results in terms of the separation analysis can be obtained.
4. The trithiocarbonate RAFT agent has an interesting theoretical ability to produce A-B-A type block copolymers in addition to the A-B type investigated in the current study. The probability is very much dependent on the monomers used and the sequence in which the block copolymer is prepared. Investigation of this property via chromatographic or chemical means will be an interesting extension of the work. With chain lengths suitable for MALDI- TOF analysis, a more detailed evaluation on the mechanism of the RAFT agent can be conducted.

## *Acknowledgements*

Firstly, I wish to acknowledge the National Research Foundation of South Africa for the financial support from a personal aspect, as well as Mondi Business Paper for funding the research project.

I would like to thank my promoter, Prof R.D. Sanderson and co-promotor, Dr J.B. McLeary for their time and efforts throughout the duration of my MSc research. Their individual contributions are greatly appreciated and will never be forgotten.

A special acknowledgement to Dr Wolfgang Weber, who was responsible for the synthesis and purification of the disulfide reagent used to prepare the trithiocarbonate RAFT agent. Your contribution played a significant role in this study and therefore I cannot thank you enough for your work and collaboration.

The following individuals are acknowledged for analytical contributions to the work presented here:

Jean McKenzie and Elsa Malherbe for NMR analysis of the RAFT agents.

Dr. V. Grumel for the introductory course to HPLC and 2-D analyses.

Mohammed Jaffer (UCT) for TEM analyses.

The staff at Barloworld Plascon Stellenbosch for the DLS analysis

In addition, I wish include my special thanks to Prof Harald Pasch and his team at DKI, Analytik for the opportunity they gave me to visit their institute and discuss my 2-D results. Their input proved to be invaluable for present and future study. Daniella Knecht, Jacques Raust, Dr Robert Brüll and Dr Wolfgang Radke deserve a special mention.

I am grateful to the staff at Polymer Science, Margie Hurndall, Erinda Cooper, Aneli Fourie, Calvin Maart and (oom) Hennie Groenewald, including Adam Keuler and the late Johan Bonthuys, for making life a little easier in Polymer Science building in terms of administration and technical assistance.

The Free Radical Group and Lab members, past and present are thanked for all the great times- Good and bad included. I would like to especially thank the group of 2003 for the great example

## *Acknowledgements*

---

they set and all the invaluable skills they taught me when I first joined the group several years ago. Students have come and gone but you guys reserved a special place in my polymer science training. To the free radical group members who attended the SML'06 conference in Il Ciocco, Tuscany Italy and supported me during my first international talk, I just want to say it would not have been half as good without you there. Crazy.....!! I'd like to thank Prof Bert Klumperman for making the transition from past to future an easy one.

On a personal note....

I'd like to thank my Libyan colleagues for their support and encouragement to not give up. To Fozi, Osama, Walid, Wael, Anwar, Reda and especially Ahmed, your positive advice, assistance, discussions and guidance are much appreciated.

To Ulli and Heide Lehman, Maggie Goosen and the Spouse group, I would like to thank all for making me feel at home and allowing me to take a breather from the madness of science at least once a week. All the Libyan woman who constantly wished me luck and supported me, you and the kids, were the silver lining of my dark clouds.

To Elana de Goede, who made my stay in Germany a less frightful experience, I will be forever grateful. On that note I would like to include Pritish Sinha and Michael Al Samman, for the best informal chats on chromatography I've ever had in my entire life.

A huge thank you to the other two musketeers, Gareth Bayley and Jacques Rinqest, for surviving my moods and endless complaining. Conspiring with Gareth to throw the HPLC/GPC instruments out of an imaginary window brightened many a dull day. Thanks bud for all the GPC/HPLC moments! Jacques will forever hold the record in my book for picking the worst times to column! From Marc Lottering shows to Pink concerts to Moyo to Fairview... from Bukhara to Brazen to Binelli's...the list goes on and on. Thanks for being there when I needed shoulders to cry on and people to share jokes with!

Importantly, I need to thank James McLeary, without whom none of this would have been possible. There are too many reasons to mention but thanks for years of working together, sharing your knowledge and experience and giving me opportunities that I only could have dreamt of. You never allowed me to give up and kept reminding me the times I needed it the most, what it's all about at

## *Acknowledgements*

---

the end of the day. “Basically- it’s complicated”. Thanks so much for making me part of a great team and supporting me thus far. Wishing you the best of luck for your future plans.

Last but not least I’d like to acknowledge those closest to me, my family...Ma, Vincent, Zoe and Micah. I’ll keep it short by saying thanks for everything and dealing with me on a daily basis. It’s a tough job-I know. Love you much. To my Dad (may he rest in peace), I finally figured it out; I am my father’s daughter. Hope I made you proud. To all the members on both sides of my hugely extended family, including Michelle and Gretchen, I appreciate you keeping me in your thoughts, your encouragements and your collective agreement that you have absolutely no idea why I’m doing this to myself! Love you all...

*“Yes, there were times, I’m sure you knew  
When I bit off more than I could chew.  
But through it all, when there was doubt,  
I ate it up and spit it out.  
I faced it all and I stood tall;  
And did it my way”  
My way- Frank Sinatra*